TU Delft

CLOSED-FORM SOLUTION FOR THE

Buckling analysis of Euler-Bernoulli columns and beam-columns with jump discontinuities

WRITTEN BY MIKHAIL JAMES

MSC. STRUCTURAL ENGINEERING

AUGUST, 2021

Closed-form solution for the

Buckling analysis of Euler-Bernoulli columns and beam-columns with jump discontinuities

The influence of step-changes of geometrical and material properties, real joints, bracing, non-propagating open edge cracks, and real support conditions

MSc Thesis by:

Mikhail James

To obtain the degree of Master of Science

at the Delft University of Technology

to be defended on Monday, 30th of August 2021

Student Number:		4815106	
Project duration:		November 2020 – August 2021	
Graduation committee:	Chair	Dr. ir. A. Cicirello	Delft University of Technology
	Member	Dr. ir. F.P. van der Meer	Delft University of Technology
	Member	Dr. ir. M. Luković	Delft University of Technology
	Member	Dr. ir. F. Giunta	ARUP

An electronic version of this thesis is available at https://repository.tudelft.nl/

Cover: Photo by Jim Pelley

TU Delft

Abstract

Structural elements under compression can fail due to instability. Such type of failure may present itself as flexural buckling, which is the sudden change of configuration of one state to another at a critical compressive load. Actual structure characteristics, such as cracks, real joints, sudden changes of flexural stiffness, bracing, and actual boundary conditions, make current analytical buckling methods inefficient. For this reason, most structures are evaluated using Finite Element (FE) software based on the Finite Element Method (FEM). However, such a numerical method may have a high computational cost when parametric studies need to be performed. The motivation for this thesis was to develop an analytical alternative for the buckling analysis of columns and beam-columns.

The thesis analyses jointed Euler-Bernoulli columns and beam-columns with N discontinuities due to step-changes of flexural stiffness, and influence of open edge cracks, real joints, bracing, and actual support conditions. The approach considered utilizes the Heaviside function to obtain a single piecewise expression for the deflection, slope, moment, and shear of columns and beam-columns. The use of the Heaviside function, along with proposed closed-form expressions, reduce the number of unknown integration constants to only four.

Main findings are listed as following: (i) Linear buckling analysis of a column only depends on solving the determinant of the 4x4 matrix of unknown coefficients, obtained by imposing four boundary conditions. (ii) Solving the four unknown constants of integration results in performing a geometrical non-linear static analysis of the beam-column, which perfectly agrees with results obtained through FE software. (iii) Closed-form expressions reduce the number of unknown constants of integrations to only four, regardless of the number of sections composing a column or beam-column.

Concluding remarks and recommendations include: (i) Closed-form expressions accurately provide linear buckling loads for columns and geometrical non-linear expressions for beam-columns. (ii) Equations solved algebraically can be stored and used for future analysis, saving the computation time of rerunning the analysis for specific columns or beam-columns. Having the equations expressed algebraically allows for the ease of performing parametric analysis and exploring the performance of new designs. (iii) Computational cost (time needed for the computer to obtain the results) may depend on the mathematical software used for the calculations. Other software may result in having lower computational time for the same calculations.

Acknowledgements

This thesis is written to obtain the Master of Science degree in Civil Engineering from Delft University of Technology.

I would like to take this opportunity to express my gratitude to my committee members: Dr. ir. Alice Cicirello, Dr.ir. Frans van der Meer, Dr. ir. Mladena Luković, and Dr. ir. Filippo Giunta, who have taken the time to guide me in this process with constructive feedback. I would like to give a special thanks to my chair supervisor Dr. ir. Alice Cicirello, for her guidance and encouragement through each stage of the process and for showing interest in not only the development of my research project, but also in my personal development.

The following people have contributed to my dissertation in their unique way, primarily by simply being great friends; Pooja, Kunal, Sali, and Raymond, who helped me validate my results. To all other people who have accompanied me on this journey with me, thank you for your friendship.

I am extremely grateful to my parents, but especially to my mother, Jeannette, for her love, prayers, caring and sacrifice to educate and set me up for my professional future. I would also like to acknowledge with gratitude the support and love of my sisters, Mayra and Asha. And finally, I would also like to thank my girlfriend Daniela, who has witnessed the countless hours dedicated to this thesis and who has supported me throughout this journey.

Table of Contents

Table of Figures

List of tables

Abbreviations

dof	degree of freedom
EB	Euler-Bernoulli
FE	Finite Element
FEA	Finite Element Analysis
FEM	Finite Element Method
PMPE	Principle of Minimum Potential Energy

1 Introduction

Structural columns, drill strings, and car driveshafts are a few examples amongst the many engineering structures that may suffer from instability. Such structures are composed of multiple components with different material and geometrical properties while being jointed together. When it comes to analyzing and validating these engineering structures, Finite Element (FE) software is widely used. However, high computational costs can be encountered when parametric investigations are carried out or during the exploration of different designs.

This chapter introduces the challenges surrounding the buckling analysis of columns and beam-columns subjected to cracks, elastic joints, bracings, and elastic boundary conditions. After, it briefly covers the different methods available in the literature for obtaining the critical values of such systems. Moreover, it explains how these complexities are idealized in analytical models. Afterwards, the identified research gap, followed by the research questions and objectives, are presented. The chapter concludes by providing the layout for the thesis.

1.1 Background and Motivation

Before breaking ground in any construction site, a team of engineers explores many designs to obtain the most economical and safe structure. Sudden changes in material and geometrical properties (Figure 1) are often implemented to reduce cost, optimize design, or be aesthetically pleasing. These structures must be checked against different kinds of failure, such as material or stability failure. Buckling is a stability failure, which is the sudden equilibrium change from one configuration to another at a critical compressive load. Actual structures present physical damage in the form of cracks, joint stiffness between consecutive segments, and bracing in a column. Such real-life occurrences may compromise the stability of a structure by lowering the compressive load necessary for a structure to buckle. Therefore, it is vital to include such complexities in the buckling analysis of columns and beam-columns to understand and avoid the sudden collapse nature inherent to buckling.

It is common to use software based on the Finite Element Method (FEM) to evaluate the buckling load or deflection of columns and beam-columns. The influence of cracks, lateral bracing, real joints between structural elements, or actual boundary conditions are complexities that can be included in models by using discrete rotational, internal, and external transversal springs [1]–[5]. Nevertheless, the use of FEM in the design exploration or parametric study can have a high computational cost to the point of becoming unfeasible. Elevated costs arise from the remodeling and remeshing of each new model for the linear buckling analysis of columns and the need for multiple loading steps to obtain accurate results for the deflection, slope, moment, and shear of beam-columns.

Figure 1: Examples of physical structures that can suffer from instability. (a) drill-strings under high compressive loads and consisting of many elements of different cross-sections. (b) structural columns that have different material properties at the column-slab-column interface. (c) stepped wind turbine subjected to high lateral loads. (d) structural columns with step-changes in their cross-section.

To overcome the mentioned FEM limitations, many authors have developed analytical methods for tackling columns with the previously mentioned complexities. Some have based their work using the Principle of Minimum Potential Energy, which can provide an approximation to the buckling load for columns with step-changes in cross-section [6], [7], with both end and intermediate axial loads [8]. Q. S. Li has proposed an approach to obtain the exact solutions of the buckling load by manipulating the governing equations into Bessel equations, followed by the *transfer matrix method* for columns with non-uniform cross-sections and multi-step non-uniform columns under different boundary conditions [9]–[12].

Additionally, Arbabi et al. [13], proposes a semi-analytical procedure for the buckling analysis of columns with variable cross-sections using the *theory of distributions.* Such a theory provides adequate mathematical tools to manipulate the governing equations of a discontinuous system to be expressed in a single equation in terms of generalized functions.

Generalized functions have unique properties that make them helpful in expressing discontinuous functions as piece-wise continues ones and by describing loading conditions, such as that of a point load, without creating a discontinuity in the loading function. Their use has been proved helpful in obtaining general closed-form solutions of complex models. Such models include the analysis of jointed Euler-Bernoulli (EB) beams with step-changes in material and cross-section [2], and the static analysis of EB beam-columns with multiple unilateral cracks [3] where the buckling load could be obtained.

The literature review has identified the lack of an effective analytical method that considers the influence of all the complexities presented in Figure 1 and Figure 2. Therefore, the main goal of this thesis is to offer a closed-form solution for the buckling analysis of columns and beam-columns with both material and cross-section step-changes while considering the influence of non-propagating cracks, bracing, real joints, and actual boundary conditions.

1.2 Analytical model to be solved

The following section presents the model of the highest complexity to be solved with its corresponding assumptions and scope.

1.2.1 Mathematical model

Discrete springs have been used in mathematical models to introduce complexities of real structures [1]–[5] as seen in Figure 2. Three main springs are contemplated:

- External transversal springs can be considered at the boundary and continuity conditions of the jointed EB beam-column to model the points where transversal displacement are restricted to some degree due to the influence of lateral bracing, diaphragms, and stabilizers of drill strings, to name a few examples.

- Internal transversal springs can be used to model real joints between two structural elements.

- Rotational springs have been used by many authors to model open cracks along the beam-column due to its effectiveness. Cracks are represented by pinning together two beam-column sections and using a rotational spring to model the increase in flexibility due to the crack [3]–[5], [14].

Figure 2: Examples of physical damage of existing structure in the form of (a) cracks in the column, (b) cracks at the location of column-slab, and (c) real joint connections.

The complexities of real structures of interest for the mathematical model are:

- Loss of stiffness due to non-propagating open cracks.
- Influence of joints between connected structural beam-column elements.
- Influence of lateral bracing.
- Influence of real boundary conditions.

Such complexities are included in Figure 3, which displays the model of the highest complexity that will be analyzed in this thesis.

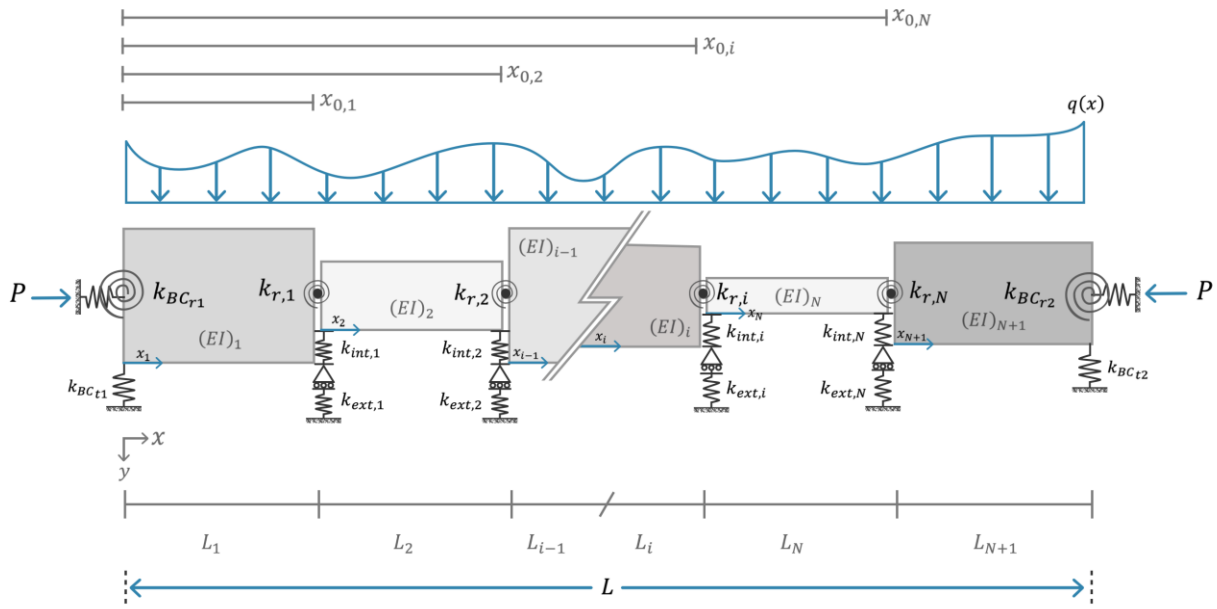

Figure 3: Model of the highest complexity: Jointed EB beam-column with multiple step-changes in flexural stiffness. Each EB structural element is pinned together with rotational and internal and external translational springs at the discontinuity location. The model has rotational and translational springs at the boundaries.

1.2.2 Model Assumptions and Scope

Given the potential complexity of such types of analysis, the following assumptions are made to formulate the new analytical solutions:

- Small deformations theory.
- Effects of shearing deformations and shortening of the beam axis are neglected.
- The material of the beam-column is homogeneous and linearly elastic. Uncertainties of material properties are not considered.
- No local buckling at any cross-section along the beam-column is allowed.
- Physical damage in the form of non-propagating open edge cracks.
- Cracks are represented by massless rotational springs at pin-connected joints to introduce slope discontinuity and loss of stiffness.
- Transversal displacement restrictions are represented by external transversal springs.
- The behavior of joints is modelled by internal transversal springs.
- Axial load acts through the axis of the beam-column.

Small deformation theory allows the kinematic relations to be developed as appropriate for linear elasticity [15].

Local buckling occurs when the strength of a member, usually a steel member, is compromised due to the stability failure of one of the steel's profile components. These can be considered as plate elements that, given the right conditions of slenderness and compressive axial load, may buckle, resulting in local buckling. Plate buckling is analyzed by its own governing equations which are dependent on two variables

as plate buckling involves the bending of two planes. Local buckling can be avoided with the correct implementation of stiffeners on the steel profile [16].

1.3 Research Questions and Objectives

The main questions this thesis will tackle are:

1. How to take advantage of the properties of generalized functions to develop a closed-form solution for the buckling analysis of columns and beam-columns with step-changes of its flexural stiffness (sudden changes of material and cross-section properties), while considering the influence of non-propagating cracks, real joints, boundary, and lateral support conditions?
2. How do different springs (rotational, external translational, and internal translational) acting in a column affect the buckling loads?

The goal of this thesis is to be achieved in the following steps:

1. Formulate a closed-form expressions for the buckling analysis of beam-column elements with step-changes of flexural stiffness and:
    a. Ideal joints and boundary conditions
    b. Ideal joints and elastic boundary conditions
    c. Ideal boundary conditions, and elastic joints which are modelled by internal translational springs between two successive elements.
    d. Ideal joints, and external along-the-axis translational springs to model external bracing.
    e. Ideal boundary conditions, and successive elements pinned together with a rotational spring to model non-propagating cracks.
    f. External along-the-axis translational springs to model external bracing, internal translational springs to model elastic joints, and internal rotational springs to model non-propagating open edge cracks.
2. Perform a parametric study to demonstrate the advantages of using the proposed closed-form solution for the buckling analysis of complex beam-columns.

1.4 Thesis Layout

Chapter 1 – Introduction

Chapter 2 – Theoretical background

Chapter 3 – Closed-form solutions for the buckling analysis of Euler-Bernoulli beam-columns and columns

Chapter 4 – Validation of the closed-form solutions for the buckling analysis of complex beam-columns

Chapter 5 – Applications and Discussion

Chapter 6 – Case Study – Wind turbine tower buckling analysis

Chapter 7 – Conclusions and recommendations

2 Theoretical background

2.1 Introduction

Extensive research has been done on the current methods for performing buckling analysis of beam-column models presenting varying complexities. This chapter explains the theoretical background necessary to understand the nature of the buckling problem and overviews the status of the field. To this end, the governing equations for beam-columns and columns are introduced in section 2.2. Afterwards, the concept of stability is briefly presented in section 2.3, including different buckling analysis methods, emphasizing Euler's buckling analysis. The modelling of physical structures and complexities in the form of cracks, bracings, and real joints is presented in section 2.4. Generalized functions of interest are discussed in section 2.5, with section 2.6 focusing on the literature takeaways and comparison between different buckling analysis methods.

2.2 Beam, Columns, and Beam-Columns

Beam-columns are structural members commonly found on frame-type structures being subjected simultaneously to both axial and transversal loads. Under these conditions, the response of the structural element is no longer linear, causing the method of superposition to no longer to be valid [17]. When no transversal loads are present, the structural member under pure compressive axial load is a column. Columns can be classified as either short, slender, or intermediate [18]. On the other hand, if only transversal loads are present, the structural element behaves as a beam.

2.2.1 Derivation of governing differential equations

The governing equations that express the behavior of beam-columns are based on Euler-Bernoulli's (EB) beam theory and can be derived from models seen in Figure 4. Figure 4a displays a structural element subjected simultaneously to a distributed lateral load $q(x)$ and a compressive axial force P. EB's main assumptions are based on the theory of small deformations, and on plain cross-sections remaining planar and normal to the undeflected beam axis in a beam subjected to bending [19]. Under such assumptions, an element of length dx between two cross-sections is presented in Figure 4b. For such a small section, the lateral load $q(x)$ is assumed to be constant. Loads acting on the y-axis direction are assumed to be positive.

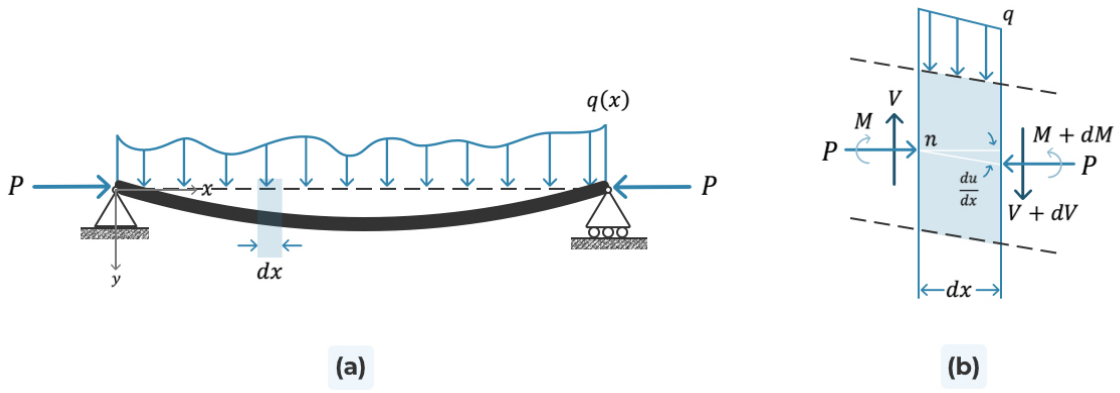

Figure 4: (a) Beam subjected to the lateral load $q(x)$ that varies with the distance x and is subjected to an axially compressive force P. (b) Element of length dx between two cross-sections taken normal to the undeflected axis of the beam shown in (a).

The governing differential equations for a beam-column are derived by considering the kinematic, constitutive, and equilibrium conditions. Under the assumption of the theory of small deformations, $\sin(\theta) \approx \tan(\theta) \approx \theta$ and $\cos(\theta) \approx 1 - \theta^2/2 \approx 1$ [15], and thus, derive the kinematic relations. The sign convention and relation to the slope can be seen in Figure 5.

$$\theta = \frac{d}{dx}u(x) \qquad \text{Eq. 1}$$

$$\kappa = \frac{1}{\rho} = \frac{d\theta}{dx} = \frac{d^2}{dx^2}u(x) \qquad \text{Eq. 2}$$

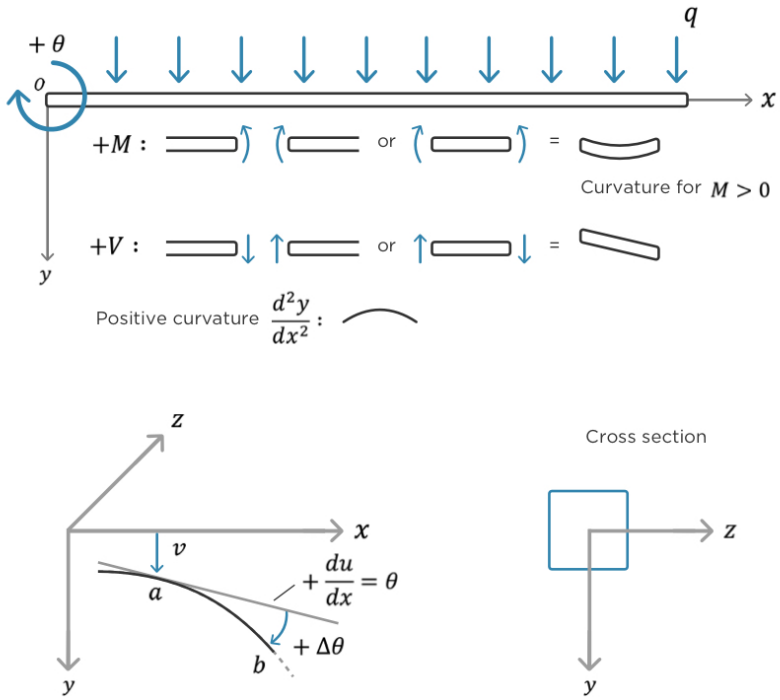

Figure 5: Sign convention adopted with the x-axis running along the column's axis and the positive y-axis acting downwards.

The relationship among the distributed load $q(x)$, shear force (V), and bending moment (M), can be obtained by inspecting the element displayed in Figure 4b. Equilibrium of vertical forces results in the relation between the distributed load and the shearing forces:

$$-V + q\,dx + (V + dV) = 0 \qquad \text{Eq. 3}$$

$$q = -\frac{dV}{dx} \qquad \text{Eq. 4}$$

Similarly, equilibrium of moments around point n of Figure 4b under the assumption of small angles results in:

$$M + q\,dx\frac{dx}{2} + (V + dV)\,dx - (M - dM) + P\frac{du}{dx}\,dx = 0 \qquad \text{Eq. 5}$$

Neglecting second-order terms, Eq. 5 reduces to:

$$V = \frac{dM}{dx} - P\frac{du}{dx} \qquad \text{Eq. 6}$$

Finally, by neglecting the effects of shearing deformation and axial shortening, the bending moment can be obtained considering the curvature of the beam and the flexural stiffness of the beam [20], resulting in:

$$-M = EI\,\kappa = EI\frac{d^2}{dx^2}u(x) \qquad \text{Eq. 7}$$

The governing equation for a beam-column can be obtained by combining Eq. 4 with Eq. 6 and Eq. 7, resulting in the following alternative forms:

$$\frac{d^2}{dx^2}\left(EI\,\frac{d^2}{dx^2}u(x)\right) + P\,\frac{d^2}{dx^2}u(x) = q(x) \qquad \text{Eq. 8}$$

Or:

$$\frac{d}{dx}\left(-EI\,\frac{d^2}{dx^2}u(x)\right) - P\,\frac{d}{dx}u(x) = V \qquad \text{Eq. 9}$$

It should be noted that when no axial force is present ($P = 0$), Eq. 8 reduces to the governing equation of a beam under pure bending due to only lateral forces [20]:

$$\frac{d^2}{dx^2}\left(EI\ \frac{d^2}{dx^2}u(x)\right) = q(x) \qquad \text{Eq. 10}$$

When no lateral load is present ($q(x) = 0$), Eq. 8 describes the behavior of an ideal column:

$$\frac{d^2}{dx^2}\left(EI\ \frac{d^2}{dx^2}u(x)\right) + P\ \frac{d^2}{dx^2}u(x) = 0 \qquad \text{Eq. 11}$$

2.2.2 General solution of the governing equation

The general solution of the governing differential equation of a beam-column (Eq. 8) with constant stiffness can be obtained in different ways. This paper's analytical solution for the buckling of a beam-column is based on the solution obtained employing the Laplace transform.

Given that the governing differential equation is fourth-order, the solution will have four unknown constants of integration. Dividing Eq. 8 by the constant stiffness EI and substituting $v^2 = P/EI$, simplifies the governing differential equation to:

$$\frac{d^4}{dx^4}u(x) + v^2\ \frac{d^2}{dx^2}u(x) = \frac{q(x)}{EI} \qquad \text{Eq. 12}$$

The introduced variable v is critical for the buckling analysis given it contains the load variable P, and will be referred to as the axial parameter or the critical variable. The Laplace transform of Eq. 12 is:

$$\mathcal{L}\{u(x)\}(s^4 + s^2\ v^2) + u(0)(-s^3 - s\ v^2) + u'(0)(-s^2 - v^2) - s\ u''(0) - u'''(0) = \frac{\mathcal{L}\{q(x)\}}{EI} \qquad \text{Eq. 13}$$

Where $\mathcal{L}\{\blacksquare\}$ stands for the Laplace transform operator and s for Laplace's variable associated with the running variable x. Isolating the term $\mathcal{L}\{u(x)\}$ and introducing the integration constants by substituting $u(0) = A,\ u'(0) = B,\ u''(0) = C,\ u'''(0) = D$ results in:

$$\mathcal{L}\{u(x)\} = A\left(\frac{s^3 + s\ v^2}{s^4 + s^2\ v^2}\right) + B\left(\frac{s^2 + v^2}{s^4 + s^2\ v^2}\right) + \frac{C\ s}{s^4 + s^2\ v^2} + \frac{D}{s^4 + s^2\ v^2} + \frac{\mathcal{L}\{q(x)\}}{EI\ (s^4 + s^2\ v^2)} \qquad \text{Eq. 14}$$

Taking the inverse Laplace transform to Eq. 14 results in:

$$u(x) = A + B\,x + C\left(\frac{1-\cos(v\,x)}{v^2}\right) + D\left(\frac{x}{v^2} - \frac{\sin(v\,x)}{v^3}\right) + \cdots$$

$$\cdots + \frac{\int_0^x (q(\tau)\sin(v\,\tau)\cos(v\,x) - q(\tau)\cos(v\,\tau)\sin(v\,x))\,d\tau}{EI\,v^3} - \cdots \qquad \text{Eq. 15}$$

$$\cdots - \frac{\int_0^x (-q(\tau)\,x + q(\tau)\,\tau)\,d\tau}{EI\,v^2}$$

Eq. 15 describes the transverse displacement of a homogeneous beam-column segment of constant stiffness subjected simultaneously to a lateral load $q(x)$, and an axial compressive load P. When no lateral load is present, Eq. 15 describes the transverse displacement of an ideal column, simplifying Eq. 15 into:

$$u(x) = A + B\,x + C\left(\frac{1-\cos(v\,x)}{v^2}\right) + D\left(\frac{x}{v^2} - \frac{\sin(v\,x)}{v^3}\right) \qquad \text{Eq. 16}$$

For the case no axial force is present $(P = 0,\ v \to 0)$, the transverse displacement is described by:

$$u(x) = A + B\,x + \frac{C\,x^2}{2} + \frac{D\,x^3}{6} + \frac{q^{[4]}(x)}{EI} \qquad \text{Eq. 17}$$

With $q^{[k]}(x)$ being the primitive of order k of the lateral loading function.

2.2.3 Beam-column conformed of multiple segments of constant stiffness

A homogeneous beam-column consisting of N discontinuities, as seen in Figure 6, is composed of $N+1$ segments. Eq. 15 is used to describe the transverse displacement of each segment, resulting in a total of $4(N+1)$ unknown constants of integrations. These are solved by enforcing $4(N+1)$ conditions. Four unknowns are evaluated by enforcing four boundary conditions, two at each boundary. The remaining $4N$ unknowns are evaluated at the location of the discontinuities, by enforcing continuity of displacements, slopes, moment, and shear, between two successive beam-column segments.

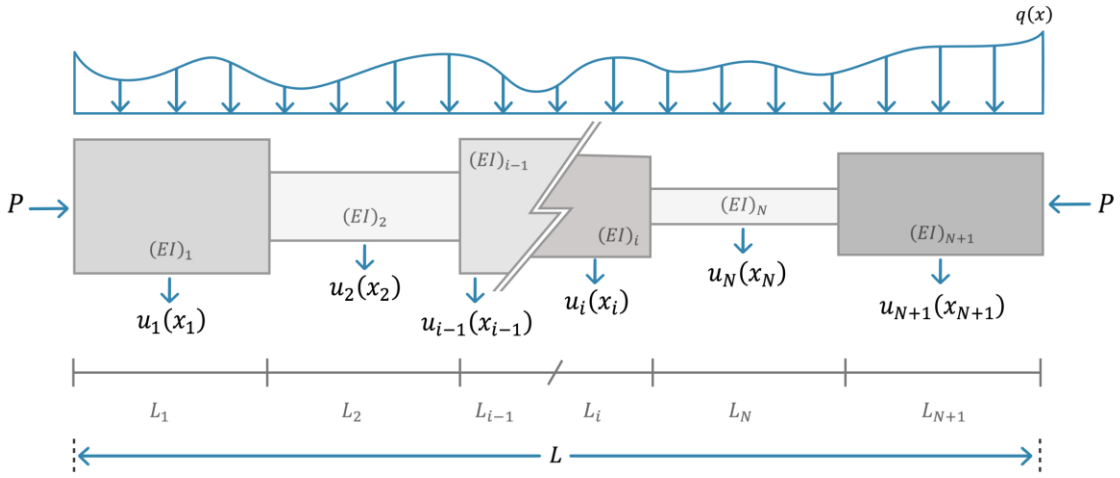

Figure 6: EB beam-column consisting of N step changes of flexural stiffness subjected to an axial load P and a lateral load $q(x)$. $N+1$ sections of constant stiffness are described by their displacement function $u_i(x_i)$.

$$u_i(x_i) = A_i + B_i\,x_i + C_i\left(\frac{1-\cos(v_i\,x_i)}{v_i^2}\right) + D_i\left(\frac{x_i}{v_i^2} - \frac{\sin(v_i\,x_i)}{v_i^3}\right) + \cdots$$

$$\cdots + \frac{\int_0^{x_i}(q_i(\tau)\sin(v_i\,\tau)\cos(v_i\,x_i) - q_i(\tau)\cos(v_i\,\tau)\sin(v_i\,x_i))\,d\tau}{EI_i\,v_i^3} - \cdots \qquad \text{Eq. 18}$$

$$\cdots - \frac{\int_0^{x}(-q_i(\tau)\,x_i + q_i(\tau)\,\tau)\,d\tau}{EI_i\,v_i^2}$$

The subscript i is used to represent the deflection, slope, moment, or shear of beam-column segment i. The relation between the slope, moment, and shear to the displacement function was presented in the previous section. Applying Eq. 15 into Eq. 1 and Eq. 7 results in:

$$\theta_i = B_i + \frac{C_i\sin(v_i\,x_i)}{v_i} + D_i\left(\frac{1}{v_i^2} - \frac{\cos(v_i\,x_i)}{v_i^2}\right) + \frac{\int_0^{x_i} q_i(\tau)\,d\tau}{EI_i\,v_i^2} - \cdots$$

$$\cdots - \frac{\int_0^{x_i}(q_i(\tau)\sin(v_i\,\tau)\sin(v_i\,x_i) + q_i(\tau)\cos(v_i\,\tau)\cos(v_i\,x_i))\,d\tau}{EI_i\,v_i^2} \qquad \text{Eq. 19}$$

$$M_i = -C_i\,EI_i\cos(v_i\,x_i) - \frac{D_i\,EI_i\sin(v_i\,x_i)}{v_i} + \cdots$$

$$\cdots - \frac{\int_0^{x_i}(-q_i(\tau)\sin(v_i\,\tau)\cos(v_i\,x_i) + q_i(\tau)\cos(v_i\,\tau)\ \sin(v_i\,x_i))\,d\tau}{v_i} \qquad \text{Eq. 20}$$

To express each equation in terms of local variables, the axial load P of Eq. 6 is substituted by $P = v_i^2\ EI_i$ allowing to write the shear on a local member as:

$$\frac{d}{dx_i}\left(-EI_i\ \frac{d^2}{dx_i^2}u_i(x_i)\right) - v_i^2\ EI_i\ \frac{d}{dx_i}u_i(x_i) = V_i \qquad \text{Eq. 21}$$

Applying Eq. 15 into Eq. 21 leads to:

$$V_i = -B_i\ EI_i\ v_i^2 - D_i\ EI_i - \int_0^{x_i} q_i(\tau)\ d\tau \qquad \text{Eq. 22}$$

The mentioned discontinuities present themselves as step-changes of stiffness, bracing influence, real joints, and non-propagating open edge cracks. For ideal columns, no lateral load is present $(q_i(x_i) = 0)$, with the local displacement, slope, moment, and shear being expressed as:

$$u_i(x_i) = A_i + B_i\ x_i + C_i\left(\frac{1-\cos(v_i\ x_i)}{v_i^2}\right) + D_i\left(\frac{x_i}{v_i^2} - \frac{\sin(v_i\ x_i)}{v_i^3}\right) \qquad \text{Eq. 23}$$

$$\theta_i(x_i) = B_i + \frac{C_i\sin(v_i\ x_i)}{v_i} + D_i\left(\frac{1}{v_i} - \frac{\cos(v_i\ x_i)}{v_i^2}\right) \qquad \text{Eq. 24}$$

$$M_i(x_i) = -C_i\ EI_i\cos(v_i\ x_i) - \frac{D_i\ EI_i\sin(v_i\ x_i)}{v_i} \qquad \text{Eq. 25}$$

$$V_i(x_i) = -B_i\ EI_i\ v_i^2 - D_i\ EI_i \qquad \text{Eq. 26}$$

This paper focuses on enforcing the boundary and continuity conditions using local coordinates. Two boundary conditions are enforced at $x_i = 0$ and the remaining two at $x_i = L_i$. The continuity of displacements, slopes, moments, and shears between two consecutive segments are enforced at $x_i = L_i$ and at $x_{i+1} = 0$.

2.3 Stability

Structural analysis is performed to find the configuration of a loaded system that satisfies different criteria to make a structure safe. Specific criteria depend on different types of failure. Two primary failure considerations for structures are

- Material failure occurs when stresses in a structure exceed an allowable value related to material properties.
- Form or configuration failure happens when a structure cannot maintain its design configuration due to external disturbances, i.e. applied loads. When tensile loads occur, the stability loss falls in

the category of material instability. On the other hand, when compressive loads are present, the stability loss is labelled as structural instability. It is more commonly known as buckling, which is a dangerous failure due to the potential collapse of the structure [16].

There are three criteria for stability:

- Euler's statical (non-trivial equilibrium state) criterion, based on the non-trivial equilibrium state approach, answers whether it exists another configuration besides the straight configuration in which the structure is in equilibrium. Figure 7 is considered to illustrate the problem. Two states of equilibrium are displayed in Figure 7(a) for a fixed-free column of uniform cross-section and elastic material under an axial load P. The axial load is increased while remaining on the straight configuration. Above a critical load, denominated as P_{cr}, the column supports the load in a bent configuration, represented by the dashed line of Figure 7(a). At the critical load, two equilibrium configurations are possible, a condition known as bifurcation or branching. The force-deformation behavior is shown in Figure 7(b). As the load increases, there is a point at which the lateral load can no longer be associated with the lateral deflection [16].
- Liapunov's dynamical criterion, based on kinetic or dynamical approach, investigates whether the amplitude of vibrations of a column diminishes or increases with time given a slight disturbance. The structure is considered as dynamically unstable for $P > P_{cr}$.
- Potential energy stability criterion, based on the work approach or energy approach, investigates at which load the potential energy of a conservative system ceases to be at a minimum [16].

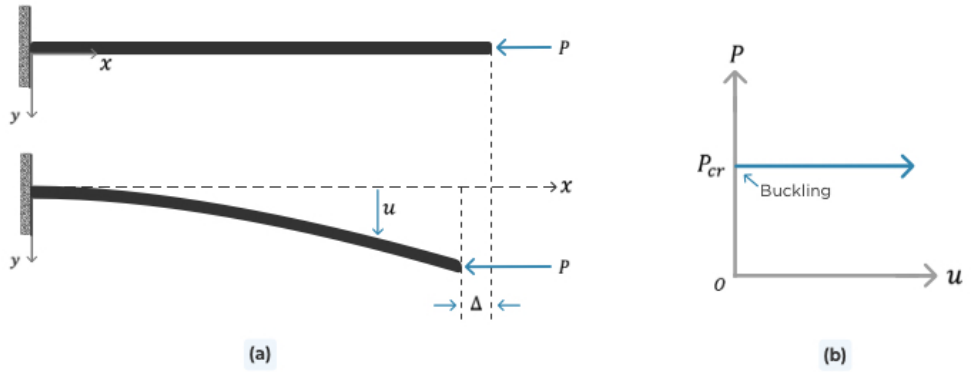

Figure 7: (a) Two equilibrium states are displayed for a fixed-free column of uniform cross-section and elastic material under an axial load P. (b) Load-deformation for the fixed-free column displayed on (a).

Buckling can be categorized further as flexural buckling, torsional buckling, torsional-flexural buckling, and snap-through buckling [16].

2.3.1 Euler Buckling analysis – non-trivial equilibrium state approach (Classical method)

This section focuses on the different methods for flexural buckling of columns and beam-columns. Emphasis will be given to the non-trivial equilibrium state approach, otherwise known as Euler's buckling criterion. An energy approach is going to be briefly introduced and discussed.

The non-trivial equilibrium state approach is also known as Euler buckling analysis, linear-buckling analysis, eigenvalue buckling; this paper refers to it as the "classical method". Such an analysis provides the theoretical buckling loads of an elastic structure. The buckling load of a structural element can be

obtained by using the governing equations of columns and beam-columns. The following assumptions are necessary for the Euler buckling analysis:

- Beam-column and column are perfectly straight.
- The cross-section is uniform throughout its length.
- The axial load acts at the centroid of the beam-column.
- Stresses are within the elastic limit.
- Material is homogeneous and isotropic.
- Self-weight is neglected.
- Failure only presents itself due to buckling.
- Axial shortening is negligible.

2.3.1.1 Column Buckling

The buckling load for a simply supported column with uniform cross-section and homogeneous material, as seen in Figure 8, can be obtained by using the governing differential equations of a column. Using the derived general solutions of the column for the displacement, slope, moment, and shear (Eq. 23 – Eq. 26), it is possible to obtain the critical buckling load.

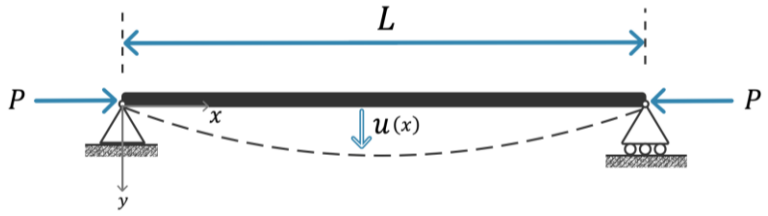

Figure 8: Simply supported column under an axial load P and constant stiffness EI. The first buckling mode is represented by the dashed line.

There are three main boundary conditions for ideal columns: fixed, pinned, or free. A fixed boundary condition requires the deflection and slope at the boundary to be zero. A pinned boundary condition requires the deflection and moment to be zero, while a free boundary condition requires both the moment and shear to be zero.

After applying the boundary conditions, a system of four equations is obtained and expressed in matrix notation. The trivial solution provides the values of the undeflected column. The non-trivial solution, according to linear algebra, is obtained by when the determinant of the matrix of unknown displacements vanishes, i.e. the determinant equals zero. This paper refers to the determinant of the system of equations as the buckling equation. It presents itself as a transcendental equation dependent on the axial parameter ν, given that the axial load P is present in such a variable ($\nu = P/EI$). The non-trivial solutions are found at the roots of the buckling equation. Each root is associated with a buckling load and its corresponding buckling mode, which is the shape that the beam-column takes at the buckling load.

Appendix 1 presents all the steps required for obtaining the buckling load of the simply supported ideal column seen in Figure 8.

The governing equations of columns and their general solution can be used for analyzing a column with sudden jumps in its flexural stiffness by either having changes of its material or geometric properties, as seen in Figure 9.

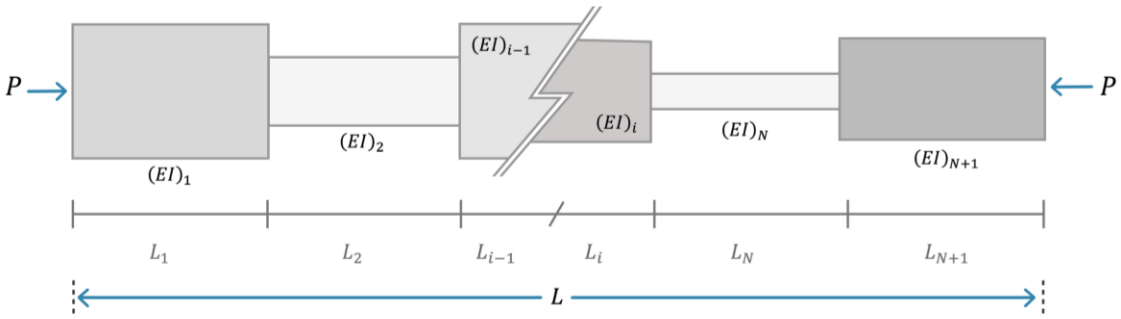

Figure 9: Ideally jointed EB column with N step changes on flexural stiffness subjected to an axial load P.

The governing equations (Eq. 23 – Eq. 26) must be applied to each section with uniform cross-section and homogeneous material properties. The application would result in four unknown constants of integration for each segment. A system of N discontinuities would have $N+1$ segments resulting in a total of $4(N+1)$ unknown constants of integration. Boundary and continuity conditions would provide the necessary equations to solve for all constants. Four equations are obtained from the boundary conditions, and the remaining equations are obtained by conditions that require a continuity of displacements, slope, shear, and moment. For the buckling analysis of a column, this means solving at least a $4(N+1) \times 4(N+1)$ matrix which non-trivial solution – having its determinant equal to zero – would result in the buckling loads and modes. Therefore, a system with N discontinuities would become computationally expensive to solve because of the large number of equations and the matrix of coefficients size.

2.3.1.2 Beam-column buckling

To effectively convey the effect of lateral loads on the buckling analysis of beam-columns, the following example is presented:

- A simply supported steel beam-column of homogeneous material under axial load P and a constant distributed lateral load q_0 (Figure 10).
- It has a length of 5000 mm
- Young's modulus of 200 000 N/mm^2
- 300x300 mm^2 square cross-section

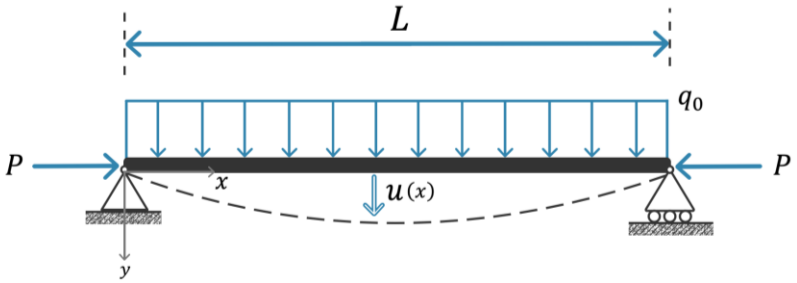

Figure 10: Simply supported beam-column under an axial load P and constant stiffness EI.

Using Eq. 23 and Eq. 25 (deflection and moment of a column), it is possible to solve for the four unknown integration constants by imposing the four boundary conditions of the simply supported beam-column $(u(0) = M(0) = u(L) = M(L) = 0)$. After solving the four unknown integration constants, it is possible to plot the deflection of the beam-column. The midspan deflection $(x = 0.5\,L)$ is plotted against the critical variable v under different values of q_0, as presented in Figure 11.

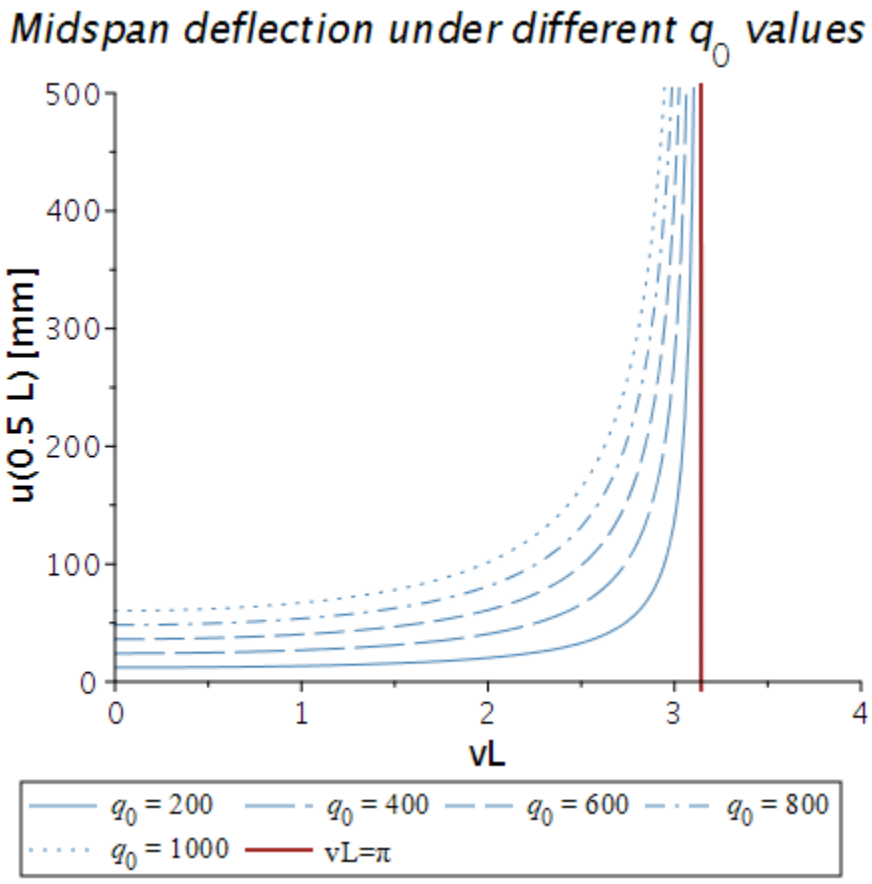

Figure 11: Midspan deflection of a simply supported beam-column under a constant lateral load q_0 in N/mm.

The red line at $vL = \pi$ corresponds to the critical load of the column counterpart of Figure 8 ($P = \pi^2 EI/L^2$). Such a value is the vertical asymptote reached in different ways, depending on the magnitude of the uniform distributed load. As seen in Figure 11, under a constant distributed load, the magnitude of the midspan deflection increases as the axial parameter v approaches the critical load of the column (red dashed line). Moreover, beam-columns under lower values of q_0 approach faster the asymptote corresponding to the buckling load of its column counterpart.

2.3.2 Work and Energy

Work is defined as the energy required to move mass around in space [19] and can be classified as internal and external work. According to the law of conservation of energy, the energy in a system cannot be created nor destroyed – it remains constant by converting one form of energy into another. For a perfectly closed elastic system, this means that the change in energy of external loads (i.e. external work done) is

equal to the change in its internal energy in the form of strain energy (i.e. internal work done) [16]. Thus, the work balance equation is:

$$-W_{in} = W_{ex} \quad \text{Eq. 27}$$

2.3.2.1 Internal Work – Bending strain energy

A one-dimensional elastic body conformed by rigid elements of infinitesimal length δx (Figure 12(a)) is connected by hinges and rotational springs (Figure 12(b)). The bending strain energy of such an elastic body is defined as the energy stored in all the rotational springs [16]. The total energy of bending stored on the rotational springs is expressed as:

$$U_r = \sum \delta U_r = \sum_{i=1}^{n} \frac{1}{2}\, k_r\, (\delta\theta_i)^2 = -W_{in} \quad \text{Eq. 28}$$

With $\delta\theta_i$ expressing the change in angle between two successive elements connected by hinge i, and k_r being the rotational stiffness of the spring. Assuming the rotational springs follow the law of linear moment springs, then:

$$M = k_r(\delta\theta) \rightarrow \delta\theta = \frac{M}{k_r} \quad \text{Eq. 29}$$

Eq. 28 can be written as:

$$U_r = \sum \delta U_r = \sum_{i=1}^{n} \frac{M_i^2}{2\, k_r} \quad \text{Eq. 30}$$

Using the relationship from the strength of materials:

$$M = EI\left(\frac{d^2u}{dx^2}\right) = EI\left(\frac{d\theta}{dx}\right) = EI \lim_{\delta x \to 0}\left(\frac{\delta\theta}{\delta x}\right) \approx EI\frac{\delta\theta}{\delta x} \quad \text{Eq. 31}$$

Solving for stiffness on Eq. 29:

$$k_r = \frac{M}{\delta\theta} = \frac{EI}{\delta x} \quad \text{Eq. 32}$$

Substituting the relation of the rotational spring stiffness of Eq. 32 in Eq. 30, the total energy due to bending is:

$$U_r = \sum \delta U_r = \sum_{i=1}^{n} \frac{M_i^2}{2\,EI}\,\delta x_i \qquad \text{Eq. 33}$$

For a continuous system, n must be infinitely large ($n \to \infty$). At the limit, $\delta()$ tends to $d()$; hence the summation Σ tends to be the integral $\int$ [16]. Thus, the strain energy is:

$$U_r = \int \frac{M^2}{2\,EI}\,dx = \frac{EI}{2}\int \left(\frac{d^2}{dx^2}u(x)\right)^2 dx \qquad \text{Eq. 34}$$

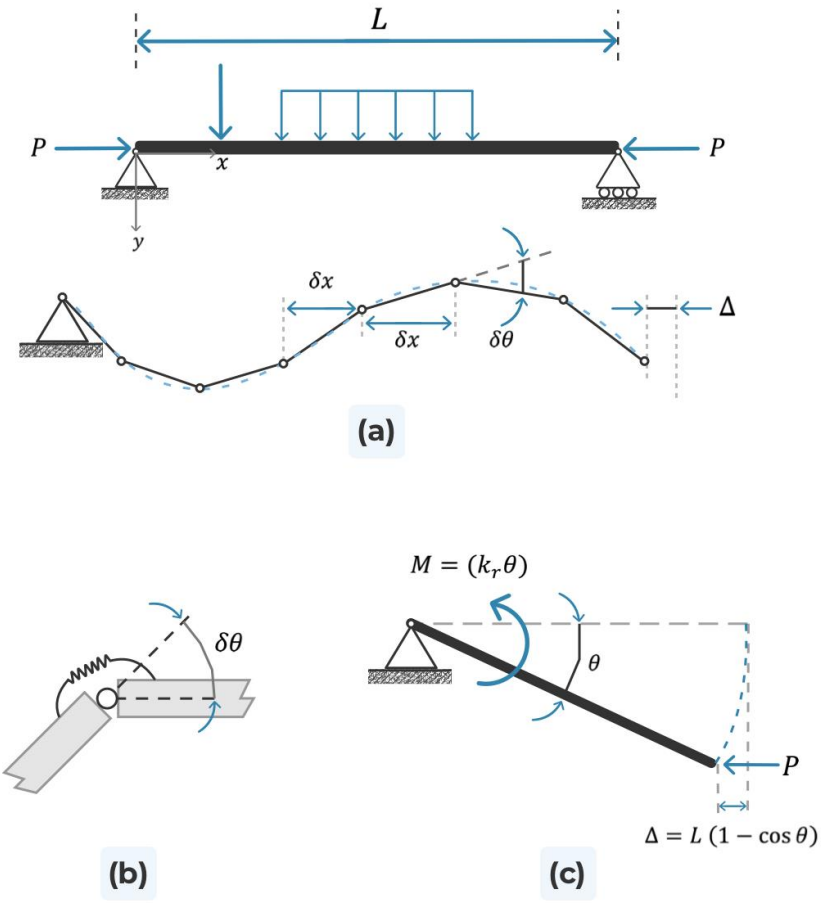

Figure 12: (a) Deflection of a simply supported beam-column modelled by discrete rigid elements with only a bending deformation. (b) Elastic rotational hinge. (c) Geometric nonlinearity.

2.3.2.2 External Work – Work done by an axial load

The external work T_p of Figure 12(c) is defined as:

$$W_{ex} = T_p = \sum \delta T_p = \sum_{i=1}^{n} P\Delta_i \qquad \text{Eq. 35}$$

Where Δ_i is the displacement of the load of segment i and can be found from geometry. Under the assumption of small displacements, $\cos(\theta) \approx 1 - \theta^2/2$, and thus the displacement of the load is:

$$\Delta = \delta x(1 - \cos(\theta)) = \delta x \left(1 - \left(1 - \frac{\theta^2}{2}\right)\right) = \delta x \frac{\theta^2}{2} \qquad \text{Eq. 36}$$

Hence, the external work can be expressed as:

$$W_{ex} = \sum \delta T_p = \sum_{i=1}^{n} P\Delta_i = \sum_{i=1}^{n} P\frac{\theta_i^2}{2}\delta x_i \qquad \text{Eq. 37}$$

For a continuous system, with $n \to \infty$, the total external work can be expressed in integral form as:

$$W_{ex} = \int \frac{P}{2}\,\theta^2\,dx = \frac{P}{2}\int \left(\frac{d}{dx}u(x)\right)^2 dx \qquad \text{Eq. 38}$$

2.3.2.3 Critical loads by the energy method

Many authors have used energy methods, such as the principle of minimum potential energy (PMPE), to obtain buckling loads of columns with a sudden change of stiffness [6]–[8]. Small lateral deflections need to be assumed when using the energy method. Such a deflection increases the strain energy, U_r, of the structure. Due to the deflection, the axial load P does work equal to the external work W_{ex} [20]. The structure is stable if the strain energy (U_r) is higher than the work done by the axial load (T_p); unstable if the strain energy (U_r) is lower than the work done by the axial load (T_p). The critical load is found when the structure changes from a stable to an unstable configuration, which occurs when the strain energy equals the work done by the axial load.

$$\begin{aligned} \text{STABLE} \quad & U_r > T_p \\ \text{UNSTABLE} \quad & U_r < T_p \\ \text{CRITICAL} \quad & U_r = T_p \end{aligned} \qquad \text{Eq. 39}$$

Exact solutions for the buckling loads are obtained using the energy method when the assumed deflection, $u(x)$, correctly satisfy the boundary conditions matching the actual deflection. Correctly assuming the deflection function for complicated systems becomes challenging when following the energy method, resulting in approximate solutions [20].

2.3.3 Numerical Approach: Finite Element Analysis

The Finite Element Method (FEM) is a numerical method that is the basis for the Finite Element Analysis (FEA). This method is a powerful tool and a favored technique for most fields of engineering. FEM is based on two fundamental concepts. The first concept is representing a continuous structure in a finite number of simple elements jointed at the nodes, known as discretization. Each node has a defined number of degrees of freedom (dof). The nodes of such elements are the primary unknowns and present themselves as displacements or stresses for structural analysis. Values between nodes are determined from polynomial interpolation. The second concept is based on obtaining the solution of differential equations by means of the weak method using numerical integration techniques. These two concepts reduce the differential equation of the complex system into a finite set of linear simultaneous equations, which can be solved through the application of matrix methods [21].

Although the FEM is powerful for analyzing complex systems, the discretization and the use of numerical methods involve errors, hence always providing approximate solutions. For simple systems, these errors can be minimized, resulting in solutions having a negligible error compared to analytical solutions [21].

Many papers have validated results obtained from proposed analytical methods for the buckling analysis of complex beams and beam-columns against those obtained through the FEM [2], [3]. For such reasons, results obtained through the proposed closed-form solution will be validated against those obtained through the FEM.

2.3.4 Discussion of current methods

All presented methods can be implemented for the analysis of beam-columns. The formulation of the proposed closed-form solution is based on the classical method. The main limitation of the latter is the number of equations required due to the unknown constants of integration. Structural elements consisting of N discontinuities require $4(N+1)$ equations that are obtained through the boundary and continuity conditions.

The relations derived for the internal and external work have been used for the analysis of structural elements. These serve as a basis for other energy methods, such as the method of real work, the method of virtual work, Castigliano's theorems, and the principle of minimum potential energy (PMPE) [22]. The main limitations in using energy methods are that the accuracy of results is dependent on being used on linear elastic structures that obey the law of superposition [23]. This may not be the case for beam-columns and columns in which the relation between applied loads and displacement are no longer linear.

The FEM is a robust method that has been used for the linear analysis of beams, columns, and beam-columns. This method provides approximate results which are dependent on the discretization of the system. The discretization may result in errors or a high computational cost when performing parametric studies using FEM.

2.4 Modelling Complexities of physical structures

Structures are idealized into simplified models to perform structural analysis. Springs are often used in such models to have a better representation of reality. The following subsection provides a brief description of the use of springs. Its influence for the buckling analysis has been proved to be crucial by M. L. Gambhir, who demonstrated that springs have an important effect on the buckling load by affecting the buckling mode [16]. Two main types of springs are considered to idealise structures: an extensional or normal spring, and a moment or rotational spring. The springs considered for the formulation of the closed-form solution are linear springs, which have a linear load-deformation relationship [16].

2.4.1 External Extensional Springs

External extensional springs can be considered at the boundary and continuity conditions of jointed EB beam-columns to model the points where transversal displacement is restricted to some degree due to the influence of lateral bracing, diaphragms, and stabilizers of drill strings, to name a few examples [20]. Linear extensional springs carry normal force only. The elongation Δ of such a linear elastic spring subjected to a force F is:

$$\Delta = \frac{F}{k_e} \qquad \text{Eq. 40}$$

Where k_e is the spring stiffness in units of force/deformation (F/Δ).

In the classical procedure, linear external translational springs between two consecutive segments, or at the boundaries, are accounted for when enforcing equilibrium of vertical forces, as seen in Figure 13.

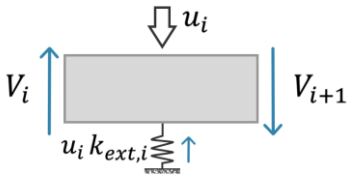

Figure 13: Diagram of vertical forces acting at the location of an external translational spring.

$$\Sigma F_y = 0$$

$$V_i + u_i\, k_{ext,i} = V_{i+1} \qquad \text{Eq. 41}$$

With V being the shear force of segment i and $i+1$, and u_i being the displacement of section i at the location of the extensional spring.

When using energy methods, the strain energy $U_{ext,spring}$ of a spring is:

$$U_{ext,spring} = \frac{1}{2} k_e\, (\Delta)^2 \qquad \text{Eq. 42}$$

2.4.2 Internal Extensional Springs

Internal extensional springs connecting two consecutive Euler-Bernoulli beam-column sections can be implemented to represent the real behavior of the joints connecting such members [2].

In the classical procedure, internal translational springs are accounted for when enforcing the continuity of displacements. The internal translational spring affects such continuity by deforming itself due to the shear force acting at the discontinuity location. Dividing the shear force of member i by the internal spring stiffness $k_{int,i}$ connecting two consecutive members provides the extra deformation required to ensure a continuity of displacements and is written as:

$$u_i + \frac{V_i}{k_{int,i}} = u_{i+1} \qquad \text{Eq. 43}$$

2.4.3 Rotational Springs

Many authors have used the discrete spring model to represent cracks along the beam-column, given its effectiveness. This modelling is performed by pinning together two beam-column sections and using a linear rotational spring to model the increase in flexibility due to the crack [3], [5], [14]. There exist various equations that define the stiffness of a rotational spring to model cracks. Such equations are dependent on the height of the cross-section as well as the depth of the crack, as proposed by Dimarogans et al. [24].

Linear rotational springs are idealized structures capable of resisting rotation but having no axial stiffness. The moment, M, is directly proportional to the angle of rotation θ for linear rotational springs [16]. Hence:

$$M = k_r\,\theta \qquad \text{Eq. 44}$$

With k_r being the rotational stiffness of the spring in units of force · deformation / radians (FL/rad).

In the classical procedure, the influence of rotational springs is accounted for when enforcing the continuity of slopes. Similar to the continuity of displacements, the moment present at the location of the rotational spring affects the slope. Dividing the moment of section i by the rotational spring stiffness $k_{rot,i}$ provides the change of slope due to the moments, and is written as:

$$\theta_i - \frac{M_i}{k_{rot,i}} = \theta_{i+1} \qquad \text{Eq. 45}$$

When using energy methods, the strain energy $U_{rot,spring}$ of a rotational spring is:

$$U_{rot,spring} = \frac{1}{2}\,k_r\,\theta^2 \qquad \text{Eq. 46}$$

2.5 Generalized Functions

Generalized functions have been defined mathematically in many ways, with the most popular definition proposed by Schwartz in his theory of distributions. Such "functions" have beneficial properties making them useful in different fields of engineering and science. One valuable property is their ability to make discontinuous functions into continuous ones [25]. The following section focuses on such property and introduces the Dirac delta function $\delta(x)$, and the Heaviside function $H(x)$.

2.5.1 Dirac delta function

The Dirac delta function $\delta(x)$ can be defined as zero for all values of x, except at $x = 0$, where at such location it has a value of infinity, as it is schematized in Figure 14. One condition that must be fulfilled is having the area under the spike equal to one. Hence it can be defined as [26]:

$$\delta(x) = \begin{cases} +\infty, & x = 0 \\ 0, & x \neq 0 \end{cases} \quad \text{Eq. 47}$$

Or as:

$$\delta(x - a) = \begin{cases} +\infty, & x = a \\ 0 & x \neq a \end{cases} \quad \text{Eq. 48}$$

while being constrained to satisfy:

$$\int_{-\infty}^{+\infty} \delta(x)\, dx = 1 \quad \text{Eq. 49}$$

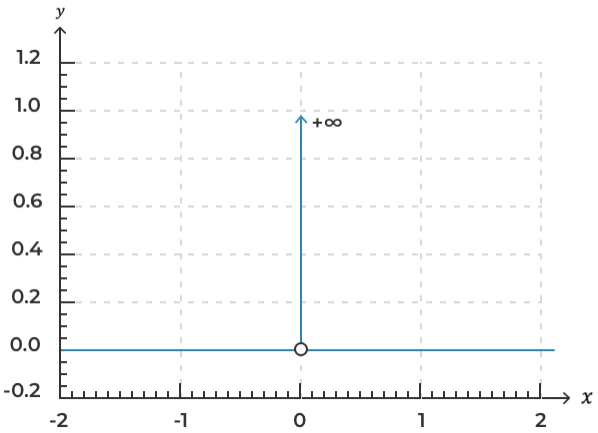

Figure 14: Schematic representation of the Dirac Delta function.

Such function has been successfully implemented in the buckling analysis of beam-columns with unilateral cracks using the flexibility model [3]. It has also been used when expressing the lateral loading function

$q(x)$ to account for a lateral point-force F_a acting at $x = a$. Thus, the lateral load is expressed as $q(x) = F_a\delta(x - a)$ [2].

2.5.2 Heaviside function

The Heaviside function is also known as the unit step function and is denoted as $\mathrm{H(x)}$ or $\theta(\mathrm{x})$. Following the half-maximum convention, the Heaviside function is defined as having a value of zero for negative arguments and a value of one for positive arguments. At an argument of zero, the Heaviside takes a value of $1/2$ [27] and can be visualized in Figure 15. Hence:

$$H(x) = \begin{cases} 0 & x < 0 \\ 0.5 & x = 0 \\ 1 & x > 0 \end{cases} \qquad \text{Eq. 50}$$

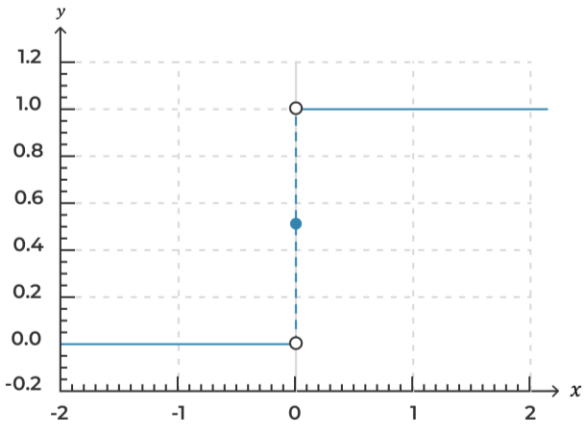

Figure 15: Heaviside function, using the half-maximum convention.

Such a function has been used to successfully express the deflection of a beam with step-changes of its stiffness [2], [3]. The Heaviside function will be implemented to represent the global deflections, slopes, moments, and shears as a single piecewise continuous equation.

2.6 Literature Takeaways

To the best of the knowledge of the author of this thesis, there is no analytical approach that considers the combination of lateral loads, non-propagating open cracks, and lateral restrictions in the buckling analysis of beam-columns with step-changes in their geometric and material properties, connected by flexible joints while having elastic boundaries. Most analytical or semi-analytical approaches in the literature review consider only the ideal column case with some complexities and approximate results.

The non-trivial equilibrium state approach provides exact solutions for the buckling analysis of structural elements with discontinuities. These appear due to the presence of springs or step-changes of flexural stiffness, and their influence is accounted for in the continuity conditions. The limitation of this approach is having to solve $4(N + 1)$ unknown constants of integration for the case of a beam-column, or obtaining the determinant of a $4(N + 1) \times 4(N + 1)$ for the case of a column.

The buckling analysis performed by different authors following the energy method [6]–[8] has provided approximate results for simple columns with step-changes of flexural stiffness. The main limitation of such a method is to accurately assume the deflection of the column. Any deflection that deviates from the actual deflection provides approximate results.

As FEM is a powerful numerical method, many authors validate their results against those obtained from FE software. However, performing parametric studies may become computational expensive or result in numerical instabilities due to the remeshing of the model.

The energy methods provide an upper bound, and their accuracy highly depends on the assumed deflection function. Moreover, although the FEM is such a powerful numerical method, it may be prone to numerical instabilities when analyzing complicated systems with a refined mesh. The ideal good practice would be to compare the results obtained through the FEM with analytical solutions. However, due to the complexity of systems and the limitations of analytical methods, it is usually not performed. It should be noted that although the FEM can perform buckling analysis for 1-D models, its computational cost can be high in the event of a parametric study.

For the design phase or a parametric study, the lack of analytical methods for the buckling analysis of complex column and beam-column models makes engineers rely on numerical methods with their own limitations. Generalized functions, precisely the Heaviside function, can express in a single equation the deflection, slope, moment, and shear of an EB structural element regardless of the number of discontinuities present. They have been successfully implemented in the analysis of models with some complexity. For such reason, expressing the buckling solution in terms of generalized functions can provide computational efficiency in exploring different designs or in the evaluation of pre-damaged structures. In combination with closed-form expressions, this efficiency reduces the number of unknown constants of integration to only four. This reduction results in only calculating the determinant of a 4×4 matrix.

Given the above and recognizing the potential for such a combination, the present thesis is focused on exploring the possibility of using the mentioned combination for the buckling analysis of columns and beam-columns.

Table 1: Comparison of the current methods for accounting for the influence of various complexities.

Influence of:	Classical method	PMPE	FEM
Step-changes of flexural stiffness	• Can obtain exact solutions • Each segment introduces 4 unknown integration constants	• Exact solution if assumed deflection matches real deflection • Difficult to assume correct deflection because of different stiffnesses	• Exact solution can be obtained • Depends on discretization
Springs	• Can obtain exact solutions • Accounted for when enforcing continuity conditions	• Accounted in the energy stored in the springs • Difficult to assume correct deflection because of springs	• Exact solution can be obtained • Depends on discretization
Elastic boundary conditions	• Accounted for when enforcing the boundary conditions	• Can be accounted in the energy stored in the boundary springs	• Exact solution can be obtained

3 Closed-form solutions for the buckling analysis of Euler-Bernoulli beam-columns and columns

The following section presents the derivation of the closed-form solution for the buckling analysis of Euler-Bernoulli beam-columns of different complexities. This section aims to formulate and offer the general closed-form solution for the main analytical model, presented in Figure 3. This formulation is performed in a stepwise approach, starting with the general procedure given in subsection 3.1. The following subsection offers the closed-form solution for an ideal beam-column with ideal boundary conditions and joints, as seen in Figure 17. Afterwards, the introduction of elastic boundary conditions to such a model, as seen in Figure 19 in subsection 3.3, is discussed. Subsection 3.4 presents the formulation of the general solution for a beam-column with elastic joints in the form of along-the-axis internal transversal springs, as seen in Figure 20. External transversal and internal rotational springs between two consecutive segments are presented in subsections 3.5 and 3.6, respectively. Finally, the closed-form solution for the buckling analysis of the model of the highest complexity, as seen in Figure 26, is presented in subsection 3.7.

3.1 Solution procedure for the derivation of the closed-form solution for the buckling analysis of complex beam-columns and columns

The procedure for finding the closed-form solution is based on normalizing Eq. 12 with respect to the length L and is expressed as:

$$\frac{d^4}{d\xi^4}\tilde{u}(\xi) + \tilde{v}^2\frac{d^2}{d\xi^2}\tilde{u}(\xi) = \frac{\tilde{q}(\xi)}{EI} \qquad \text{Eq. 51}$$

Eq. 51 is dependent on the normalized abscissa $\xi = x/L$, which ranges from 0 to 1. The normalized quantities in Eq. 51 are as follow:

$$\tilde{u}(\xi) = \frac{u(\xi\, L)}{L} \qquad \text{Eq. 52}$$

$$\tilde{v}^2 = \frac{P\, L^2}{EI} \qquad \text{Eq. 53}$$

$$\tilde{q}(\xi) = q(\xi L)L^3 \qquad \text{Eq. 54}$$

For a beam-column with step-changes of its flexural stiffness, the solution of the normalized differential equation, Eq. 51, is implemented to each section with its local normalized coordinate ξ_i, transforming Eq. 51 into:

$$\frac{d^4}{d\xi^4}\tilde{u}_i(\xi_i) + \tilde{v}^2\frac{d^2}{d\xi^2}\tilde{u}_i(\xi_i) = \frac{\tilde{q}_i(\xi)}{EI_i} \qquad \text{Eq. 55}$$

With $0 \le \xi_i \le \tilde{L}_i$, $\tilde{L}_i = \frac{L_i}{L}$, and $\tilde{v}_i^2 = \frac{P\,L^2}{EI_i}$. Figure 16 represents the normalized counterpart of the highest-complex model, which will be analyzed.

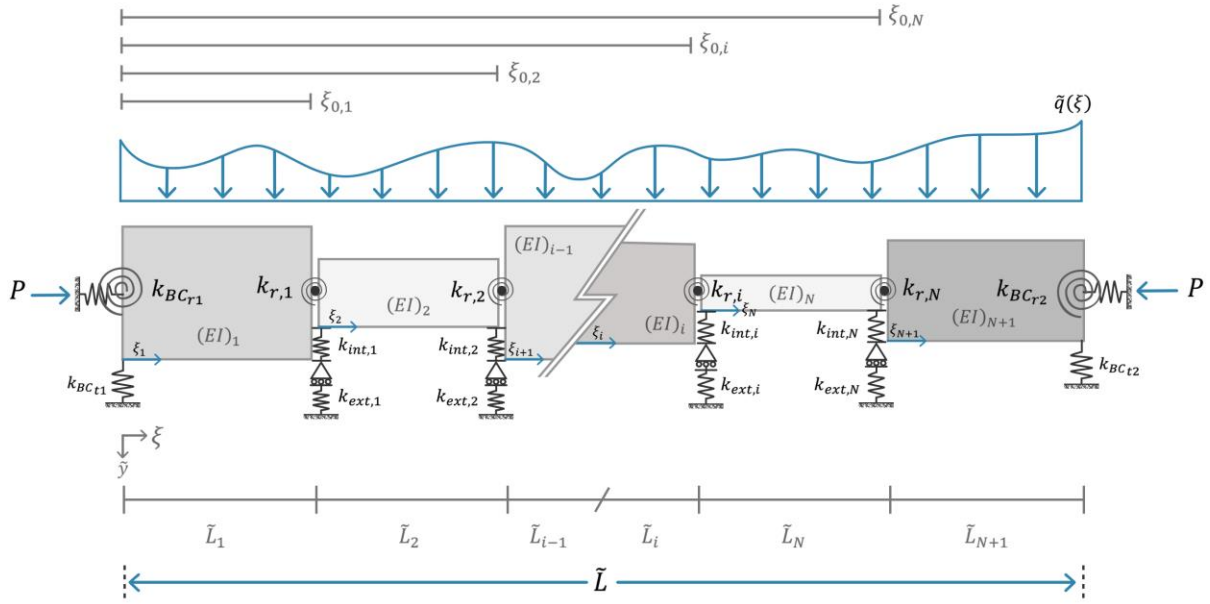

Figure 16: Normalized counterpart of the model of highest complexity to be analyzed, consisting of N discontinuities due to step-changes of flexural stiffness, or the presence of springs. Each section has a constant flexural stiffness EI_i and is described in terms of a local dimensionless axis, ξ_i.

The term $\xi_{0,i}$ represents the location of a discontinuity due to a step-change in flexural stiffness or the presence of a spring. It is expressed in terms of the global abscissa ξ_G. The Heaviside function is implemented to express a single piecewise continuous function using the local functions of each segment. The global deflection of the beam-column is defined as:

$$U(\xi_G) = \tilde{u}_1(\xi_1) + \sum_{i=2}^{N+1}\left[\tilde{u}_i(\xi_i) - \tilde{u}_{i-1}(\xi_{i-1})\right] H\left(\xi_G - \xi_{0,i-1}\right) \qquad \text{Eq. 56}$$

Similarly to Eq. 56, the slope, moment, and shear of the beam-column are expressed as:

$$\Theta(\xi_G) = \tilde{\theta}_1(\xi_1) + \sum_{i=2}^{N+1}\left[\tilde{\theta}_i(\xi_i) - \tilde{\theta}_{i-1}(\xi_{i-1})\right] H\left(\xi_G - \xi_{0,i-1}\right) \qquad \text{Eq. 57}$$

$$\mathrm{M}(\xi_G) = \widetilde{M}_1(\xi_1) + \sum_{i=2}^{N+1} \left[\widetilde{M}_i(\xi_i) - \widetilde{M}_{i-1}(\xi_{i-1})\right] H\left(\xi_G - \xi_{0,i-1}\right) \quad \text{Eq. 58}$$

$$T(\xi_G) = \tilde{V}_1(\xi_1) + \sum_{i=2}^{N+1} [\tilde{V}_i(\xi_i) - \tilde{V}_{i-1}(\xi_{i-1})] H\left(\xi_G - \xi_{0,i-1}\right) \quad \text{Eq. 59}$$

The relationship between the global normalized coordinate (ξ_G) and local coordinate (ξ_i) is:

$$\xi_i = \xi_G - \sum_{j=1}^{i-1} L_j$$

A beam-column with N discontinuities due to step-changes of flexural stiffness, or the presence of springs, would consist of $N+1$ segments. These discontinuities lead to each section introduce four unknown integration constants, making it necessary to obtain the determinant of a $4(N+1) \times 4(N+1)$ system of equations to obtain the buckling equation for a column, or solving for $4(N+1)$ integration constants for a beam-column, and thus getting the critical buckling loads. To reduce the number of $4(N+1)$ unknown integration constants and therefore the number of required conditions, the relation between the integration constant of two successive beam-column elements are found by imposing the continuity conditions. For the normalized case, the continuity conditions are imposed at $\xi_i = \tilde{L}_i$ and at $\xi_{i+1} = 0$, with subscript i used to represent segment i, and consists of enforcing continuity of displacement (u), slope (θ), moment (M), and shear (V).

When enforcing the continuity conditions, it is essential to remain dimensionally consistent. Normalizing the displacement with respect to the length makes the displacement function and its derivatives dimensionless. The local displacement and slope have the form of:

$$\tilde{u}_i(\xi_i) = A_i + B_i\,\xi_i + C_i\left(\frac{1}{\tilde{v}_i^2} - \frac{\cos(\tilde{v}_i\,\xi_i)}{\tilde{v}_i^2}\right) + D_i\left(\frac{\xi_i}{\tilde{v}_i^2} - \frac{\sin(\tilde{v}_i\,\xi_i)}{\tilde{v}_i^3}\right) + \cdots$$

$$\cdots + \frac{\int_0^{\xi_i}(\tilde{q}_i(\tau)\sin(\tilde{v}_i\,\tau)\cos(\tilde{v}_i\,\xi_i) - \tilde{q}_i(\tau)\cos(\tilde{v}_i\,\tau)\sin(\tilde{v}_i\,\xi_i))\,d\tau}{EI_i\,\tilde{v}_i^3} - \cdots \quad \text{Eq. 60}$$

$$\cdots - \frac{\int_0^{\xi_i}(-\tilde{q}_i(\tau)\,\xi_i + \tilde{q}_i(\tau)\,\tau)\,d\tau}{EI_i\,\tilde{v}_i^2}$$

$$\tilde{\theta}_i(\xi_i) = B_i + \frac{C_i \sin(\tilde{v}_i\,\xi_i)}{\tilde{v}_i} + D_i\left(\frac{1}{\tilde{v}_i^2} - \frac{\cos(\tilde{v}_i\,\xi_i)}{\tilde{v}_i^2}\right) + \frac{\int_0^{\xi_i} \tilde{q}_i(\tau)\,d\tau}{EI_i\ \tilde{v}_i^2} + \cdots$$

$$\cdots - \frac{\int_0^{\xi_i}(\tilde{q}_i(\tau)\sin(\tilde{v}_i\,\tau)\sin(\tilde{v}_i\,\xi_i) + \tilde{q}_i(\tau)\cos(\tilde{v}_i\,\tau)\cos(\tilde{v}_i\,\xi_i))\,d\tau}{EI_i\ \tilde{v}_i^2} \qquad \text{Eq. 61}$$

Both $\tilde{u}_i(\xi_i)$ and $\tilde{\theta}_i(\xi_i)$ are dimensionless. On the other hand, the moment and shear have units of $Force \cdot Length^2$ given that the second and third derivatives of the dimensionless displacement function are multiplied by Young's Modulus (E) and the second moment of inertia (I) of their respective segment. The moment and shear of segment i have the form of:

$$M_i(\xi_i) = -C_i\,EI_i\cos(\tilde{v}_i\,\xi_i) - \frac{D_i\,EI_i\sin(\tilde{v}_i\,\xi_i)}{\tilde{v}_i} + \cdots$$

$$\cdots - \frac{\int_0^{\xi_i}(-\tilde{q}_i(\tau)\sin(\tilde{v}_i\,\tau)\ \cos(\tilde{v}_i\,\xi_i) + \tilde{q}_i(\tau)\cos(\tilde{v}_i\,\tau)\ \sin(\tilde{v}_i\,\xi_i))\,d\tau}{\tilde{v}_i} \qquad \text{Eq. 62}$$

$$V_i(\xi_i) = -EI_i\left(\tilde{v}_i^2\,B_i + D_i\right) - \int_0^{\xi_i} \tilde{q}_i(\tau)\,d\tau \qquad \text{Eq. 63}$$

Finding the relation between two successive beam-column segments reduces the number of unknown integration constants to only four, which are solved by imposing the four boundary conditions. The procedure of relating the integration constants has been successfully implemented by F. Giunta on the analysis of jointed Euler-Bernoulli beams with step changes in material and cross-section under static and dynamic loads [2].

The normalized equations for the local displacement, slope, moment, and shear for a column are:

$$\tilde{u}_i(\xi_i) = A_i + B_i\,\xi_i + C_i\left(\frac{1}{\tilde{v}_i^2} - \frac{\cos(\tilde{v}_i\,\xi_i)}{\tilde{v}_i^2}\right) + D_i\left(\frac{\xi_i}{\tilde{v}_i^2} - \frac{\sin(\tilde{v}_i\,\xi_i)}{\tilde{v}_i^3}\right) \qquad \text{Eq. 64}$$

$$\tilde{\theta}_i(\xi_i) = B_i + \frac{C_i \sin(\tilde{v}_i\,\xi_i)}{\tilde{v}_i} + D_i\left(\frac{1}{\tilde{v}_i^2} - \frac{\cos(\tilde{v}_i\,\xi_i)}{\tilde{v}_i^2}\right) \qquad \text{Eq. 65}$$

$$M_i(\xi_i) = -C_i\,EI_i\cos(\tilde{v}_i\,\xi_i) - \frac{D_i\,EI_i\sin(\tilde{v}_i\,\xi_i)}{\tilde{v}_i} \qquad \text{Eq. 66}$$

$$V_i(\xi_i) = -EI_i\,\tilde{v}_i^2\,B_i - EI_i\,D_i$$ Eq. 67

For the buckling analysis of a column, as explained in Section 2.3.1.1, the next step is to obtain the buckling equation by computing the determinant of the system of four equations. As explained in 2.3.1.2, the next step is to solve the four unknown integration constants for the buckling analysis of a beam-column. In either case, it is necessary to express all variables that account for the step changes in flexural stiffness $(\tilde{v}_i)$ in terms of a stiffness of reference. This thesis takes the stiffness of the first segment as a reference for calculating the critical load P_{cr}. This is done by substituting:

$$\tilde{v}_1 = \sqrt{\frac{P\,L^2}{EI_1}} = \alpha$$ Eq. 68

$$\tilde{v}_i = \frac{\sqrt{\frac{P\,L^2}{EI_i}}}{\sqrt{\frac{P\,L^2}{EI_1}}} \cdot \alpha$$ Eq. 69

After the substitution, the buckling equation is dependent on the variable α, which will be referred to as the critical variable. The roots of such an equation are associated with the buckling loads. Hence, at the roots, the critical buckling load can be found and is expressed as:

$$P_{cr} = \frac{\alpha_{root}^2\,EI_1}{L^2}$$ Eq. 70

3.2 Formulation of a closed-form expression for the buckling analysis of ideal Euler-Bernoulli beam-column

Let us consider an EB beam-column consisting of N discontinuities of flexural stiffness resulting on $N+1$ sections of uniform stiffness, as seen in Figure 17.

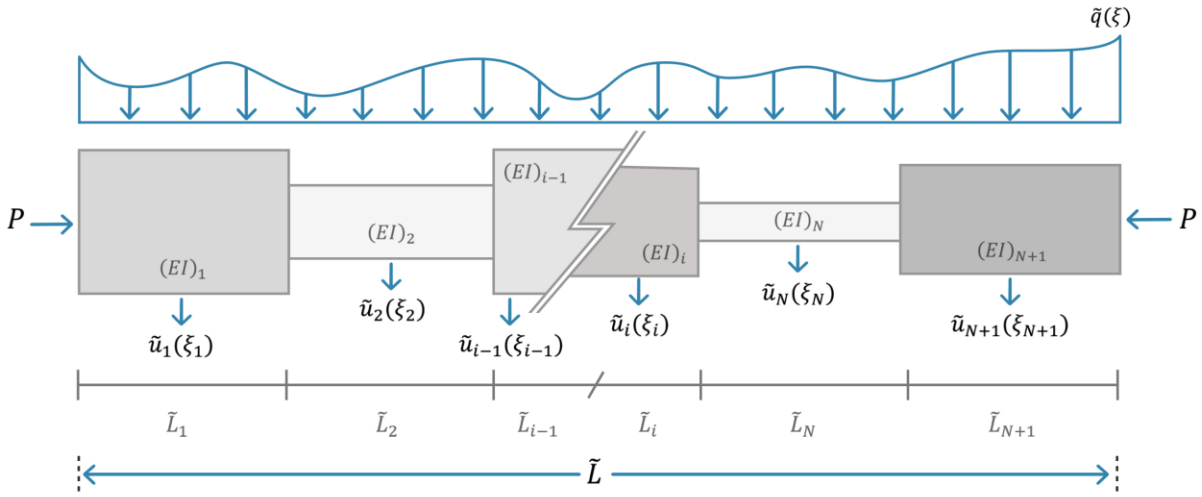

Figure 17: Normalized ideally jointed EB beam-column with step changes in flexural stiffness and ideal boundary conditions subjected to lateral and axial load.

As described in Section 3.1, the number of unknown constants of integration is reduced to only four unknowns. This is done by relating constants of integration between two successive segments by imposing continuity conditions. The continuity conditions are enforced at $\xi_i = \tilde{L}_i$ and at $\xi_{i+1} = 0$, with the continuity conditions being:

$$\tilde{u}_i(\tilde{L}_i) = \tilde{u}_{i+1}(0) \qquad \text{Eq. 71}$$

$$\tilde{\theta}_i(\tilde{L}_i) = \tilde{\theta}_{i+1}(0) \qquad \text{Eq. 72}$$

$$\tilde{M}_i(\tilde{L}_i) = \tilde{M}_{i+1}(0) \qquad \text{Eq. 73}$$

$$\tilde{V}_i(\tilde{L}_i) = \tilde{V}_{i+1}(0) \qquad \text{Eq. 74}$$

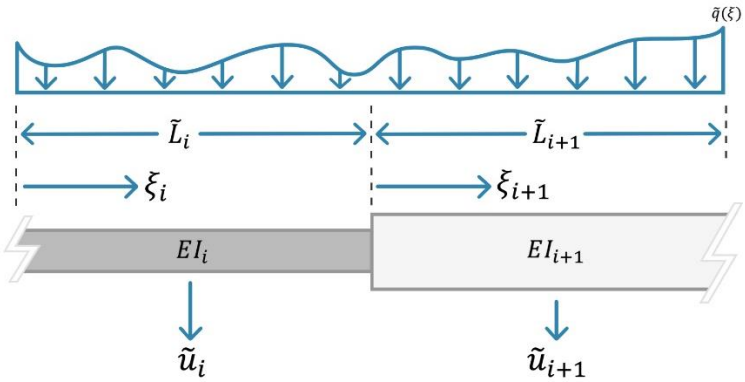

Figure 18: Two normalized ideally jointed consecutive segments where continuity of deflection, slope, moment, and shear needs to be enforced.

For ease of notation, dimensionless quantities, β_i, are introduced to describe the relationships between the flexural rigidities of two successive segments:

$$\beta_i = \frac{EI_i}{EI_{i+1}} \qquad \text{Eq. 75}$$

The relation between two successive constants of integration is:

$$A_{i+1} = A_i + B_i\, L_i + \left(\frac{1}{\tilde{v}_i^2} - \frac{\cos(\tilde{v}_i\, L_i)}{\tilde{v}_i^2}\right) C_i + \left(\frac{L_i}{\tilde{v}_i^2} - \frac{\sin(\tilde{v}_i\, L_i)}{\tilde{v}_i^3}\right) D_i + \cdots$$
$$\cdots + \frac{\int_0^{\tilde{L}_i} (\tilde{q}_i(\tau)\sin(\tilde{v}_i\,\tau)\cos(\tilde{v}_i\, L_i) - \tilde{q}_i(\tau)\cos(\tilde{v}_i\,\tau)\sin(\tilde{v}_i\, L_i))\, d\tau}{EI_i\, \tilde{v}_i^3} - \cdots \qquad \text{Eq. 76}$$
$$\cdots + \frac{\int_0^{\tilde{L}_i} \left(\tilde{q}_i(\tau)\, \tilde{L}_i - \tilde{q}_i(\tau)\, \tau\right) d\tau}{EI_i\, \tilde{v}_i^2}$$

$$B_{i+1} = B_i + \frac{C_i \sin(\tilde{v}_i\, L_i)}{\tilde{v}_i} + \left(\frac{1}{v_i^2} - \frac{\cos(\tilde{v}_i\, L_i)}{\tilde{v}_i^2}\right) D_i + \frac{\int_0^{\tilde{L}_i} \tilde{q}(\tau)\, d\tau}{EI_i\, \tilde{v}_i^2} + \cdots$$
$$\cdots - \frac{\int_0^{\tilde{L}_i} (\tilde{q}(\tau)\sin(\tilde{v}_i\,\tau)\ \sin(\tilde{v}_i\, L_i) + \tilde{q}_i(\tau)\cos(\tilde{v}_i\,\tau)\ \cos(\tilde{v}_i\, L_i))\, d\tau}{EI_i\, \tilde{v}_i^2} \qquad \text{Eq. 77}$$

$$C_{i+1} = C_i\, \beta_i \cos(\tilde{v}_i\, L_i) + \frac{D_i\, \beta_i \sin(\tilde{v}_i\, L_i)}{\tilde{v}_i} + \cdots$$
$$\cdots + \frac{\int_0^{\tilde{L}_i} \left(-\tilde{q}_i(\tau)\sin(\tilde{v}_i\,\tau)\ \cos\left(\tilde{v}_i\, \tilde{L}_i\right) + \tilde{q}_i(\tau)\cos\left(\tilde{v}_{\mathrm{i}}\, \tilde{L}_{\mathrm{i}}\right)\sin\left(\tilde{v}_i\, \tilde{L}_i\right)\right) d\tau}{\tilde{v}_{\mathrm{i}}\, EI_{i+1}} \qquad \text{Eq. 78}$$

$$D_{i+1} = B_i\, \tilde{v}_i^2\, \beta_i + D_i\, \beta_i - B_{i+1}\, \tilde{v}_{i+1}^2 + \int_0^{\tilde{L}_i} \frac{\tilde{q}_i(\tau)\, d\tau}{EI_{i+1}} \qquad \text{Eq. 79}$$

Using the derived relation between constants of integration (Eq. 76 –Eq. 79) in the global equations of deflection, slope, moment, and shear functions (Eq. 56 – Eq. 59) reduces the system of equations being expressed to only four unknown integration constants, which are solved through the boundary conditions.

3.3 Introduction of elastic boundary conditions to the closed-form solution for the buckling analysis of ideally jointed Euler-Bernoulli beam-column

Let us consider an EB beam-column consisting of N discontinuities of flexural stiffness resulting on $N+1$ sections of uniform stiffness subjected to elastic boundaries, as seen in Figure 19.

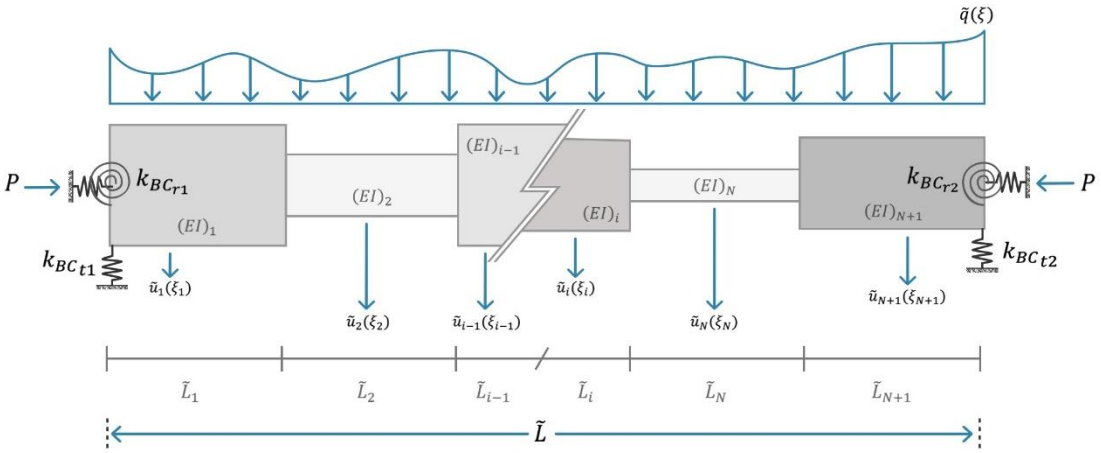

Figure 19: Normalized ideally jointed EB beam-column with step changes in flexural stiffness and elastic boundary conditions subjected to lateral and axial load.

The elastic boundaries are accounted for in the four necessary equations to solve the four unknown constants of integration. The four equations are dependent on the equilibrium of moments and vertical forces, hence the equations at the boundaries ($\xi_G = 0$ and at $\xi_G = \tilde{L}$) are:

$$T(0) = U(0) \cdot k_{BC_{t1}} \cdot L^3 \qquad \text{Eq. 80}$$

$$\mathrm{M}(0) = -\Theta(0) \cdot k_{BC_{r1}} \cdot L \qquad \text{Eq. 81}$$

$$T(L) = -U\left(\tilde{L}\right) \cdot k_{BC_{t2}} \cdot L^3 \qquad \text{Eq. 82}$$

$$\mathrm{M}(L) = \Theta\left(\tilde{L}\right) \cdot k_{BC_{r2}} \cdot L \qquad \text{Eq. 83}$$

The terms of L^3 and L are added to Eq. 80 – Eq. 83 to remain dimensionally consistent, given that the units of the translational and rotational springs are of $Force/Length$ and $(Force \cdot Length)/Rad$, respectively.

3.4 Introduction of internal translational springs to the closed-form solution for the buckling analysis of elastic jointed Euler-Bernoulli beam-columns

Let us consider an EB beam-column consisting of N discontinuities due to step-changes of flexural stiffness and the presence of internal springs resulting on $N+1$ sections of uniform stiffness, as seen in Figure 20.

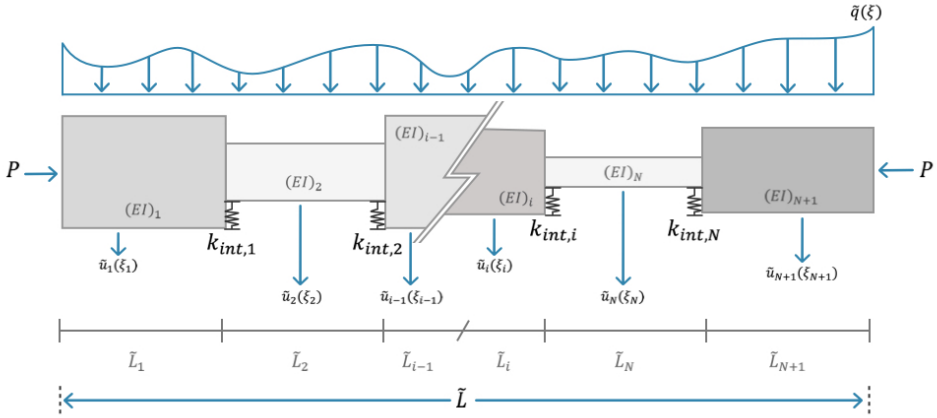

Figure 20: Normalized ideally jointed EB beam-column with N step-changes of flexural stiffness and N along-the-axis internal translational springs while being subjected to a lateral load $\tilde{q}(\xi)$ and axial load P.

Following the same procedure, as described in section 3.1, it is possible to account for internal springs by relating constants of integration between two successive segments. As described in the procedure, the influence of internal springs is accounted for at the continuity conditions, as seen in Figure 21.

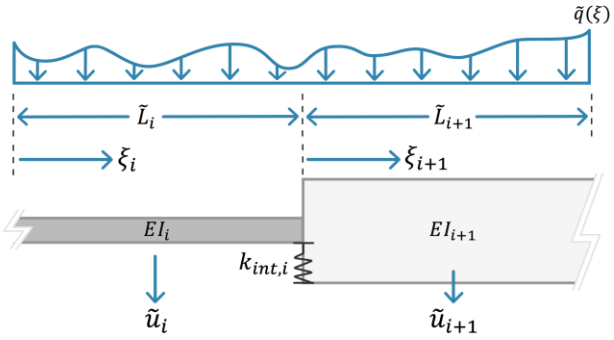

Figure 21: Continuity condition between two dimensionless successive beam-column segments with an internal translational spring at discontinuity i.

At the location of $\xi_i = \tilde{L}_i$ and at $\xi_{i+1} = 0$, the continuity of deflections, slopes, moments, and shears are enforced.

$$\tilde{u}_i(\tilde{L}_i) + \frac{\tilde{V}_i(\tilde{L}_i) \cdot \eta_{int,i}}{k_{int,i}\, L^3} = \tilde{u}_{i+1}(0) \qquad \text{Eq. 84}$$

$$\tilde{\theta}_i(\tilde{L}_i) = \tilde{\theta}_{i+1}(0) \qquad \text{Eq. 85}$$

$$\tilde{M}_i(\tilde{L}_i) = \tilde{M}_{i+1}(0) \qquad \text{Eq. 86}$$

$$\tilde{V}_i(\tilde{L}_i) = \tilde{V}_{i+1}(0) \qquad \text{Eq. 87}$$

Internal springs are accounted for on the continuity of displacements by dividing the shear of segment i by the internal spring stiffness at such a location. The term of L^3 is introduced in Eq. 84 to remain dimensionally consistent. Moreover, the term $\eta_{int,i}$ receives a value of zero when no internal spring is present and one when an internal spring is present. It is introduced to indicate when a spring is present between two segments. Given that the influence of internal springs only affects the continuity of displacements (Eq. 84), the derived relation between constants of integration for the ideal case on section 3.2 remains the same for B_{i+1}, C_{i+1}, D_{i+1} (Eq. 77 – Eq. 79). The only term that changes is A_{i+1} and is equal to:

$$A_{i+1} = A_i + \left(\tilde{L}_i - \frac{\tilde{v}_i^2\, EI_i\, \eta_{int,i}}{k_{int,i}\, L^3}\right) B_i + \left(\frac{1}{\tilde{v}_i^2} - \frac{\cos(\tilde{v}_i\, \tilde{L}_i)}{\tilde{v}_i^2}\right) C_i + \left(\frac{\tilde{L}_i}{\tilde{v}_i^2} - \frac{\sin(\tilde{v}_i\, \tilde{L}_i)}{\tilde{v}_i^3} - \frac{EI_i\, \eta_{int,i}}{k_{int,i}\, L^3}\right) D_i - \cdots$$

$$\cdots - \frac{\eta_{int,i} \int_0^{\tilde{L}_i} \tilde{q}_i(\tau)\, d\tau}{k_{int,i}\, L^3} + \frac{\int_0^{\tilde{L}_i} \left(\tilde{q}_i(\tau)\, \tilde{L}_i - \tilde{q}_i(\tau)\, \tau\right) d\tau}{\tilde{v}_i^2\, EI_i} + \cdots \qquad \text{Eq. 88}$$

$$\cdots + \frac{\int_0^{\tilde{L}_i} \left(\tilde{q}_i(\tau) \sin(\tilde{v}_i\, \tau) \cos(\tilde{v}_i\, \tilde{L}_i) - \tilde{q}_i(\tau) \cos(\tilde{v}_i\, \tau) \sin(\tilde{v}_i\, \tilde{L}_i)\right) d\tau}{\tilde{v}_i^3\, EI_i} - \cdots$$

Using the newly derived relation between constants of integration between two consecutive segments, the buckling analysis of elastic jointed EB beam-columns with N step-changes of flexural stiffness can be performed depending only on the four boundary conditions.

3.5 Introduction of external translational springs to the closed-form solution for the buckling analysis of ideally jointed Euler-Bernoulli beam-column

Let us consider an EB beam-column consisting of N discontinuities due to step-changes of flexural stiffness and the presence of external springs resulting on $N + 1$ sections of uniform stiffness, as seen in Figure 22.

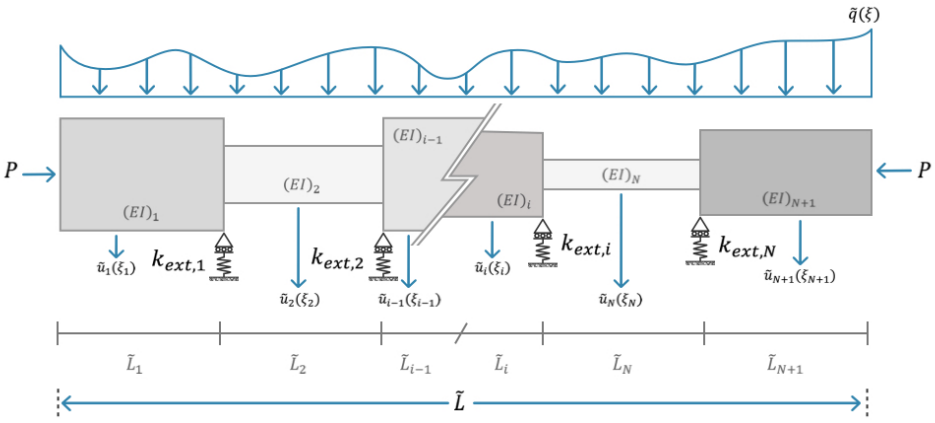

Figure 22: Normalized ideally jointed EB beam-column with N step-changes of flexural stiffness and N along-the-axis external translational springs while being subjected to a lateral $\tilde{q}(\xi)$ and axial load P.

External springs are accounted for when enforcing the continuity of vertical forces. As in previous sections, the continuity conditions are enforced at $\xi_i = \tilde{L}_i$ and at $\xi_{i+1} = 0$ as seen in Figure 23.

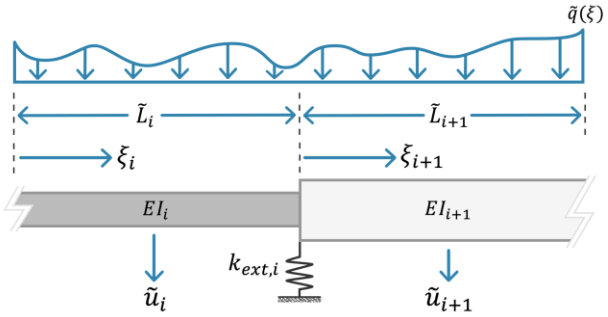

Figure 23: Continuity condition between two normalized successive beam-column segments with an external translational spring at discontinuity i.

To avoid coupling problems when both internal and external springs act on the same discontinuity for future models, the external spring is considered acting on segment $i+1$, given that the internal spring was associated with the shear of segment i in section 3.4. This results in the continuity of shears being:

$$\tilde{V}_i + \tilde{u}_{i+1} \cdot k_{ext,i} \cdot L^3 \cdot \eta_{ext,i} = \tilde{V}_{i+1} \qquad \text{Eq. 89}$$

The term of L^3 is introduced to remain dimensionally consistent. The term $\eta_{ext,i}$ receives the value of zero when no external spring is present and one when it is present. This term is used to indicate the presence of a spring between consecutive segments. This continuity condition only affects the relation of constants of integration for term D_{i+1} with A_{i+1}, B_{i+1}, and C_{i+1} remaining the same as in Eq. 76 – Eq. 78. The continuity of displacement, slope, and moment are the same as in the ideal case (Eq. 71 – Eq. 73) and are in the form of:

$$\tilde{u}_i(\tilde{L}_i) = \tilde{u}_{i+1}(0) \qquad \text{Eq. 90}$$

$$\tilde{\theta}_i(\tilde{L}_i) = \tilde{\theta}_{i+1}(0) \qquad \text{Eq. 91}$$

$$\tilde{M}_i(\tilde{L}_i) = \tilde{M}_{i+1}(0) \qquad \text{Eq. 92}$$

The newly derived relation for D_{i+1} is equal to:

$$D_{i+1} = -\frac{A_{i+1}\, L^3\, k_{ext,i}\, \eta_{ext,i}}{EI_{i+1}} + B_i \tilde{v}_i^2\, \beta_i + D_i \beta_i - B_{i+1} \tilde{v}_{i+1}^2 + \int_0^{\tilde{L}_i} \frac{\tilde{q}_i(\tau)\, d\tau}{EI_{i+1}} \qquad \text{Eq. 93}$$

This newly derived relation successfully accounts for the influence of external springs in ideally connected EB beam-columns with step-changes of flexural stiffness. Implementing such relation on the global equations Eq. 56 – Eq. 59, along with enforcing the boundary conditions, results in having a system of four equations expressed in terms of only four unknown constants of integration.

3.6 Introduction of rotational springs to the closed-form solution for the buckling analysis of an ideally jointed Euler-Bernoulli beam-column

Let us consider an EB beam-column consisting of N discontinuities due to step-changes of flexural stiffness and the presence of rotational springs resulting on $N+1$ sections of uniform stiffness, as seen in Figure 24.

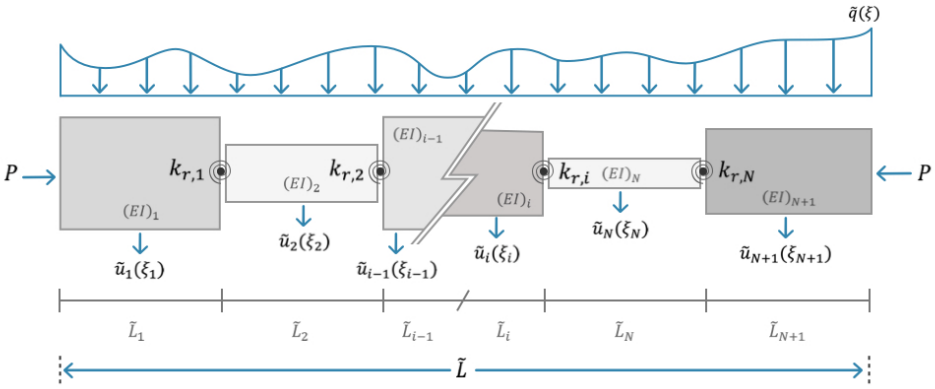

Figure 24: Normalized ideally jointed EB beam-column with N step-changes of flexural stiffness and N rotational springs while being subjected to a lateral $\tilde{q}(\xi)$ and axial load P.

As in previous sections, the influence of rotational springs is accounted for when enforcing the continuity conditions. The presence of rotational springs affects the continuity of slopes when trying to relate the constants of integration between two consecutive segments at $\xi_i = \tilde{L}_i$ and at $\xi_{i+1} = 0$, as seen in Figure 25.

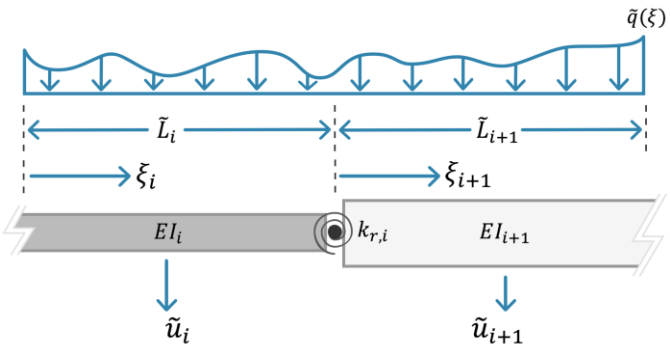

Figure 25: Continuity condition between two normalized successive beam-column segments with a rotational spring at discontinuity i.

The continuity of displacement, moment, and shear remains the same as in Eq. 71, Eq. 73, and Eq. 74. The continuity of slopes is:

$$\tilde{\theta}_i(\tilde{L}_i) - \frac{\tilde{M}_i(\tilde{L}_i) \cdot \eta_{rot,i}}{k_{rot,i}\, L} = \tilde{\theta}_{i+1}(0) \qquad \text{Eq. 94}$$

With L being introduced to remain dimensionally consistent. The term of $\eta_{rot,i}$ receives the value of zero when no rotational spring is present and a value of one when it is. This term accounts for the absence or presence of rotational springs between two consecutive segments. Such a continuity condition only affects the term B_{i+1}, leaving the remaining terms A_{i+1}, C_{i+1}, and D_{i+1} equal to Eq. 76, Eq. 78, and Eq. 79 from the ideal case in section 3.2.

$$\tilde{u}_i(\tilde{L}_i) = \tilde{u}_{i+1}(0) \qquad \text{Eq. 95}$$

$$\tilde{M}_i(\tilde{L}_i) = \tilde{M}_{i+1}(0) \qquad \text{Eq. 96}$$

$$\tilde{V}_i(\tilde{L}_i) = \tilde{V}_{i+1}(0) \qquad \text{Eq. 97}$$

The new relation of B_{i+1} is:

$$B_{i+1} = B_i + C_i\left(\frac{EI_i \cos(\tilde{v}_i\tilde{L}_i)\ \eta_{rot,i}}{k_{rot,i}\, L} + \frac{\sin(\tilde{v}_i\tilde{L}_i)}{\tilde{v}_i}\right) + \cdots$$

$$\cdots + D_i\left(\frac{EI_i \sin(\tilde{v}_i\tilde{L}_i)\ \eta_{rot,i}}{\tilde{v}_i\, k_{rot,i}\, L} - \frac{\cos(\tilde{v}_i\tilde{L}_i)}{\tilde{v}_i^2} + \frac{1}{\tilde{v}_i^2}\right) + \frac{\int_0^{\tilde{L}_i} \tilde{q}_i(\tau)\, d\tau}{\tilde{v}_i^2\, EI_i} + \cdots \qquad \text{Eq. 98}$$

$$\cdots + \frac{\eta_{rot,i} \int_0^{\tilde{L}_i} \left(-\tilde{q}_i(\tau) \sin(\tilde{v}_i\, \tau)\ \cos\left(\tilde{v}_i\, \tilde{L}_i\right) + \tilde{q}_i(\tau) \cos(\tilde{v}_i\, \tau)\ \sin\left(\tilde{v}_i\, \tilde{L}_i\right)\right) d\tau}{\tilde{v}_i\, k_{rot,i}\, L} + \cdots$$

$$\cdots - \frac{\int_0^{\tilde{L}_i} \left(\tilde{q}_i(\tau) \sin(\tilde{v}\, \tau) \sin\left(\tilde{v}\, \tilde{L}_i\right) + \tilde{q}_i(\tau) \cos(\tilde{v}_i\, \tau) \cos\left(\tilde{v}\, \tilde{L}_i\right)\right) d\tau}{\tilde{v}_i^2\, EI_i}$$

When implementing the newly developed relation into the global equations, it is possible to reduce such equation to only having four unknown constants of integration. Applying four boundary conditions provides the necessary system of four equations to solve the four unknown integration constants.

3.7 Closed-form solution for the buckling analysis of EB beam-column subjected to step-changes of flexural stiffness, external and internal translational springs, as well as rotational springs

Let us consider an EB beam-column consisting of N locations where complexities in the form of internal translational, external translational, and rotational springs are present, as well as step-changes of flexural stiffness. These complexities create $N+1$ segments of uniform stiffness, as seen in Figure 26.

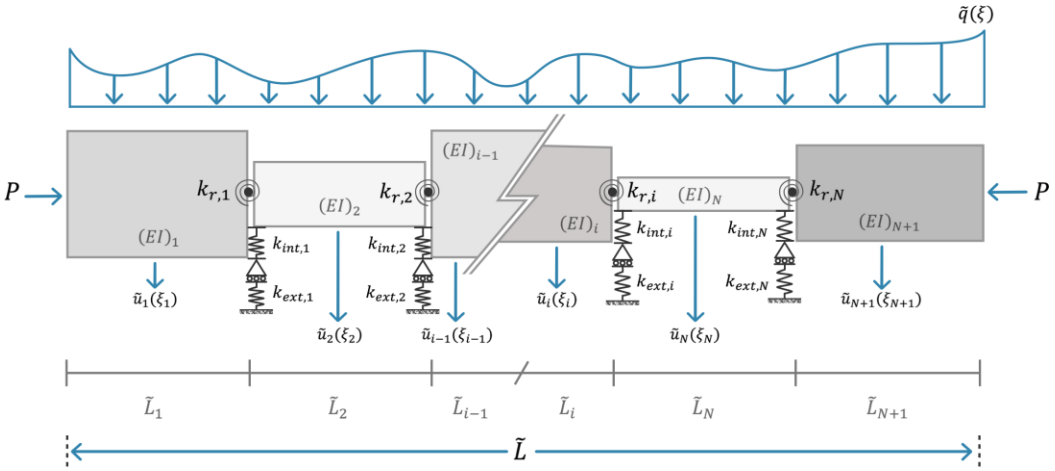

Figure 26: Normalized ideally jointed EB beam-column with N step-changes of flexural stiffness and N along-the-axis external, internal translational springs, and rotational springs while being subjected to a lateral $\tilde{q}(\xi)$ and axial load P.

Analyzing the relation of constants of integration between two consecutive segments subjected to different complexities from section 3.4 to section 3.6, it is noted that each complexity in the form of a spring affects the relation of a different constant of integration. The influence of internal springs only affects the term A_{i+1}, the influence of external springs only affects the term D_{i+1}, the influence of rotational springs only influences the term B_{i+1}, and finally the term C_{i+1} remaining the same as in Eq. 78.

The final form of the relation of constants of integration between two consecutive segments is defined as:

$$A_{i+1} = A_i + \left(\tilde{L}_i - \frac{\tilde{v}_i^2\, EI_i\, \eta_{int,i}}{k_{int,i}\, L^3}\right) B_i + \left(\frac{1}{\tilde{v}_i^2} - \frac{\cos(\tilde{v}_i\, \tilde{L}_i)}{\tilde{v}_i^2}\right) C_i + \cdots$$

$$+ \left(\frac{\tilde{L}_i}{\tilde{v}_i^2} - \frac{\sin(\tilde{v}_i\, \tilde{L}_i)}{\tilde{v}_i^3} - \frac{EI_i\, \eta_{int,i}}{k_{int,i}\, L^3}\right) D_i - \frac{\eta_{int,i} \int_0^{\tilde{L}_i} \tilde{q}_i(\tau)\, d\tau}{k_{int,i}\, L^3} + \cdots$$

Eq. 99

$$\cdots + \frac{\int_0^{\tilde{L}_i} \left(\tilde{q}_i(\tau) \sin(\tilde{v}_i\, \tau) \cos(\tilde{v}_i\, \tilde{L}_i) - \tilde{q}_i(\tau) \cos(\tilde{v}_i\, \tau) \sin(\tilde{v}_i\, \tilde{L}_i)\right) d\tau}{\tilde{v}_i^3\, EI_i} - \cdots$$

$$\cdots - \frac{\int_0^{\tilde{L}_i} \left(-\tilde{q}_i(\tau)\, \tilde{L}_i + \tilde{q}_i(\tau)\, \tau\right) d\tau}{\tilde{v}_i^2\, EI_i}$$

$$B_{i+1} = B_i + C_i \left(\frac{EI_i \cos(\tilde{v}_i \tilde{L}_i)\ \eta_{rot,i}}{k_{rot,i}\, L} + \frac{\sin(\tilde{v}_i \tilde{L}_i)}{\tilde{v}_i}\right) + \cdots$$

$$\cdots + D_i \left(\frac{EI_i \sin(\tilde{v}_i \tilde{L}_i)\ \eta_{rot,i}}{\tilde{v}_i\, k_{rot,i}\, L} - \frac{\cos(\tilde{v}_i \tilde{L}_i)}{\tilde{v}_i^2} + \frac{1}{\tilde{v}_i^2}\right) + \frac{\int_0^{\tilde{L}_i} \tilde{q}_i(\tau)\, d\tau}{\tilde{v}_i^2\, EI_i} + \cdots$$

Eq. 100

$$\cdots + \frac{\eta_{rot,i} \int_0^{\tilde{L}_i} \left(-\tilde{q}_i(\tau) \sin(\tilde{v}_i\, \tau)\ \cos(\tilde{v}_i\, \tilde{L}_i) + \tilde{q}_i(\tau) \cos(\tilde{v}_i\, \tau)\ \sin(\tilde{v}_i\, \tilde{L}_i)\right) d\tau}{\tilde{v}_i\, k_{rot,i}\, L} + \cdots$$

$$\cdots - \frac{\int_0^{\tilde{L}_i} \left(\tilde{q}_i(\tau) \sin(\tilde{v}\, \tau) \sin(\tilde{v}\, \tilde{L}_i) + \tilde{q}_i(\tau) \cos(\tilde{v}_i\, \tau) \cos(\tilde{v}\, \tilde{L}_i)\right) d\tau}{\tilde{v}_i^2\, EI_i}$$

$$C_{i+1} = C_i\, \beta_i \cos(\tilde{v}_i\, L_i) + \frac{D_i\, \beta_i \sin(\tilde{v}_i\, L_i)}{\tilde{v}_i} + \cdots$$

Eq. 101

$$\cdots + \frac{\int_0^{\tilde{L}_i} \left(-\tilde{q}_i(\tau) \sin(\tilde{v}_i\, \tau)\ \cos(\tilde{v}_i\, \tilde{L}_i) + \tilde{q}_i(\tau) \cos(\tilde{v}_{\mathrm{i}}\, \tilde{L}_{\mathrm{i}}) \sin(\tilde{v}_i\, \tilde{L}_i)\right) d\tau}{\tilde{v}_i\, EI_{i+1}}$$

$$D_{i+1} = -\frac{A_{i+1}\, L^3\, k_{ext,i}\, \eta_{ext,i}}{EI_{i+1}} + B_i \tilde{v}_i^2\, \beta_i + D_i \beta_i - B_{i+1} \tilde{v}_{i+1}^2 + \int_0^{\tilde{L}_i} \frac{\tilde{q}_i(\tau)\, d\tau}{EI_{i+1}} \qquad \text{Eq. 102}$$

Adopting such expressions between constants of integration reduces the global functions to depend only on four unknown integration constants. Applying four boundary conditions results in a system of four equations sufficient to perform the buckling analysis of beam-columns.

When there is no lateral load present (column case), Eq. 99 – Eq. 102 is reduced to:

$$A_{i+1} = A_i + \left(\tilde{L}_i - \frac{\tilde{v}_i^2\, EI_i\, \eta_{int,i}}{k_{int,i}\, L^3}\right) B_i + \left(\frac{1}{\tilde{v}_i^2} - \frac{\cos(\tilde{v}_i\, \tilde{L}_i)}{\tilde{v}_i^2}\right) C_i + \left(\frac{\tilde{L}_i}{\tilde{v}_i^2} - \frac{\sin(\tilde{v}_i\, \tilde{L}_i)}{\tilde{v}_i^3} - \frac{EI_i\, \eta_{int,i}}{k_{int,i}\, L^3}\right) D_i \qquad \text{Eq. 103}$$

$$B_{i+1} = B_i + C_i \left(\frac{EI_i \cos(\tilde{v}_i \tilde{L}_i)\ \eta_{rot,i}}{k_{rot,i}\, L} + \frac{\sin(\tilde{v}_i \tilde{L}_i)}{\tilde{v}_i}\right) + D_i \left(\frac{EI_i \sin(\tilde{v}_i \tilde{L}_i)\ \eta_{rot,i}}{\tilde{v}_i\, k_{rot,i}\, L} - \frac{\cos(\tilde{v}_i \tilde{L}_i)}{\tilde{v}_i^2} + \frac{1}{\tilde{v}_i^2}\right) \qquad \text{Eq. 104}$$

$$C_{i+1} = C_i\, \beta_i \cos(\tilde{v}_i\, \tilde{L}_i) + \frac{D_i\, \beta_i \sin(\tilde{v}_i\, \tilde{L}_i)}{\tilde{v}_i} \qquad \text{Eq. 105}$$

$$D_{i+1} = -\frac{A_{i+1}\, L^3\, k_{ext,i}\, \eta_{ext,i}}{EI_{i+1}} + B_i \tilde{v}_i^2\, \beta_i + D_i \beta_i - B_{i+1} \tilde{v}_{i+1}^2 \qquad \text{Eq. 106}$$

Eq. 103 – Eq. 106 are used to relate the constants of integration between two successive EB column segments. Applying the four boundary conditions results in a system of four equations whose determinant is the buckling equation of the column. The roots of such an equation are associated with the buckling loads.

For the case no axial load is present (beam), the expressions that relate constants of integration can be obtained from F. Giunta's work "On the analysis of jointed Euler-Bernoulli beams with step changes in material and cross-section under static and dynamic loads " [2].

3.8 Implementation of the closed-form solution

In this section, the procedure to implement the closed-form solution is presented on a step-by-step approach.

1. Express the local displacement, slope, moment, and shear equations (Eq. 60 – Eq. 67) using the closed-form expressions. Use Eq. 95 – Eq. 98 for beam-columns, and Eq. 99 – Eq. 102 for columns. This step expresses all local functions in terms of only four unknown constants of integration.
2. Express if a spring is absent or present by defining the appropriate η to equal zero or one, respectively.

3. Use the Heaviside function to obtain a single continuous piece-wise function to describe each deflection, slope, moment, and shear (Eq. 56 – Eq. 59).
4. Impose the four boundary conditions to obtain a system of four equations.
5. Obtain the buckling equation by computing the determinant of the system of equations for the buckling analysis of a column. Solve for the four unknown constants of integration For a beam-column.
6. Apply variables $(L_i,\ \eta,\ \beta_i,\ \nu_i,\ EI_i)$
7. Express all critical variables with respect to a single critical variable of reference (e.g. segment 1)

$$\tilde{\nu}_1 = \frac{\sqrt{P\ L^2}}{EI_1} = \alpha$$

$$\tilde{\nu}_i = \frac{\frac{\sqrt{P\ L^2}}{EI_i}}{\frac{\sqrt{P\ L^2}}{EI_1}} \cdot \alpha$$

8. Plot the buckling equation. Obtain the critical loads which are associated with the roots of the buckling equation of a column:

$$P_{cr} = \frac{\alpha^2\ EI_1}{L^2}$$

4 Validation of the closed-form solutions for the buckling analysis of complex beam-columns

The purpose of the following section is to validate the formulated closed-form solution from section 3 against the results obtained from the finite element software DIANA. The jointed beam-column presented in Figure 27 consists of an assembly of four EB beam-columns of constant stiffness. Step-changes of flexural stiffness between sections and the presence of springs are located at three discontinuities $(x_{0,1} = 3\,m,\ x_{0,2} = 6\,m,\ x_{0,3} = 9\,m)$. The material, section length, cross-section and flexural stiffness properties are presented in Table 2.

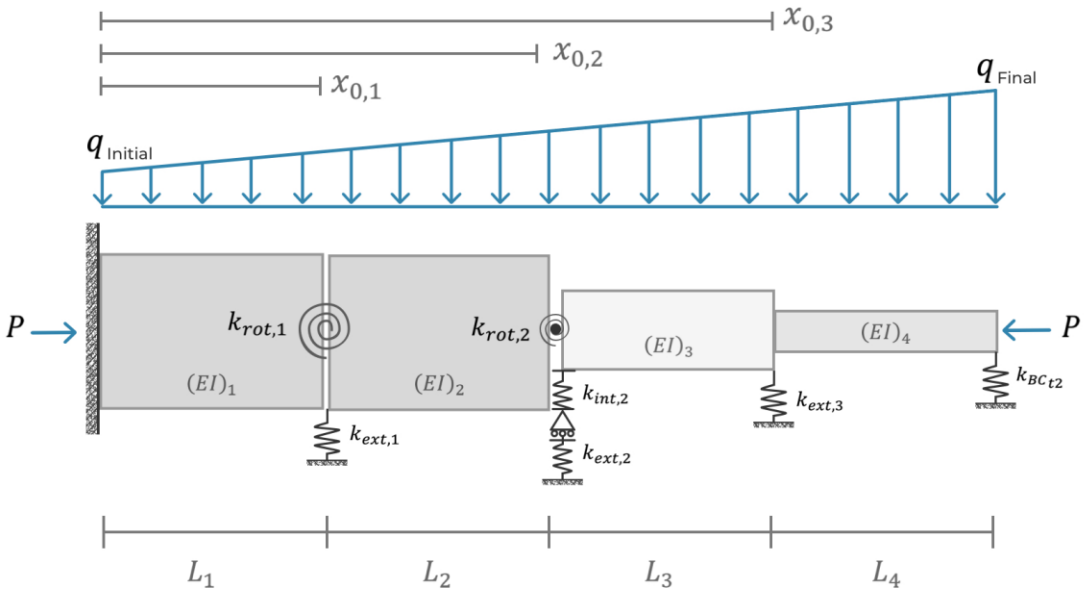

Figure 27: EB beam-column subjected to an axial load P, with a rotational and external spring at the discontinuity $x_{0,1}$, flexural stiffness step-change, rotational, internal, and external spring at the discontinuity $x_{0,2}$, flexural stiffness step-change, and external spring at the discontinuity $x_{0,3}$. The beam-column has a fixed boundary at $x = 0$, and only an elastic translational condition at $x = L$.

The beam-column displayed in Figure 27 is subjected to an axial load P. The boundary condition at $x = 0$ is considered as fixed, while it is subjected to only a translational boundary spring at $x = L$. The presence of a rotational spring and along-the-axis external translational spring creates a discontinuity at $x_{0,1}$. Step-changes of flexural stiffness, along with the presence of rotational and both internal and external along-the-axis translational springs, produces a discontinuity at $x_{0,2}$. The discontinuity at $x_{0,3}$ is caused by the presence of an along-the-axis external translational spring, along with step-changes of flexural stiffness between two consecutive beam-column elements. The properties of all springs acting on the beam-column are presented in Table 3.

Buckling analysis is performed using the proposed closed-form solution in section 3. The influence of springs is successfully accounted for by defining the correct value of $\eta_{spring,i}$. Such a variable receives a value of one when a spring is present and zero when the spring is absent.

Table 2: Flexural rigidity, material, length, and cross-section properties for each section of the beam-column in Figure 27.

Section	Material	Length $[mm]$	Young's modulus $[N/mm^2]$	Height $[mm]$	Width $[mm]$	Second moment of area $[mm^4]$	Flexural rigidity $[Nmm^2]$
1	Concrete C25/30	3000	31476	500	500	5.2083E+09	1.639375E+14
2	Concrete C25/30	3000	31476	500	500	5.2083E+09	1.639375E+14
3	Steel	3000	200000	300	300	6.7500E+08	1.350000E+14
4	Steel	3000	200000	200	200	1.3333E+08	2.666667E+13

Table 3: Boundary conditions and spring properties.

Discontinuity point $[i]$	Translational spring		Rotational spring $[k_{rot,i}]$ $[Nmm/rad]$
	Internal $[k_{int,i}]$ $[N/mm]$	External $[k_{ext,i}]$ $[N/mm]$	
1	-	1.00E+06	3.00E+12
2	7.00E+04	2.20E+05	9.00E+10
3	-	9.00E+04	-

Boundary conditions		
Location	$[k_{rot_{BC}}]$ $[Nmm/rad]$	$[k_{trans_{BC}}]$ $[N/mm]$
0	FIXED	
L	0	3.00E+04

The analysis aims to find the critical buckling loads given the properties of Table 2 and Table 3. As mentioned in section 2.3.1, the lateral load does not influence the theoretical buckling loads. For such a reason, no lateral load was considered acting on the beam-column of Figure 27.

The boundary conditions provide a system of four equations that are expressed with the appropriate global equation for the deflection, slope, moment, and shear. All critical local variables $\tilde{v}_i$ are expressed in terms of the same critical variable. Defining $\tilde{v}_1 = \alpha$ and representing all other local critical variables in the same parameter, as seen in Eq. 69, results in $\tilde{v}_2 = \alpha$, $\tilde{v}_3 = 1.1019\,\alpha$, and $\tilde{v}_4 = 2.4794\,\alpha$.

The determinant of such a system of equations is the buckling equation, and the buckling loads are obtained at their roots, which are associated with α. Figure 28 displays the first three roots of the buckling equation of the beam-column of Figure 27.

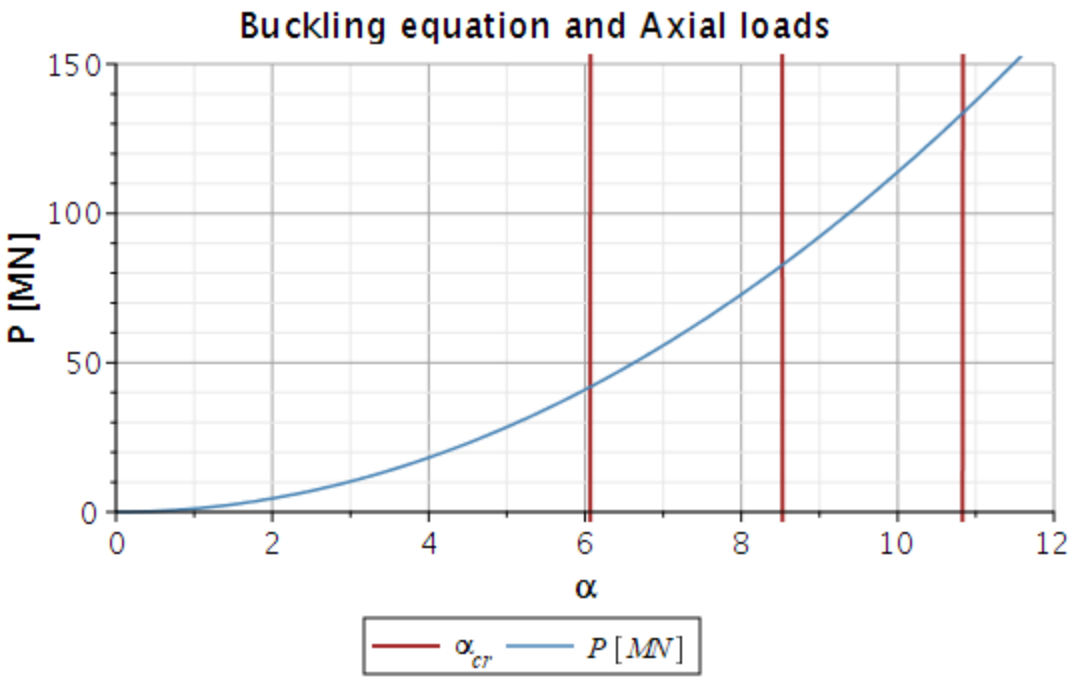

Figure 28: First three roots of the beam-column of Figure 28 are expressed in terms of $\alpha = \tilde{v}_1 = \sqrt{\frac{P\,L^2}{EI_1}}$. *Axial load* P *is related to the critical variable* α.

The buckling load is found by solving for the load term P, which is associated to α by:

$$\alpha_{cr} = \sqrt{\frac{P\,L^2}{EI_1}} \qquad \text{Eq. 107}$$

Hence, the buckling load is:

$$P_{cr,i} = \frac{\alpha_{cr,i}^2\,EI_1}{L^2} \qquad \text{Eq. 108}$$

Eq. 108 shows the positive relationship between the critical load P and the critical root α_{cr}. Using Eq. 108, the first three buckling loads are computed and compared to the values obtained through DIANA in Table 4. The percentage error between the results obtained through DIANA against those obtained through the proposed closed-form solution is calculated as:

$$\varepsilon(\%) = \left(\frac{P_{cr_{DIANA}} - P_{cr_{Proposed}}}{P_{cr_{DIANA}}}\right) \cdot 100 \qquad \text{Eq. 109}$$

With $P_{cr_{DIANA}}$ being the critical load obtained through DIANA and $P_{cr_{Prosposed}}$ being the critical load obtained through the proposed method.

Table 4: Comparison between the buckling loads obtained through the proposed closed-form solution to those obtained through DIANA.

Mode	Closed-form solution		DIANA	% Error
	Root No. α_i	$P_{cr_{Proposed}}$ [N]	$P_{cr_{DIANA}}$ [N]	[%]
1	6.0414	4.155E+07	4.155E+07	0.00021%
2	8.5218	8.268E+07	8.268E+07	0.00000%
3	10.8520	1.341E+08	1.341E+08	0.00093%

Each buckling load is associated with a buckling mode, which is the shape the beam-column takes under the influence of its respective buckling load. Solving for the constants of the system of equations would result in the trivial solution along with the trivial mode, which is an undeflected beam-column. The non-trivial mode is avoided by assigning a value to one of the four unknown constants of integration, and then solving the remaining three unknown constants. If no mode is obtained, another constant of integration must be chosen. The local dimensionless buckling mode is obtained after introducing the solved constants of integration and critical value α_{cr} to the local dimensionless deflection function. The global dimensionless buckling mode is obtained after combining in a piece-wise manner all the local modes. A comparison between the global modes obtained through the closed-form solution and those obtained through DIANA is displayed in Figure 29.

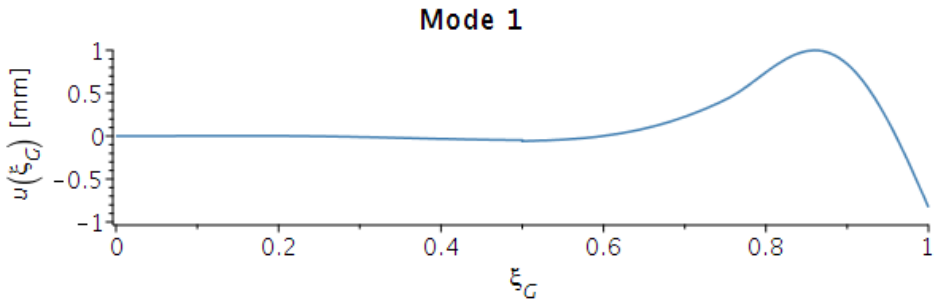

(a) Mode 1 was obtained through the closed-form solution. Min: -0.828 mm. Max: 1.00 mm.

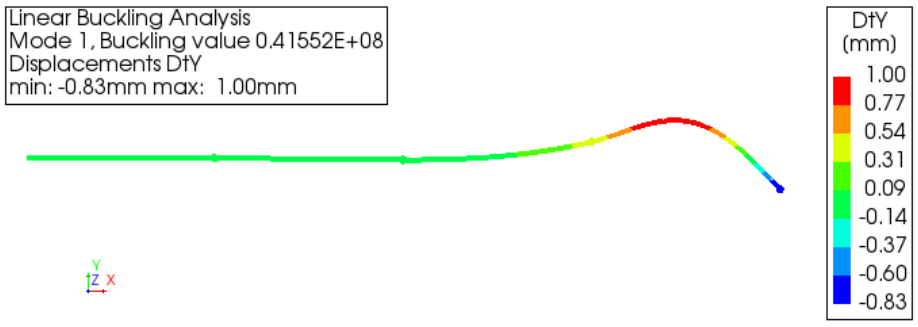

(b) Mode 1 obtained through DIANA

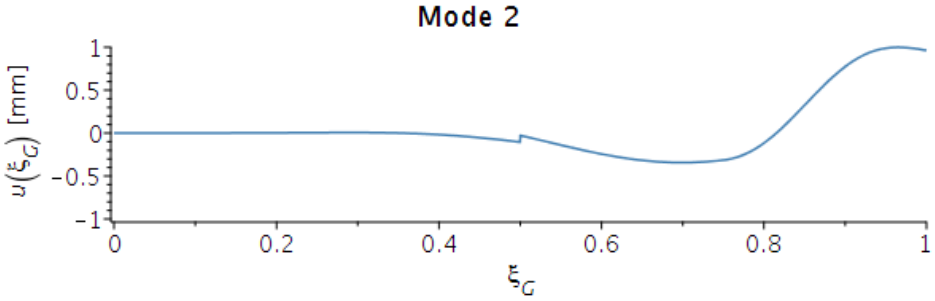

(c) Mode 2 was obtained through the closed-form solution. Min: -0.343 mm. Max: 1.00 mm

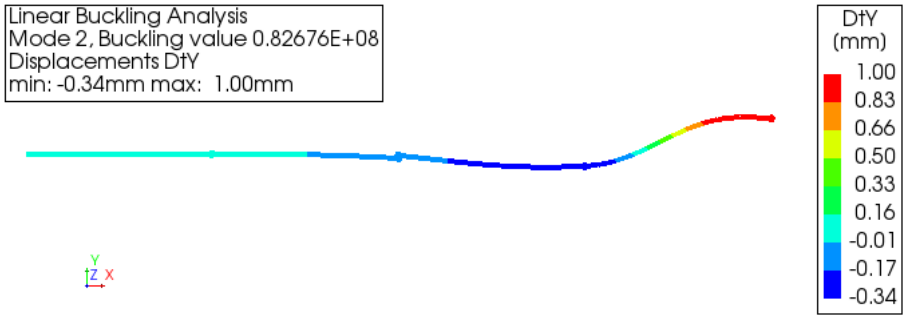

(d) Mode 2 obtained through DIANA

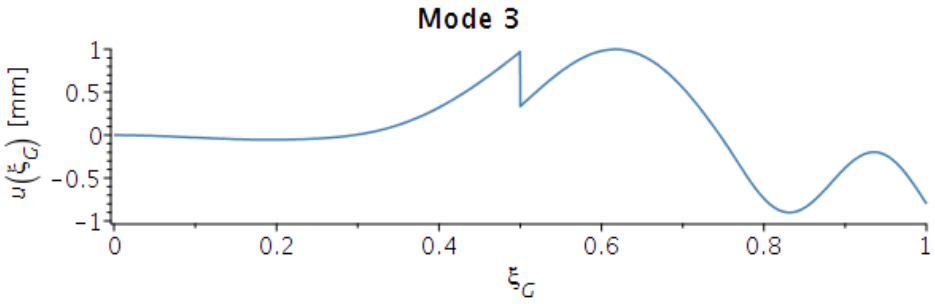

(e) Mode 3 was obtained through the closed-form solution. Min: -0.902 mm. Max: 1.00 mm.

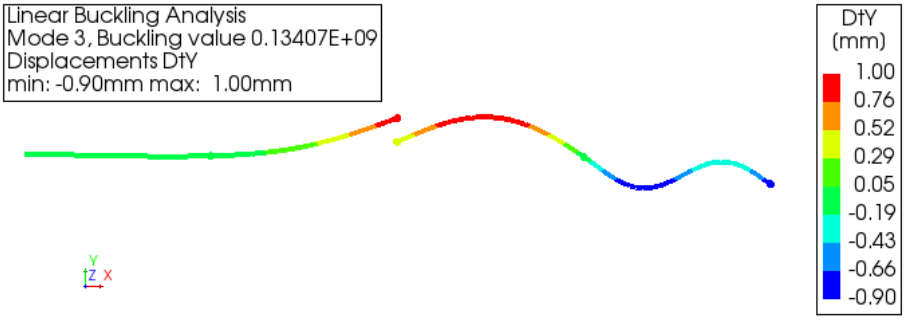

(f) Mode 3 obtained through DIANA

Figure 29: Comparison between the first three buckling modes obtained from the closed-form solution to those obtained through DIANA. (a) Buckling mode one was obtained using the closed-form solution. (b)Buckling mode one was obtained through DIANA. (c) Buckling mode two was obtained using the closed-form solution. (d) Buckling mode two was obtained through DIANA. (e) Buckling mode three was obtained using the closed-form solution. (f) Buckling mode three was obtained through DIANA.

For axial loads below the first critical load, solving the four constants of integration of the beam-column using the closed-form expressions can successfully describe the displacement, slope, moment, and shear. Assuming the compressive load P has a value of $1000\ kN$, and being subjected to a trapezoidal load function with $q_1 = 1N/mm$ and $q_2 = 4\ N/mm$, the beam-column's deflection, slope, moment, and shear are presented and compared to values obtained from a geometrical non-linear static analysis on DIANA, as shown in Figure 30 – Figure 33. All diagrams have a perfect agreement with the results obtained from the proposed closed-form expressions. The values not in agreement in the shear diagram in Figure 33 are due to singularities at the location of external springs acting on the beam-column.

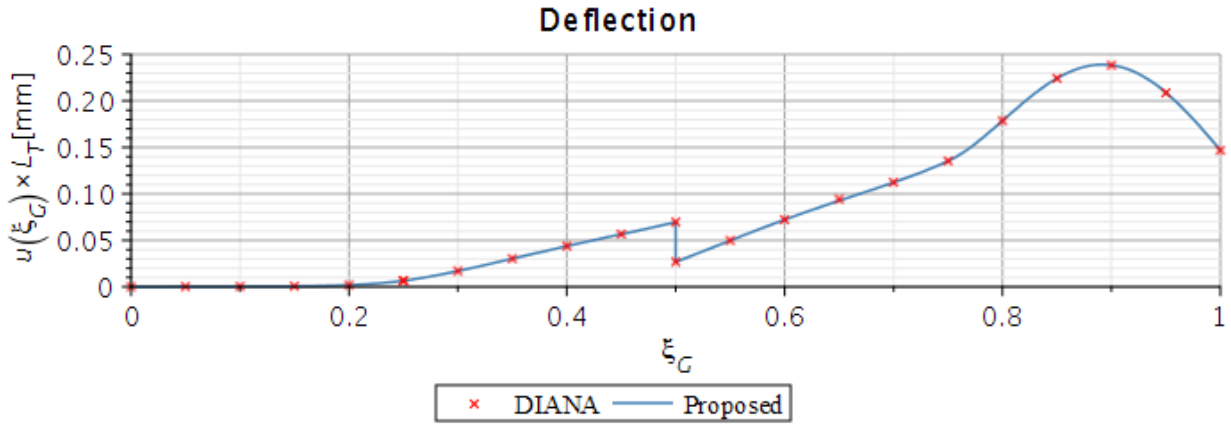

Figure 30: Comparison between deflection obtained from DIANA and proposed closed-form expressions.

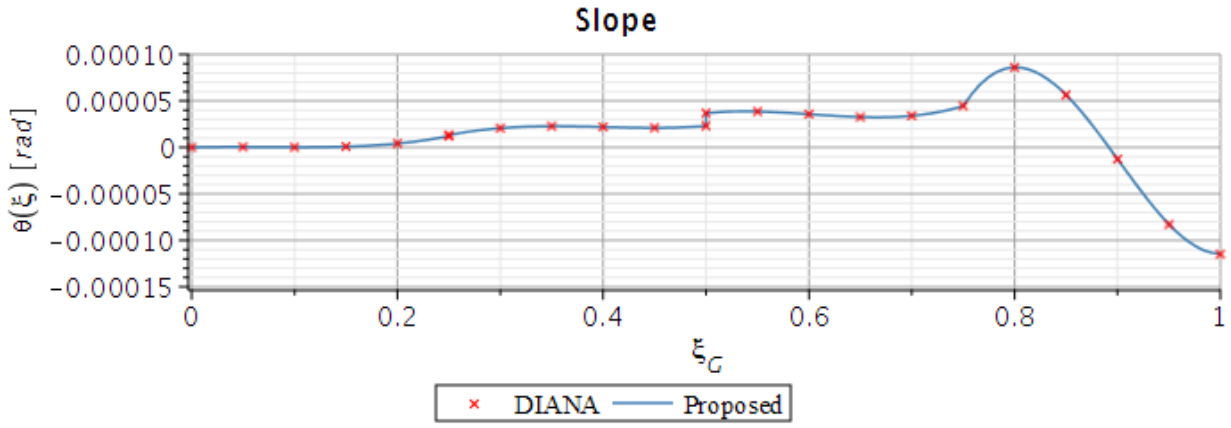

Figure 31: Comparison between slope obtained from DIANA and proposed closed-form expressions.

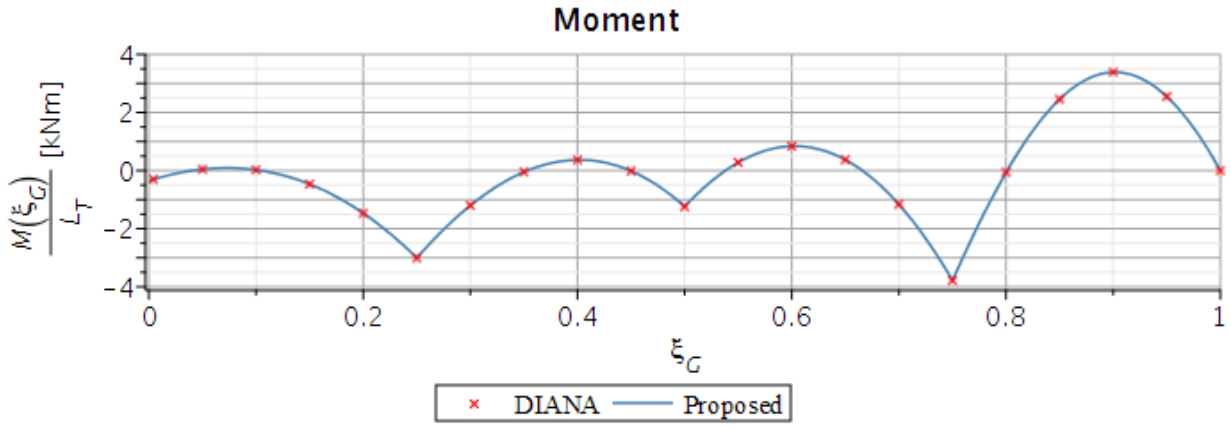

Figure 32: Comparison between moment obtained from DIANA and proposed closed-form expressions.

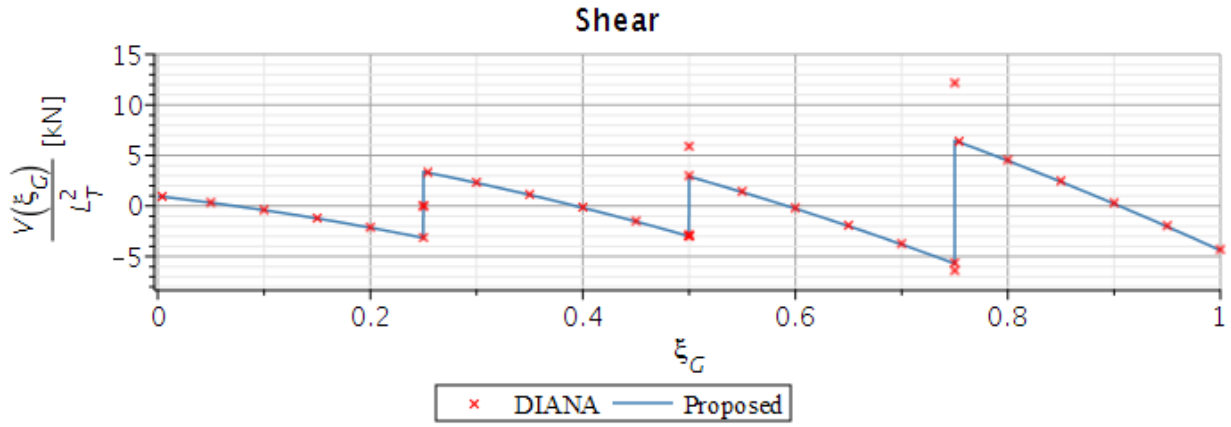

Figure 33: Comparison between shear obtained from DIANA and proposed closed-form expressions.

The takeaways for this chapter are that the proposed closed-form expressions can be used to perform a buckling analysis of a column with N discontinuities due to a combination of step-changes of flexural stiffness, internal and external translational springs, internal rotational springs, and elastic boundary conditions. The buckling analysis accurately calculates the buckling loads and captures their respective buckling modes. It is also possible to accurately obtain the deflection, slope, moment, and shear of beam-columns under a compressive axial load and a varying lateral load. Using the closed-form expressions and solutions avoids the need to perform a geometrical non-linear structural static analysis on FEM software, which requires the discretization of the system and multiple loading steps to obtain such results accurately.

5 Applications and Discussion

The purpose of the following chapter is to discuss and present possible applications for the proposed closed-form solution. Section 5.1 offers a brief discussion of the computational cost when obtaining the buckling equation of columns. A simple parametric study is performed in Section 5.2 to see how different kinds of springs and their location influence the critical loads of a simply supported column.

5.1 Computational Cost of closed-form expressions

The advantages of using the proposed closed-form expressions when performing a linear buckling analysis are: (i) to only solve for the determinant of a 4x4 system of equations, regardless of the number of discontinuities present of a column, (ii) to only solve for four unknown constants of integration to obtain the deflection, slope, moment, and shear of a beam-column. Nonetheless, there is a computational cost that is related to the number of discontinuities. Figure 34 displays the computation time required in seconds for obtaining the buckling equation of a column with N discontinuities and having ideal boundary conditions. Figure 35 depicts the computation time required in seconds for obtaining the buckling equation of a column with N discontinuities and having elastic boundary conditions.

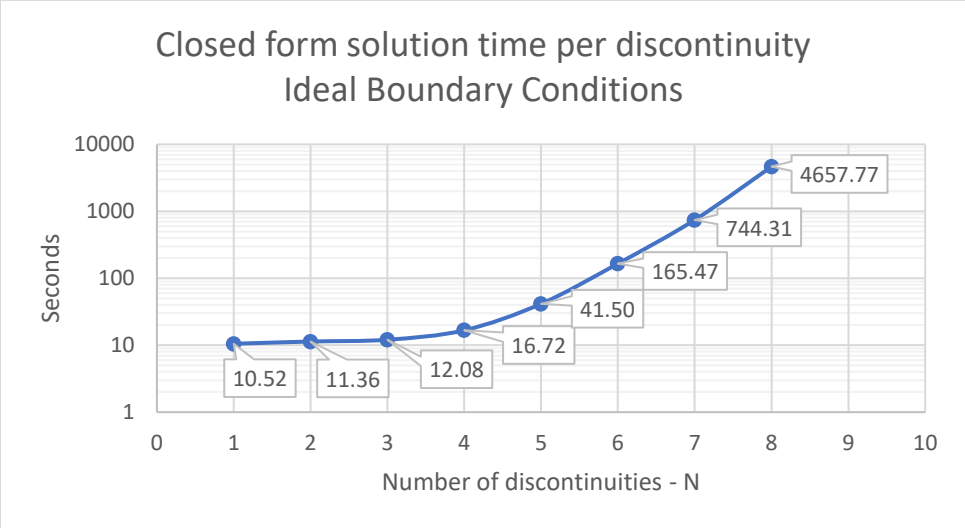

Figure 34: Computation time for obtaining the algebraic buckling equation of a column with ideal boundary conditions in Maple.

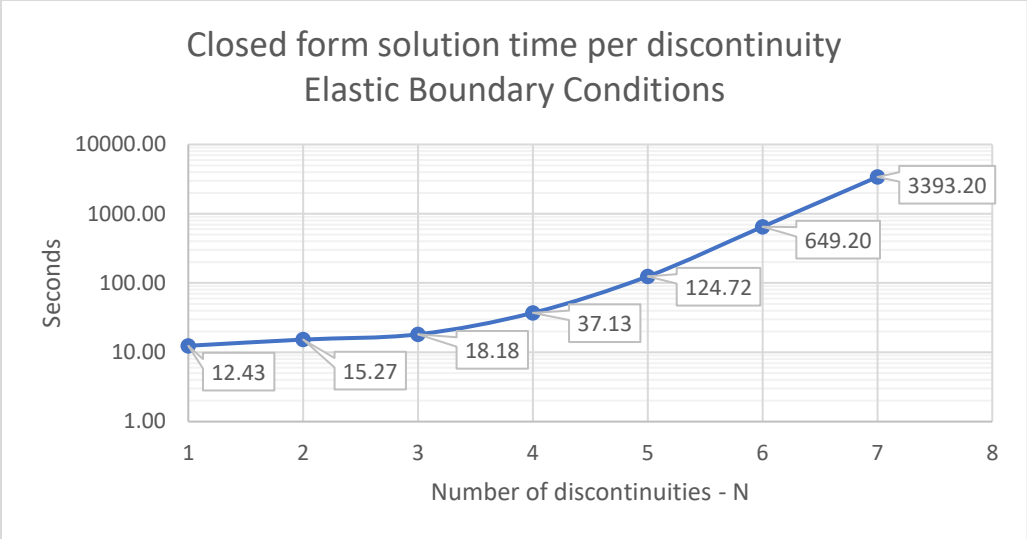

Figure 35: Computation cost for obtaining the algebraic buckling equation of a column with elastic boundary conditions.

The computation cost starts becoming expensive for a column with ideal boundary conditions after six discontinuities are present (column of seven segments). For a column with elastic boundary conditions, such a cost starts becoming expensive after five discontinuities (column of six segments). It is worth noting that such computational costs are associated with solving and expressing the buckling equation algebraically in terms of lengths, flexural stiffness, spring stiffness, and critical variables using the mathematical software Maple. Other mathematical software might be more efficient in obtaining algebraically the determinant of a 4x4 system of equations.

Although the computation time starts increasing after five discontinuities for a column with ideal boundary conditions, or after six discontinuities for a column with elastic boundary conditions, the buckling equation would only have to be computed once and stored for future use giving it a comparative advantage when compared to numerical methods.

5.2 Parametric study

The following subsection presents a simple parametric study using the proposed closed-form expressions to visualize the effect on the critical roots resulting from changes in the stiffness and location of different springs acting on a simply supported column with the following properties:

- A square cross-section of 200×200 mm
- Made of steel with an elastic modulus of 200 000 N/mm^2

Sections 5.2.1 – 5.2.3 focus on the effect that the stiffness of external translational, internal translational, and rotational springs have on the critical roots. In turn, sections 5.2.4 – 5.2.6 examine how the roots of the buckling equation are affected by a spring acting at different locations, as seen in Figure 36.

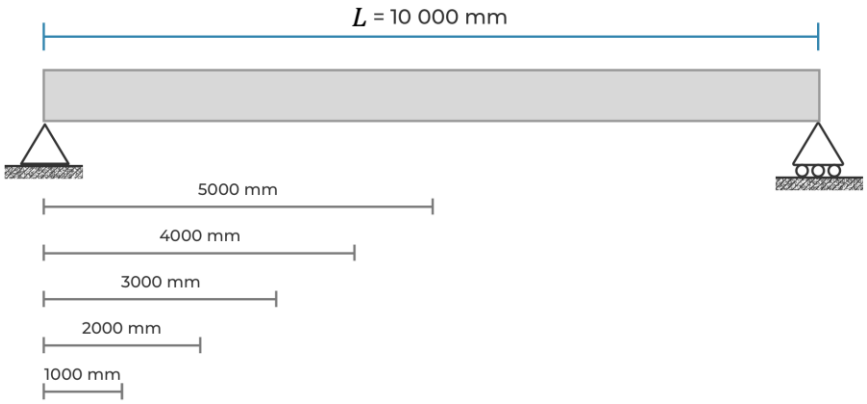

Figure 36: Simply supported column under an axial load P displaying the location of springs for five different cases for Sections 5.2.4 – 5.2.6.

5.2.1 Influence of external translational springs

To only account for the influence of springs, the flexural stiffness will be assumed to be constant throughout the column presented in Figure 37. Springs are introduced at locations to create three segments of equal length. Moreover, Figure 37 displays a simply supported column with a span of 15 000 mm.

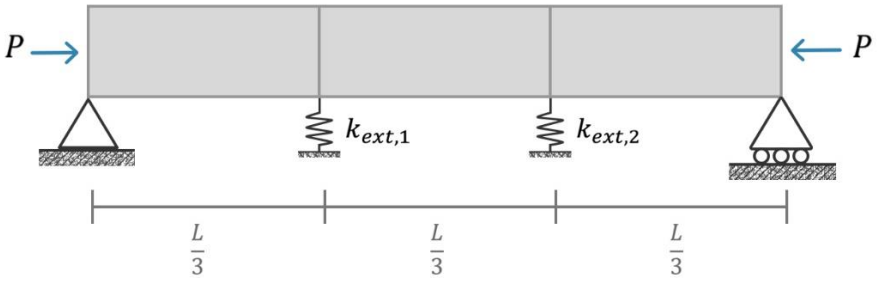

Figure 37: Simply supported column of constant stiffness under an axial load P. Each section is of the same length. External springs are located at $x = L/3$ and at $x = 2L/3$.

The first parameter to be analyzed is the influence of only translational springs. Using the closed-form solution proposed in section 3, it is possible to visualize how the critical roots are affected by external springs of different stiffnesses. Figure 38 displays the buckling equation of the column presented in Figure 37 under seven different external translational spring's stiffnesses. This simple case study solely focuses on the first three roots associated with the first three critical loads.

In Figure 38(A), an external spring stiffness of zero results in the same critical roots as that of the unsupported column. With an increase of external spring stiffness, as seen in Figure 38(A) – (E), the first and second critical roots increase, and the third one remains unchanged because the external springs are located at the inflection points (points with no displacement) associated to the third buckling mode.

Using the information from Figure 38, the relationship between an increase in stiffness to an increase of critical load (P_{cr}) is obtained and plotted in Figure 39. The first and second critical loads follow their almost

linear trend (segment A-B and D-B) and are associated with their respective buckling mode (half-sine wave shape for segment A-B, and sine wave shape for segment D-B). From such a plot, it is possible to visualize at which stiffness both critical loads equal each other. The buckling modes still seem to follow the almost linear trend they had for segments A-B and D-B, meaning that there is a change in buckling modes between the first and second critical loads. Segment B-C belongs to the first critical load but has a buckling mode of a sine-wave shape, while segment B-E describes the second critical load but has a half-sine wave buckling mode.

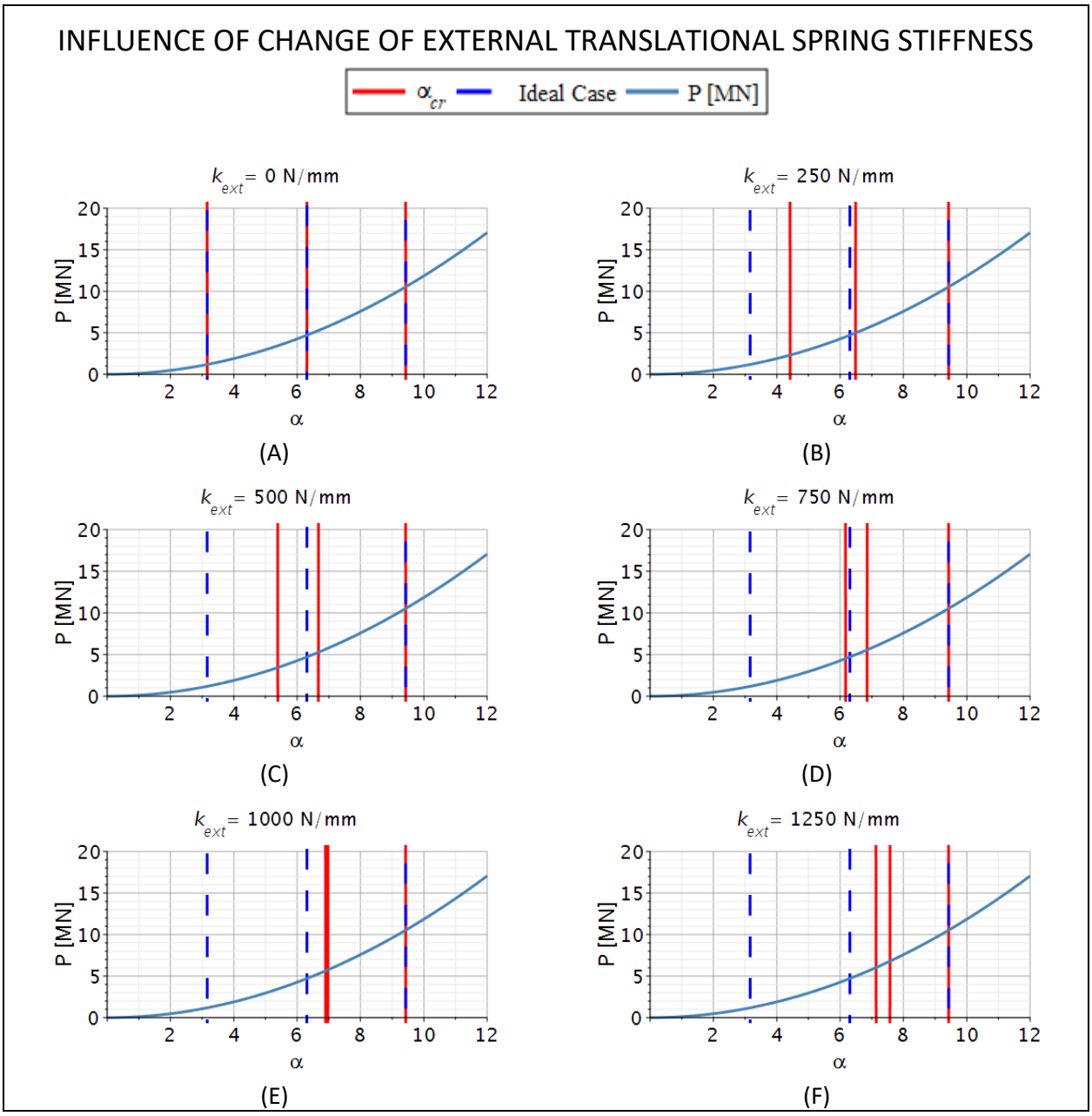

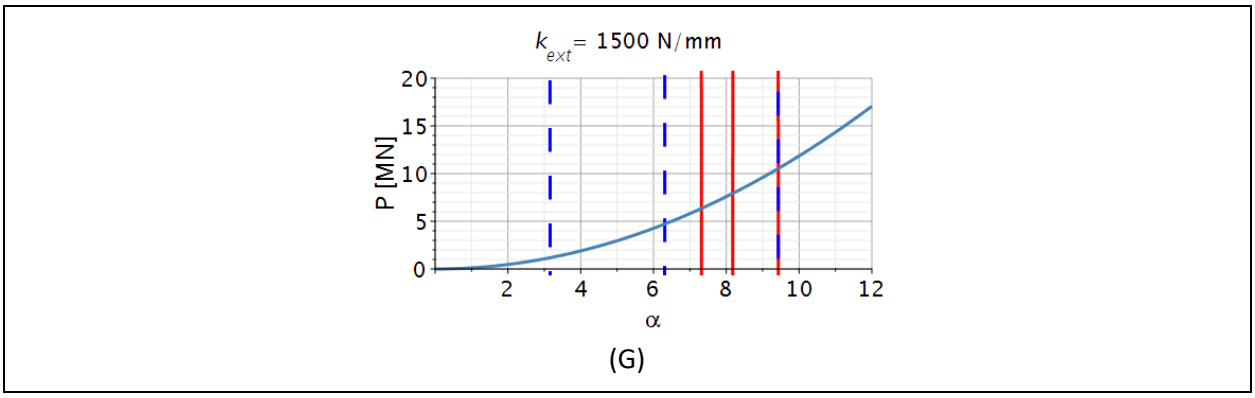

Figure 38: Plots obtained using the proposed closed-form solution to illustrate the change of critical roots due to the influence of external translational springs of different stiffnesses located at a third of the span from both supports.

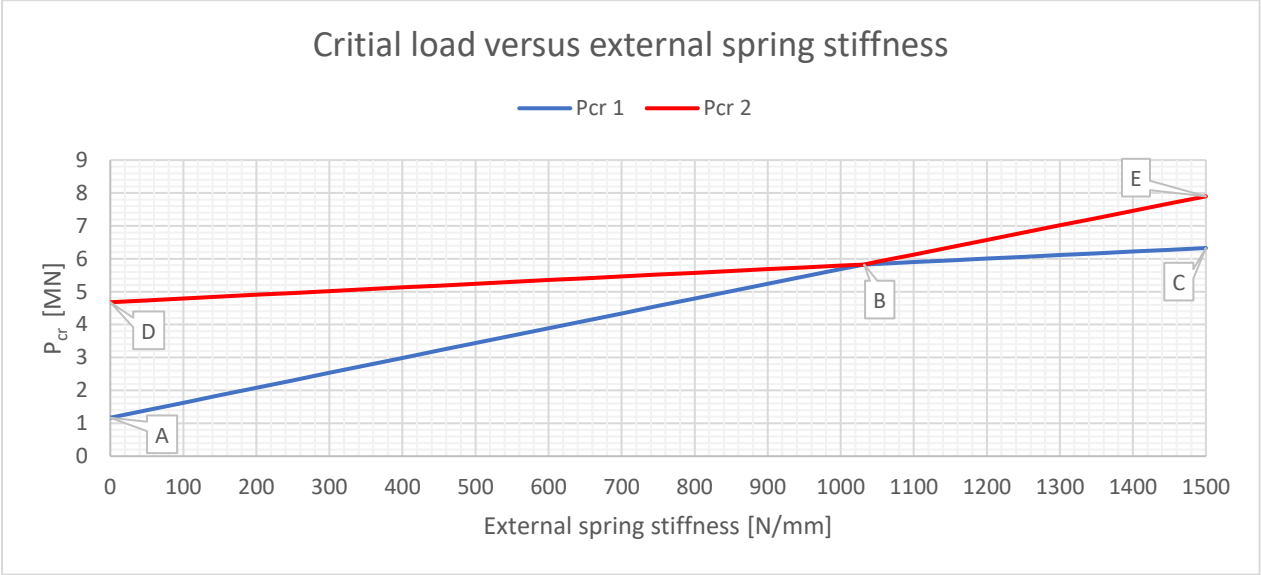

Figure 39: Critical load of first and second critical root versus External spring stiffness. Line ABE is associated with buckling mode 1 of its ideal counterpart (half-sine wave shape). Line DBC is associated with buckling mode 2 of its ideal counterpart (sine wave shape).

5.2.2 Influence of internal translational springs

To only account for the influence of internal springs, the flexural stiffness is assumed to be constant throughout the beam-column presented in Figure 40. Springs are introduced to create three segments of equal length. Moreover, Figure 40 is simply supported with a span of 15 000 mm.

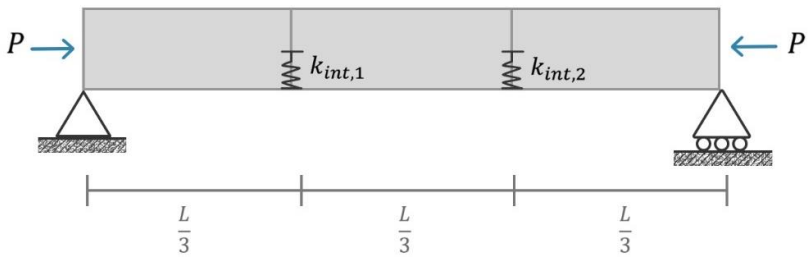

Figure 40: Simply supported beam-column of constant stiffness under an axial load P. Each section is of the same length. Internal springs are located at $x = L/3$ and at $x = 2L/3$.

As in the previous subsection, it is possible to visualize the influence of internal springs with different stiffnesses on the critical roots by using the developed closed-form solution. Figure 41 displays the buckling equation of the column displayed in Figure 40 under different internal translational spring stiffnesses. Figure 41 shows how the increase of stiffness of the internal translational springs affects one critical root at a time. There is also a linear trend between the critical roots and the increase of stiffness of the spring. This relation can be seen in Figure 43, where the critical load of each root is plotted against the stiffness of the spring.

When the roots match those of the ideally jointed column ($\alpha_{cr} = \pi$ & 2π), their respective buckling mode is the same as well. When the critical roots do not match those of its ideally jointed counterpart, the buckling mode is the extension of the internal translational springs, with each segment remaining straight, as seen in Figure 42.

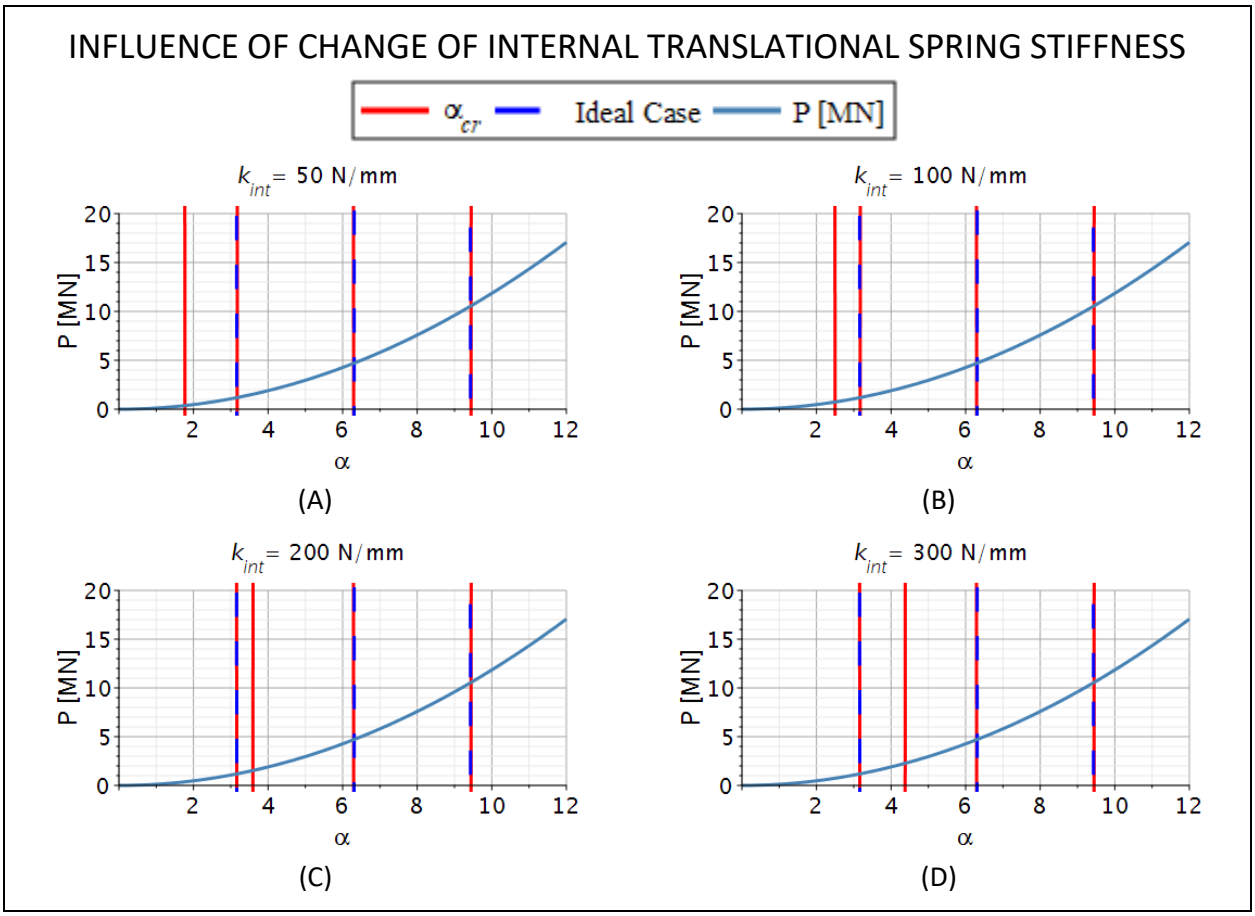

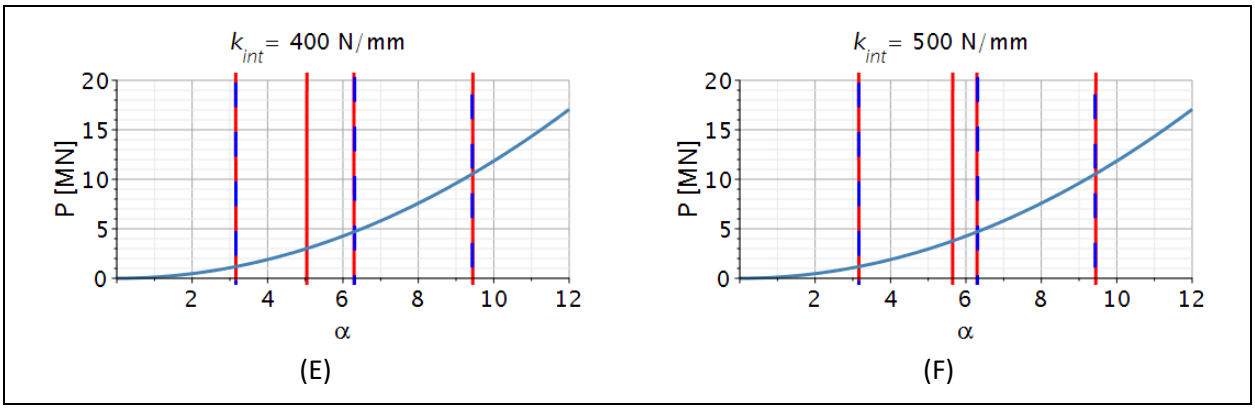

Figure 41: Plots obtained using the proposed closed-form solution to illustrate the change of critical roots due to the influence of internal translational springs with different stiffnesses located at a third of the span from both supports.

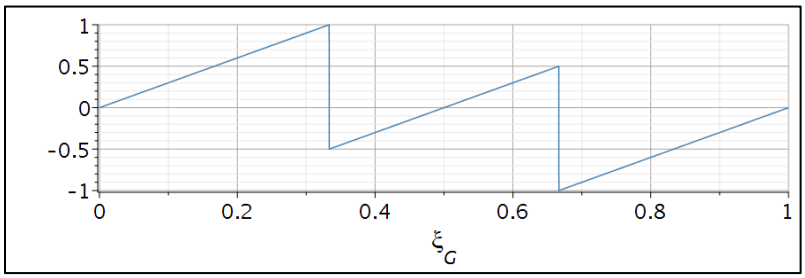

Figure 42: Buckling mode when critical roots are not equal to that of its ideally jointed counterpart due to the influence of internal translational springs.

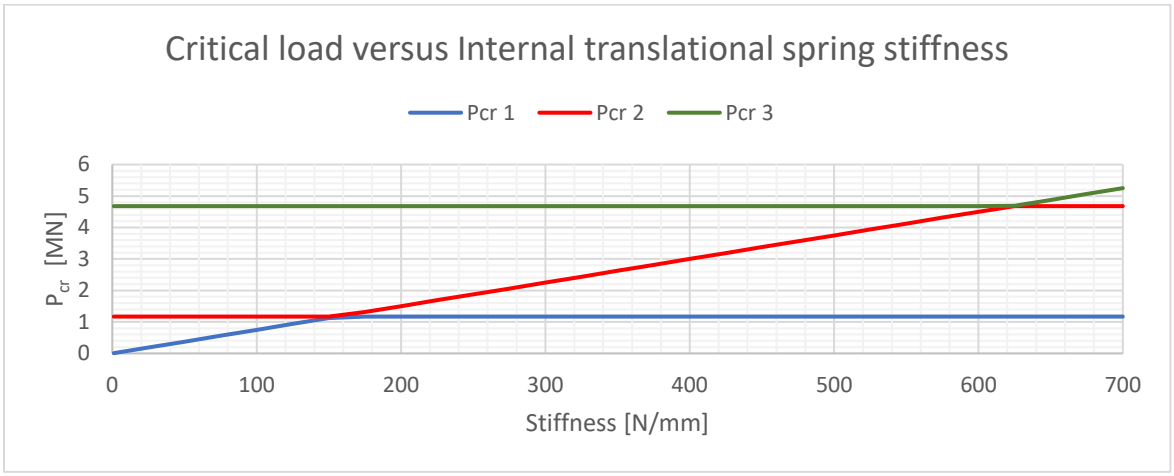

Figure 43: Change of first three critical loads due to changes of internal translational spring stiffness.

5.2.3 Influence of rotational springs

To only account for the influence of springs, the flexural stiffness will be assumed to be constant throughout the column presented in Figure 44. Springs are introduced at locations to create three segments of equal length. Moreover, Figure 44 is going to be simply supported. The square cross-section of the beam-column is 200×200 mm^2, resulting in a flexural stiffness of about 2.667E+13 Nmm^2.

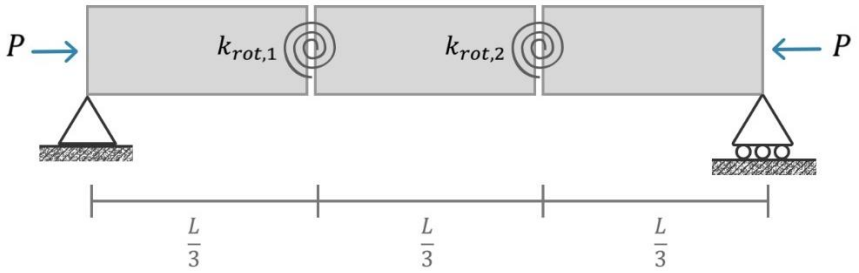

Figure 44: Simply supported column of constant stiffness under an axial load P. Each section is of the same length with a square cross-section of 200x200 mm². Rotational springs are located at $x = L/3$ and at $x = 2L/3$.

Using the closed-form solution proposed in section 3, it is possible to visualize how rotational springs affect the critical roots of the simply supported column of Figure 44. Such plots are displayed in Figure 45, where five buckling load plots showing the critical roots are presented for five different rotational spring stiffnesses. Unlike internal springs that only affect one root at a time, the stiffnesses of the rotational springs influence all buckling modes compared to their ideal case.

Under the influence of large cracks, characterized by having a low rotational stiffness compared to the flexural stiffness of the segment, all critical roots are greatly affected. Increasing the rotational spring stiffness from that presented in Figure 45(A) has a higher effect on the critical roots associated with higher modes. Data can also be obtained from Figure 45 to visualize at which rotational stiffness there is a negligible change in critical loads. This data is presented in Figure 46, where after certain stiffness, any increase stops having a great influence on the critical loads.

Once again, the third critical root is unaffected by the change of stiffness of the rotational springs. This lack of change is because the springs are located at the inflection points associated with the third buckling mode.

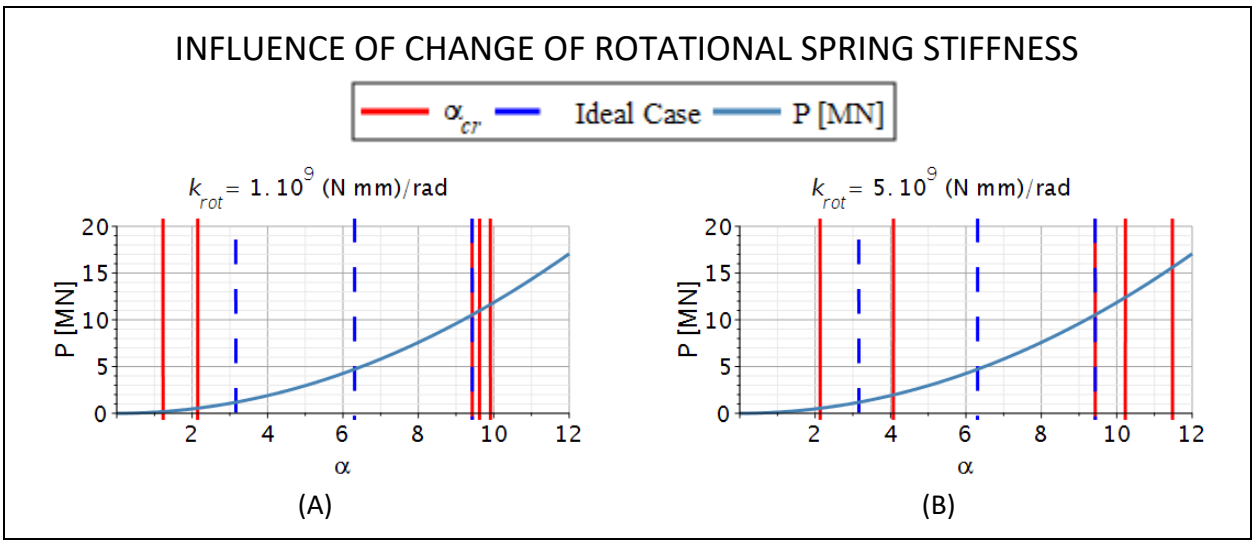

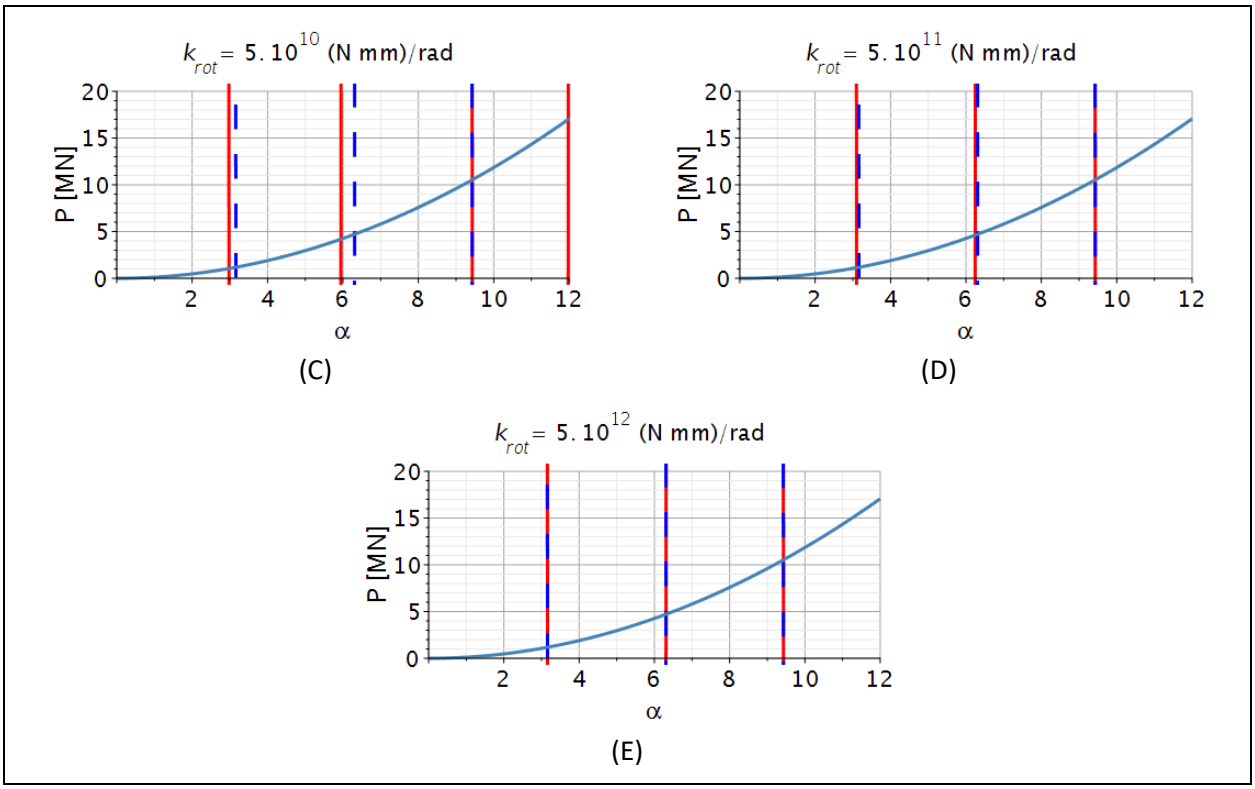

Figure 45: Plots obtained using the proposed closed-form solution to illustrate the change of critical roots due to the influence of internal rotational springs with different stiffnesses located at a third of the span from both supports.

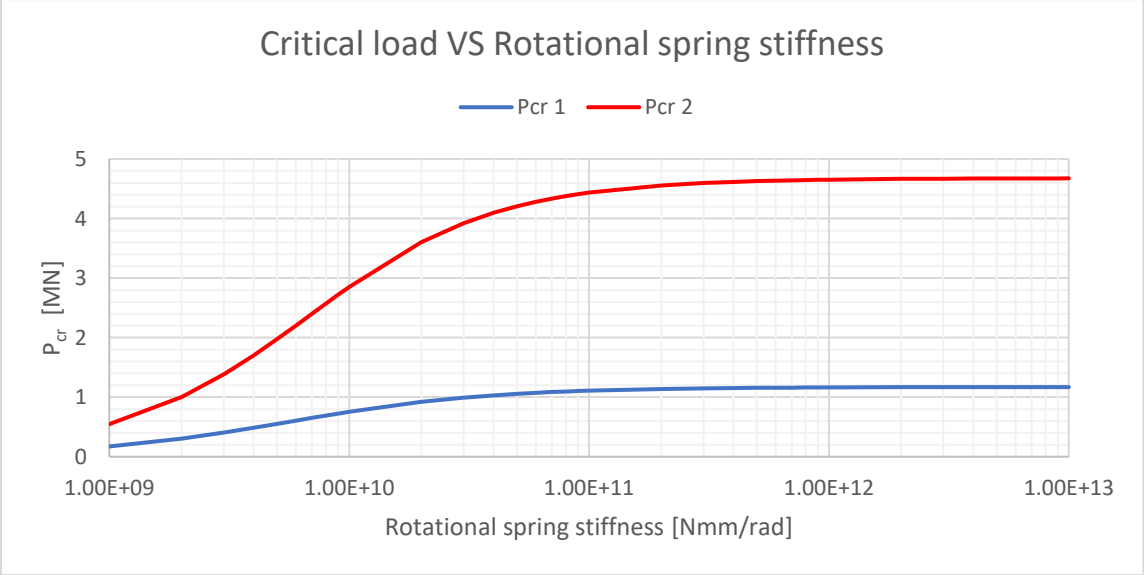

Figure 46: Change of first two critical loads due to changes of rotational spring stiffness.

5.2.4 Location of external translational spring

This subsection studies the effects of the location of a single external spring with stiffness of 5 000 N/mm acting on five different locations of a simply supported column of 10 000 mm, as seen in Figure 36. As described previously, the column is made of steel with a Young's Modulus of 200 000 N/mm^2 and a square cross section of 200×200 mm^2.

Figure 47 displays how the external spring at five different locations from one of the pin supports affects the critical roots of the mentioned column. It should be noted that the location of the external spring affects the various critical roots in different ways. Using the proposed closed-form expressions, Figure 48 displays the effect of the location of the external springs on the critical loads associated with each critical root. It is possible to identify the location of the highest impact on the critical loads using the closed-form expressions. Such a tool helps the user determine how the location of single supports affects higher buckling loads.

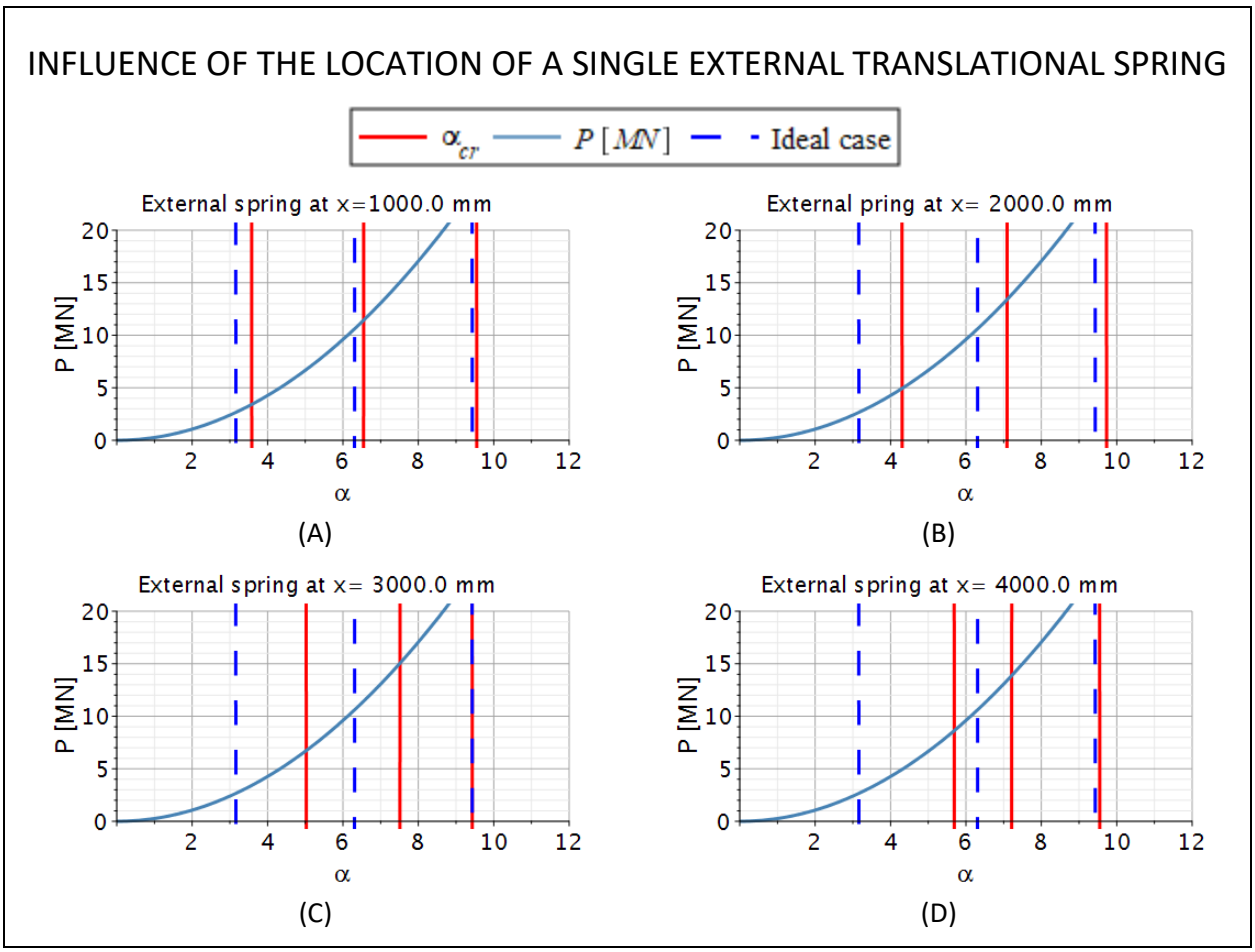

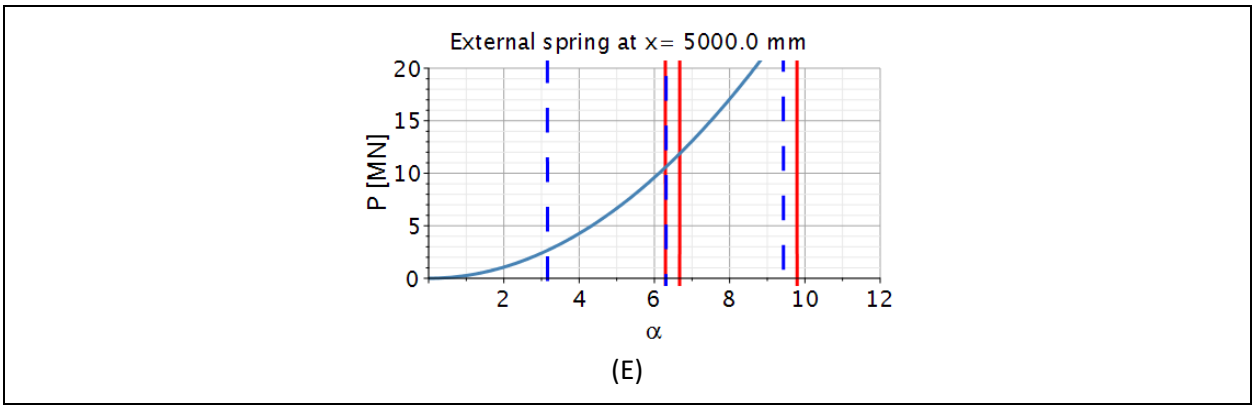

Figure 47: Plots obtained using the proposed closed-form solution to illustrate the change of critical roots due to the influence of an external translational spring with stiffness of 5 000 N/mm acting at different locations from the supports.

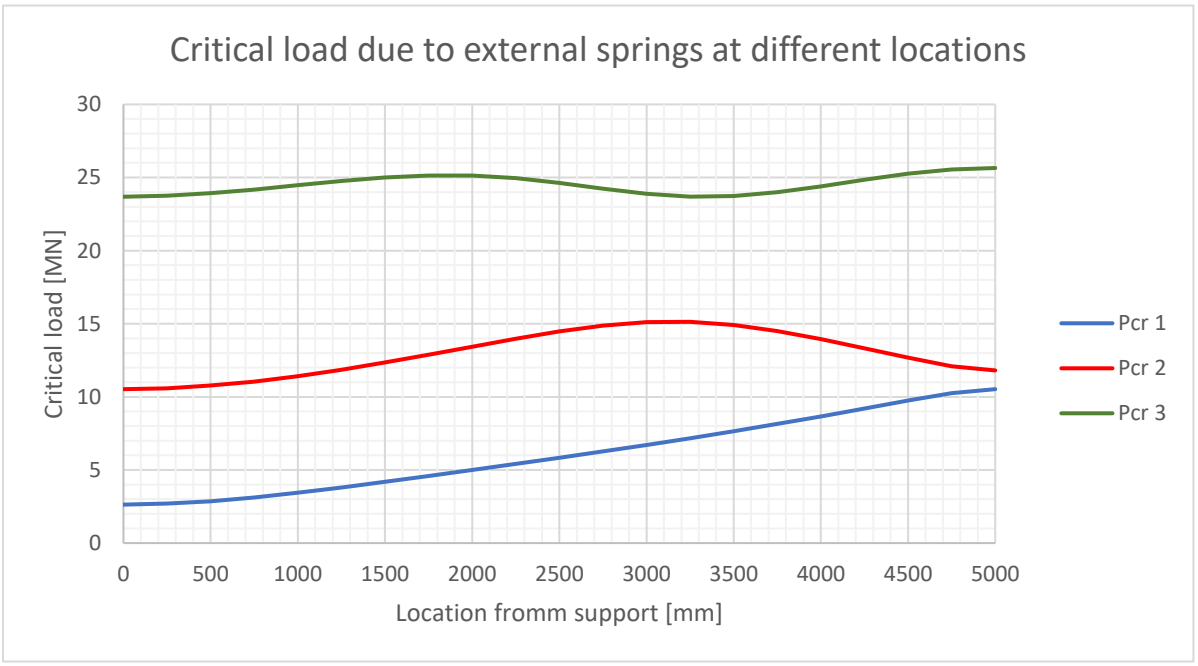

Figure 48: Effect of critical loads due to a single external spring at different distances from left pin support of a 10 000 mm simply supported column.

5.2.5 Location of internal translational spring

This subsection studies the effects of the location of a single internal spring with a stiffness of 100 N/mm acting on five different positions of a simply supported column of 10 000 mm, as seen in Figure 36. The column is made of steel with a Young's Modulus of 200 000 N/mm^2 and a square cross section of 200×200 mm^2.

The proposed closed-form expressions have been used to obtain the graphs in Figure 49 displaying how the location of the single internal translational spring (representing the stiffness of joints between two consecutive column segments) affects the critical roots and loads of the column. From such a graph, it is

evident that the location does not affect the critical loads of the simply supported column, thus making the stiffness of the internal translational springs critical on the buckling loads.

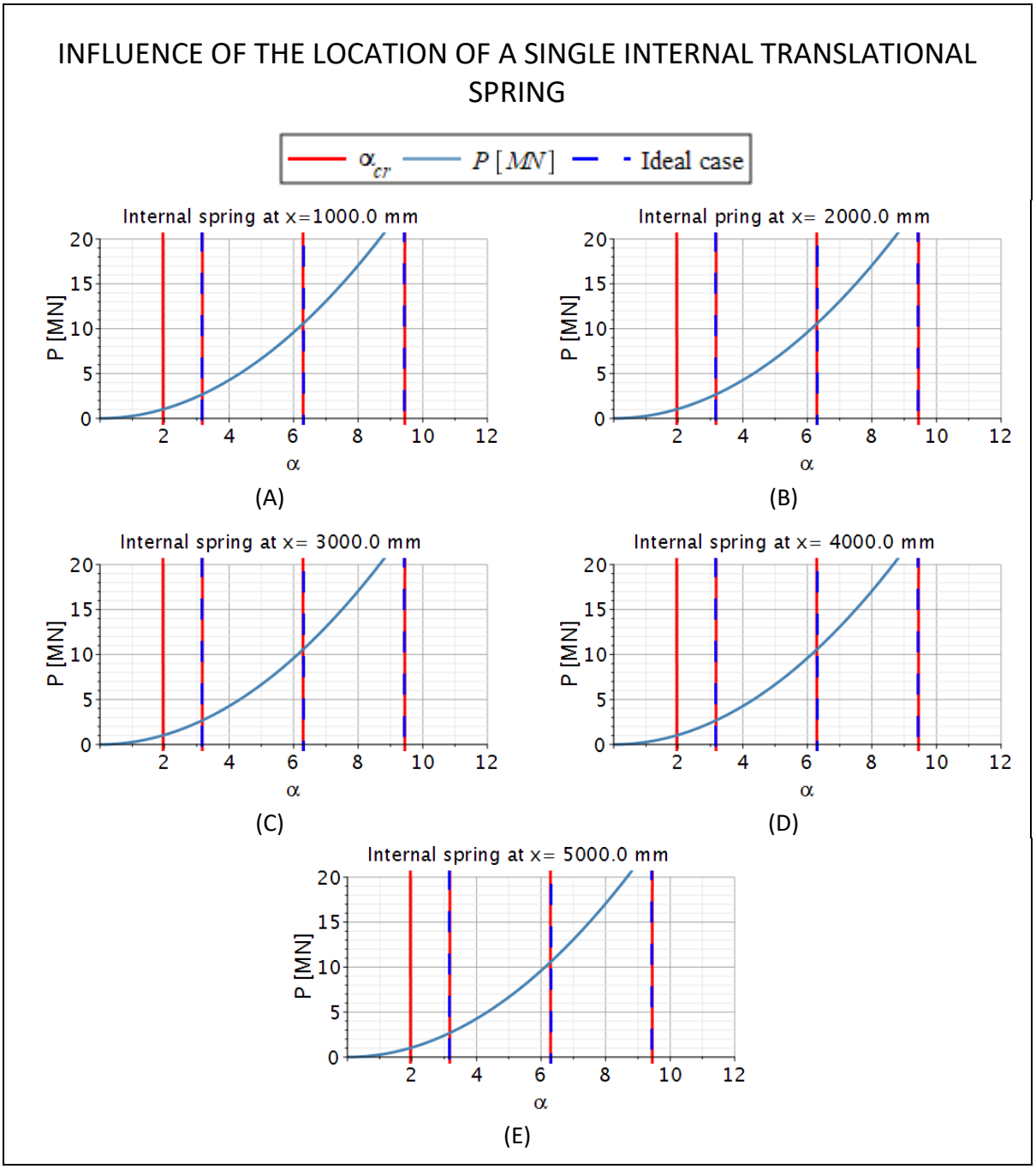

Figure 49: Plots obtained using the proposed closed-form solution to illustrate the change of critical roots due to the influence of an internal translational spring with a stiffness of 100 N/mm acting at different locations from the supports.

5.2.6 Location of rotational spring

This subsection studies the effects of the location of an internal rotational spring with stiffness of 5e+9 Nmm/rad acting on a simply supported column of 10 000 mm. The column is made of steel with a Young's Modulus of 200 000 N/mm^2 and a square cross-section of 200×200 mm^2.

The proposed closed-form expressions have been used to obtain the five graphs displayed within Figure 50, presenting the effect of a single internal rotational spring with a stiffness of 5e+9 Nmm/rad acting at five different locations from the left pin support, as depicted in Figure 36. The data in Figure 50 is extracted and displayed in Figure 51 to represent better how the location of a single rotational spring affects the first three buckling loads. From such a figure, the position of highest interest can be easily identified. It can also be concluded that having the rotational spring present at the inflection points corresponding to their respective buckling mode results in the lowest negative impact on the critical buckling loads.

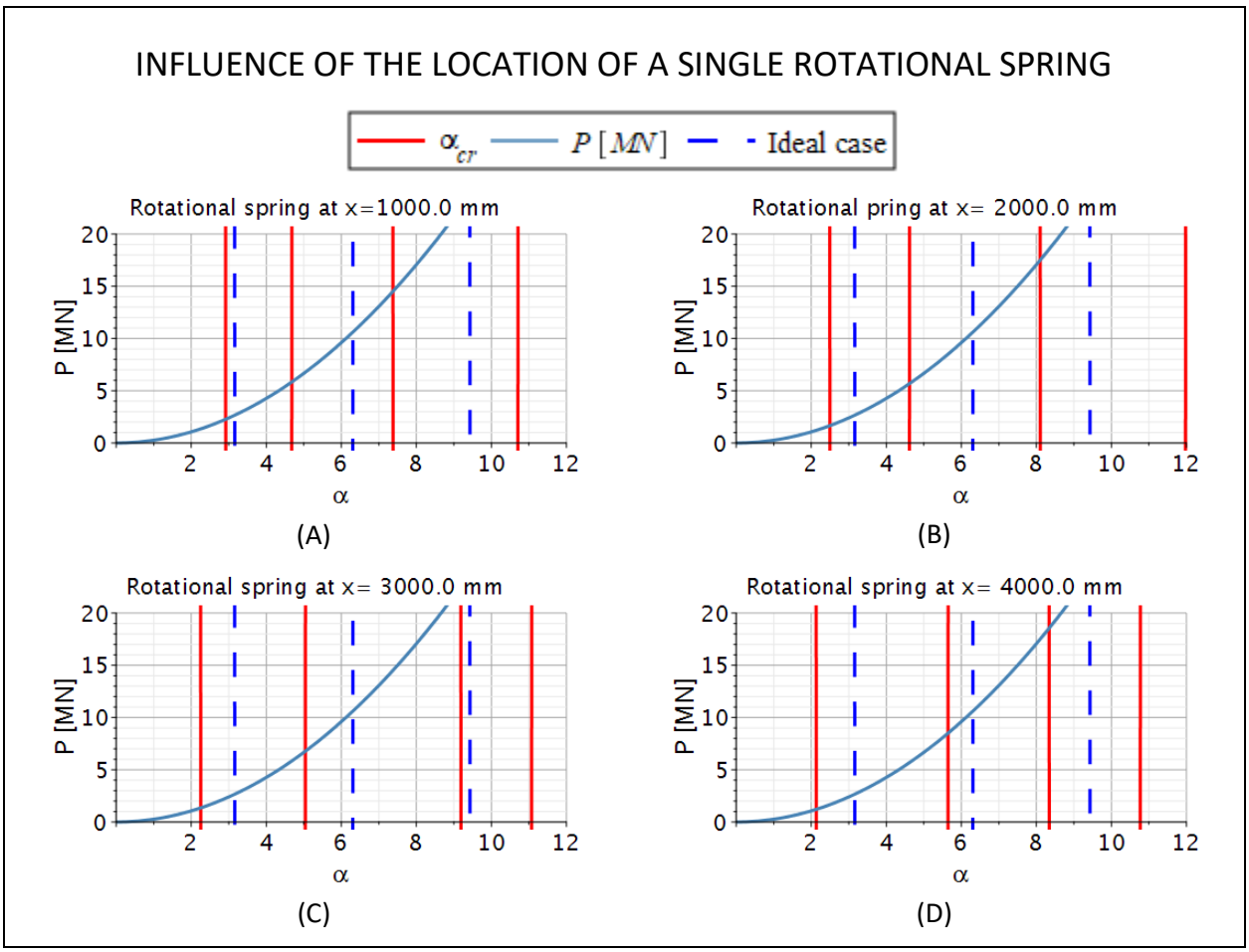

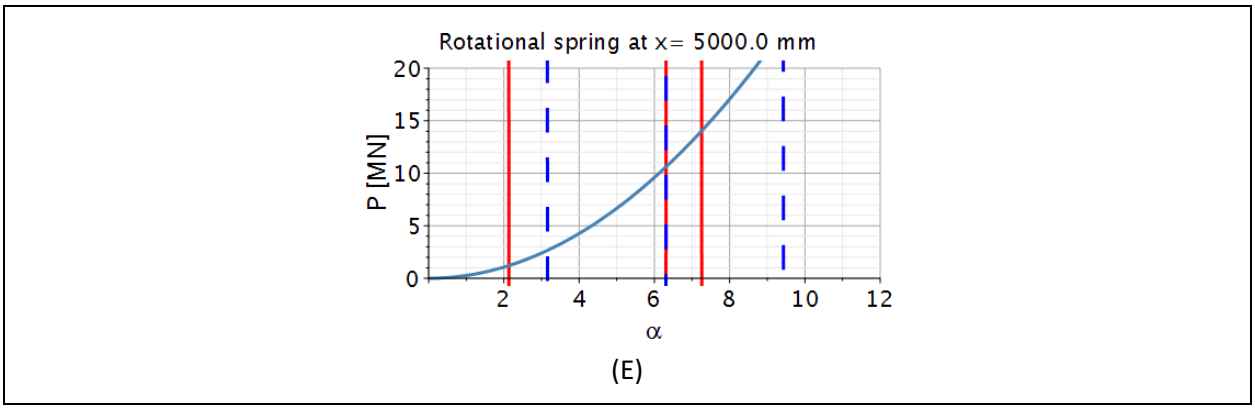

Figure 50: Plots obtained using the proposed closed-form solution to illustrate the change of critical roots due to the influence of an internal rotational springs with a stiffness of 100 N/mm acting at different locations from the supports.

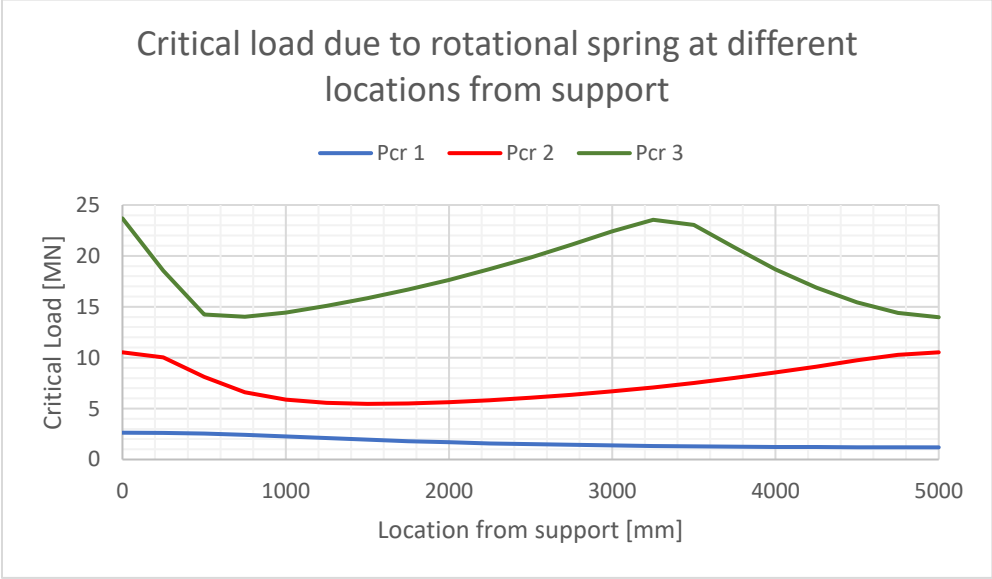

Figure 51: Effect of critical loads due to a single internal rotational spring at different distances from the left pin support of a 10 000 mm simply supported column

6 Case Study – Wind turbine tower buckling analysis

The following section uses the proposed closed-form expressions to obtain charts to explore different designs of wind turbine towers. Two approaches are considered: the first consists of finding the material properties of each section that can withstand known forces, such as those experienced due to a lateral wind load and the axial compression load of the generator itself. The second approach focuses on obtaining deflection plots due to different combinations of lateral and axial forces, given the known properties of a structure.

It should be noted that the proposed closed-form solutions only provide critical loads by performing a linear buckling analysis. The deflections obtained from the closed-form solutions can account for the geometrically non-linear static analysis of the wind tower.

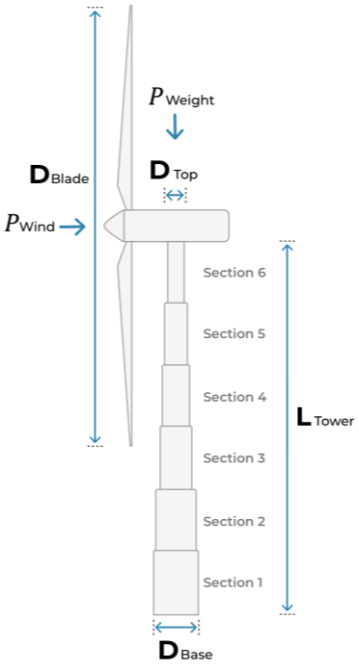

Figure 52: Wind tower structure consisting of six hollow circular sections of equal span and varying diameter.

6.1 Finding the best cross-section properties given known loads

This first section focuses on employing the proposed closed-form expressions to obtain useful plots in finding the best combination of material properties for a 30 kW wind turbine (Figure 52). Such a turbine located at the free end of a cantilever column exerts 3480 kg of compressive force, according to Aeolos Wind Energy Ltd technical charts. The rotor blade diameter for such a wind turbine is 15.6 m, which can be supported by a 24 m wind tower. Plots are obtained assuming a lateral point load due to the wind of 10 000 N acting at the free end of the cantilever beam-column. Seven models of a wind tower consisting of six sections are considered. Table 5 presents the cross-sectional and material properties of such models.

The proposed closed-form expressions are used to solve the four unknown constants of integration algebraically. Such solutions, and the data of Table 5, result in the deflection of seven different wind towers, as seen in Figure 53. If a maximum allowable displacement is known, the plot can identify the tower models that satisfy such a condition.

Table 5: Cross-sectional and material properties of seven considered models in the design exploration of a wind tower structure. Section 1 represents the base of the tower, and section 6 the top of the tower.

	Section 1 (Elastic Mod.) $[N/mm^2]$	Section 2 (Elastic Mod.) $[N/mm^2]$	Section 3 (Elastic Mod.) $[N/mm^2]$	Section 4 (Elastic Mod.) $[N/mm^2]$	Section 5 (Elastic Mod.) $[N/mm^2]$	Section 6 (Elastic Mod.) $[N/mm^2]$
Model 1	Steel (2.00E+05)	Steel (2.00E+05)	Steel (2.00E+05)	Steel (2.00E+05)	Steel (2.00E+05)	Steel (2.00E+05)
Model 2	Concrete (3.00e+04)	Steel (2.00E+05)	Steel (2.00E+05)	Steel (2.00E+05)	Steel (2.00E+05)	Steel (2.00E+05)
Model 3	Concrete (3.00e+04)	Concrete (3.00e+04)	Steel (2.00E+05)	Steel (2.00E+05)	Steel (2.00E+05)	Steel (2.00E+05)
Model 4	Concrete (3.00e+04)	Concrete (3.00e+04)	Concrete (3.00e+04)	Steel (2.00E+05)	Steel (2.00E+05)	Steel (2.00E+05)
Model 5	Concrete (3.00e+04)	Concrete (3.00e+04)	Concrete (3.00e+04)	Concrete (3.00e+04)	Steel (2.00E+05)	Steel (2.00E+05)
Model 6	Concrete (3.00e+04)	Concrete (3.00e+04)	Concrete (3.00e+04)	Concrete (3.00e+04)	Concrete (3.00e+04)	Steel (2.00E+05)
Model 7	Concrete (3.00e+04)	Concrete (3.00e+04)	Concrete (3.00e+04)	Concrete (3.00e+04)	Concrete (3.00e+04)	Concrete (3.00e+04)
Outer radius $[mm]$	350	330	310	290	270	250
Inner radius $[mm]$	150	130	110	90	70	50
Thickness $[mm]$	200	200	200	200	200	200
Second moment of area $[mm^4]$	1.139E+10	9.090E+09	7.138E+09	5.503E+09	4.155E+09	3.063E+09

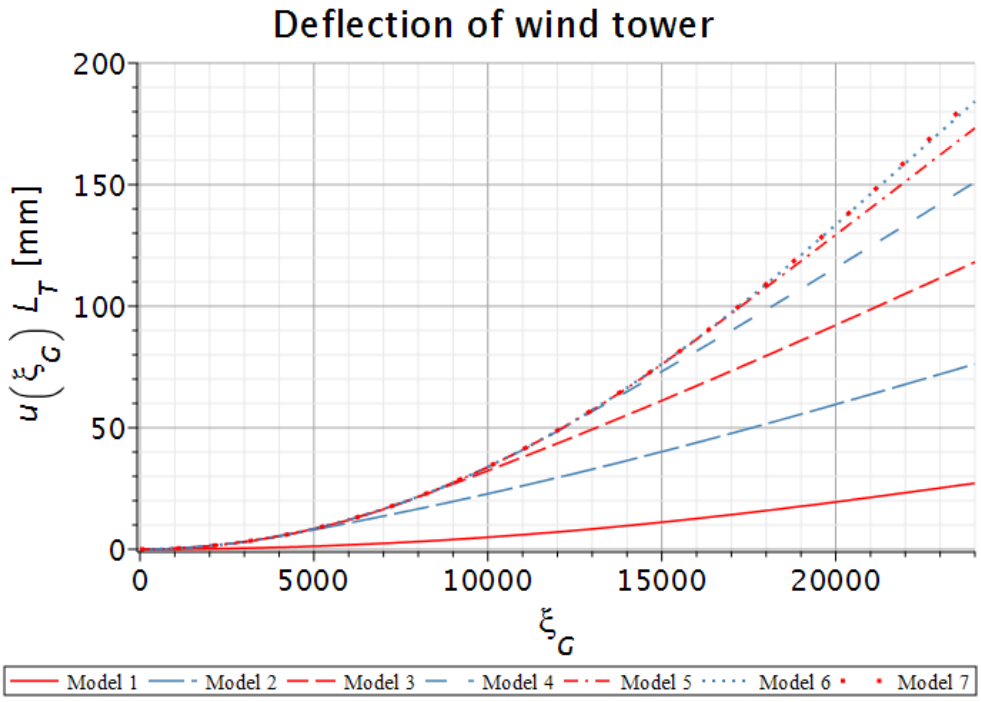

Figure 53: Deflection of seven wind tower structures with different material properties under an axial load of 35 000 N and a lateral point load of 10 000 N acting at the free end.

The solved unknown constants of integration expressed algebraically allow for the further consideration of other parameters, such as different cross-sectional properties, or lengths of each section, without the need to obtain new solutions for the constants of integration.

6.2 Finding allowable loads given known structural properties

This section employs the proposed closed-form expressions to obtain geometrical non-linear deflection under different axial and lateral load combinations at the free end of a telescopic wind tower. Model 1 from Table 5 is analysed. It is possible to plot the deflection experienced at the free-end under different combinations of axial compressive loads (related to the axial parameter ν) and wind point load (Figure 54). Such a plot is valuable when a maximum allowable deflection is considered as a design criterion. From such a plot, the first critical buckling variable (ν_{crit_1}) of its column counterpart is presented as the asymptote of the graph. Under such a compressive load, the column bifurcates from one configuration to another. The closed-form expressions can capture the effect of the point load acting on the free end of the structure, with the deflection reaching the bifurcation point in different manners, depending on the lateral load.

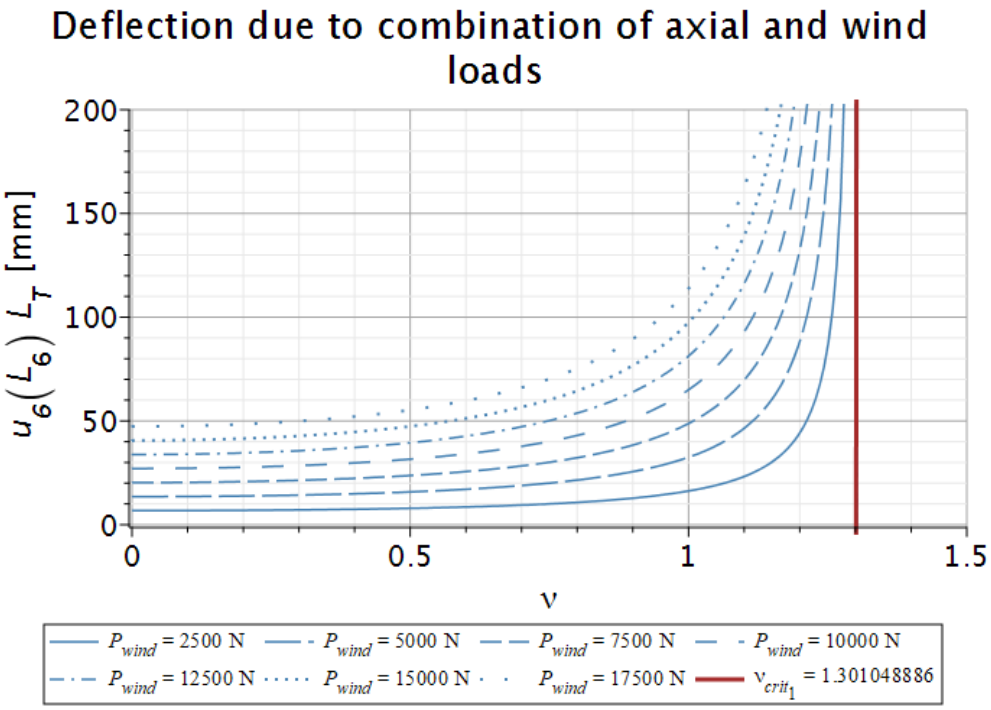

Figure 54: Deflection at the free end of model 7 under the combination of wind load (P_{wind}) and axial parameter ν.

The closed-form expressions can obtain the linear buckling loads and capture the geometrical non-linear effects experienced by beam-columns. Such expressions can be used to obtain displacement plots due to a combination of axial and lateral loads acting on beam-columns. Getting the solutions algebraically allows the user the freedom of changing parameters without drawbacks from the FE method, such as having a new model for each analysis, avoiding the re-discretization of each model, and the need of multiple load steps to capture the geometrical non-linear effects due to the axial and lateral loads.

7 Conclusions and recommendations

This chapter first discusses the research questions follower by the thesis concluding remarks. Finally, some recommendations are presented for future improvements of analysis of beam-columns.

7.1 Answers to the research questions

The first research questions proposed in section 1.3 was:

"How to take advantage of the properties of generalized functions to develop a closed-form solution for the buckling analysis of columns and beam-columns with step-changes of its flexural stiffness (sudden changes of material and cross-section properties), while considering the influence of non-propagating cracks, real joints, boundary, and lateral support conditions?"

- The most effective way of using generalized functions for the buckling analysis of columns and beam-columns is by employing the governing equations of each section between discontinuities and expressing the global behavior of the column or beam-column by creating a piecewise equation by means of the Heaviside function. It should be noted that such a procedure does not tackle the issue of having many integration constants; it just helps in expressing the global behavior of the structure in a single equation.

- Point loads create discontinuities when analyzing columns and beam-columns. They can be avoided by expressing such load types in the loading function utilizing the Dirac delta function.

The second research question was:

"How do different springs (rotational, external translational, and internal translational) acting in a column affect the buckling loads?"

- The parametric study performed in section 5.2 using the closed-form expressions provides some insight into how different springs (external and internal translational, and internal rotational) affect the roots of the buckling equations, which are related to the critical buckling loads of a column and beam-column. The stiffness and location of springs affect such roots.

    - External springs can increase the value of all of their critical roots compared to their ideal counterpart. Under the right stiffnesses, they behave as intermediate supports affecting the buckling modes the columns undergo, as seen in Figure 39, where the change of buckling modes between roots can be identified. Moreover, the location of the external spring has an added effect on the critical loads of a column. However, the spring location has different impacts on the higher buckling loads, as seen in Figure 48.

    - Internal springs can decrease the value of the critical roots compared to their ideal counterpart. Unlike external springs, the change of stiffness of internal springs affects one critical root at a time. The buckling mode is associated with that of its ideal counterpart. Trends of the buckling modes related to loads can be seen in Figure 43. Critical values that differ from those of their ideal counterparts have a special buckling mode, as displayed in

Figure 42. Finally, the spring stiffness of an internal spring is the sole factor affecting the critical roots of a column.

- Low rotational spring stiffnesses reduce all critical roots until the rotational spring stiffness matches that of one of the connected segments. However, the change of critical load due to variations of rotational spring stiffness is not constant nor linear, as in the case of internal translational springs or external translational springs. After reaching a specific stiffness, any further increase would not significantly affect the critical loads, as seen in Figure 46. The location of rotational springs also plays a considerable role in its effect on the critical roots. However, the location impacts the critical roots of higher-order, as seen in Figure 51.

- A common relation of all springs is that it does not affect the critical roots whenever they are located at an inflection point associated with one of the buckling modes of the column.

7.2 Concluding remarks

This thesis proposes a closed-form solution for the buckling analysis of Euler-Bernoulli columns and beam-columns with step-changes of flexural stiffness with real boundaries, as well as external translational, internal translational, and internal rotational springs. The analyzed column or beam-column consists of $N+1$ sections of constant stiffness, N being the number of discontinuities present on the column or beam-column. The discontinuities present themselves where step-changes of flexural stiffness occur or due to springs' presence between two consecutive segments. The deflection, slope, moment, and shear are expressed locally for every segment. The Heaviside function is used to combine in a piece-wise manner all local functions to obtain a single expression for the global deflection, slope, moment, and shear.

A system of N discontinuities presents $4(N+1)$ unknown constants of integration. The proposed closed-form expressions reduce the number of unknown to only four unknown constants of integration which are solved by enforcing four boundary conditions. This reduction of unknown constants also results in computing the determinant of a 4×4 matrix of unknown coefficients to obtain the buckling equation that provides the critical loads for a column. Moreover, after solving for the constants of integration when analyzing the static behavior of a beam-column, the closed-form expression can accurately describe the geometrically non-linear deflection, slope, moment, and shear. Such results have been validated utilizing the FE software DIANA.

Computational time starts taking a toll after six discontinuities. However, the advantages of using the proposed closed-form expressions are that the buckling equation or the four unknown integration constants are solved algebraically. Such algebraic expressions allow the possibility of storing the resulting equations for future use without recomputing them. Having the solutions expressed algebraically also allows the manipulation and change of parameters to explore different structural designs.

7.3 Recommendation and further improvements

- The proposed closed-form solutions prove that a linear buckling analysis can be performed analytically on a column with N discontinuities while only depending on obtaining the determinant of a 4×4 system of equations or solving for the four unknown constants of integration. The computational time it takes to perform such calculations can vary depending on the mathematical software used for the variable manipulation required for such an analysis.

- It is recommended to store the buckling equation and the constants of integration after solving them algebraically, avoiding the need to recompute such expressions. Having the solutions saved and expressed algebraically allows direct use in the parametric study of columns and beam-columns.

- The closed-form expressions can be expanded to include more complexities acting on columns and beam-columns, such as the influence of being on an elastic foundation.

Appendix 1: Pin-pin column buckling example

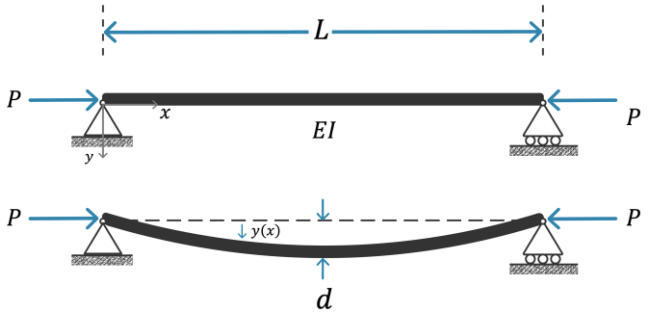

Figure A1.1: Pin-pin column under an axial load P

The column presented in Figure A1.1 can be analyzed using equation (A *1*).

$$u'''' + v^2 \cdot u'' = \frac{q}{EI} \qquad (A\ 1)$$

The general solution of equation (A *1*) is

$$u(x) = A + B\,x + C\left(\frac{1}{v^2} - \frac{\cos(\mathrm{v}\,\mathrm{x})}{\mathrm{v}^2}\right) + D\left(\frac{x}{v^2} - \frac{\sin(v\,x)}{v^3}\right) + Q \qquad (A\ 2)$$

With

$$Q = \frac{\int_0^x (-q(\tau)\,x + q(\tau)\,\tau)\,d\tau}{EI\,v^2} + \frac{\int_0^x (q(\tau)\sin(v\,\tau)\cos(v\,x) - q(\tau)\cos(v\,\tau)\sin(v\,x))\,d\tau}{EI\,v^3} \qquad (A\ 3)$$

The four constants of integration require four equations for them to be solved. Such equations are obtained using the boundary conditions. The boundaries of a pin-pin column dictate that the displacements and moments are zero at $x = 0$ and $x = L$ giving us the four necessary equations for the system of equations.

The constitutive relation of the displacement to the moments is found in equation (A 4).

$$M = -EI \cdot u'' \qquad (A\ 4)$$

After applying the boundary conditions, the matrix of the system of equations for a pin-pin column is:

$$\begin{bmatrix} 1 & 0 & 0 & 0 \\ 0 & 0 & -EI & 0 \\ 0 & 0 & -EI\cos(v\,L) & -\dfrac{EI\sin(v\,L)}{v} \\ 1 & L & -\dfrac{\cos(v\,L)}{v^2} & -\dfrac{\sin(v\,L)}{v^3} + \dfrac{L}{v^2} \end{bmatrix} \qquad (A\ 5)$$

The transcendental buckling equation is obtained from the determinant of the matrix of the system of equations. From (A 5), it can be noted that the loading function is not present; hence it has no effect on the theoretical buckling load. The determinant of the matrix in equation (A 5) is:

$$Buckling\ equation = \frac{L\,EI^2 \sin(v\,L)}{v} \qquad (A\ 6)$$

The non-trivial solutions associated with the buckling loads can be found by setting the buckling equation to zero, which is the same as finding its roots, which are associated with the term vL. The first and second roots can be seen in Figure A1.2:

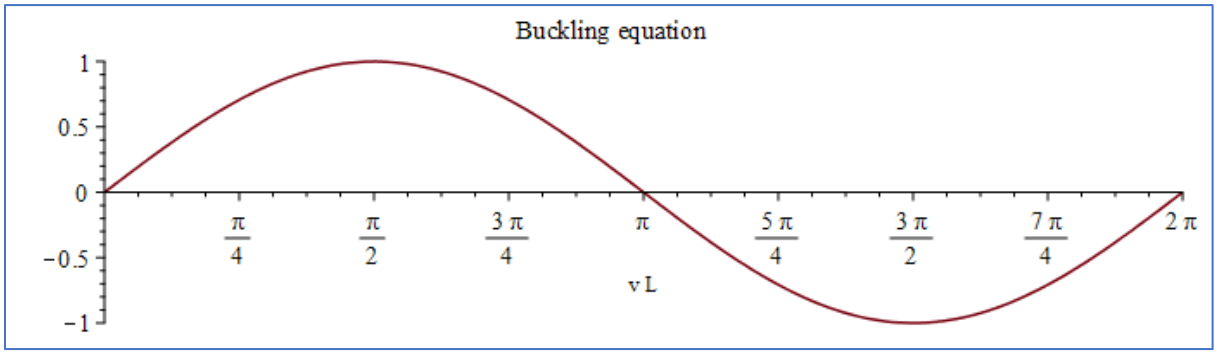

Figure A1.2: Transcendental buckling equation of a pin-pin column

The first and second buckling load, $P_{cr,1}$ and $P_{cr,2}$ respectively, can be found by solving for P considering that $v^2 = \frac{P}{EI}$. Hence:

$$P_{cr,1} = \frac{\pi^2\,EI}{L^2} \text{ and } P_{cr,2} = \frac{4\,\pi^2\,EI}{L^2}$$

These critical loads are associated with their respective buckling shapes that can be seen in Figure A1.3, assuming a length of 10 m for the column.

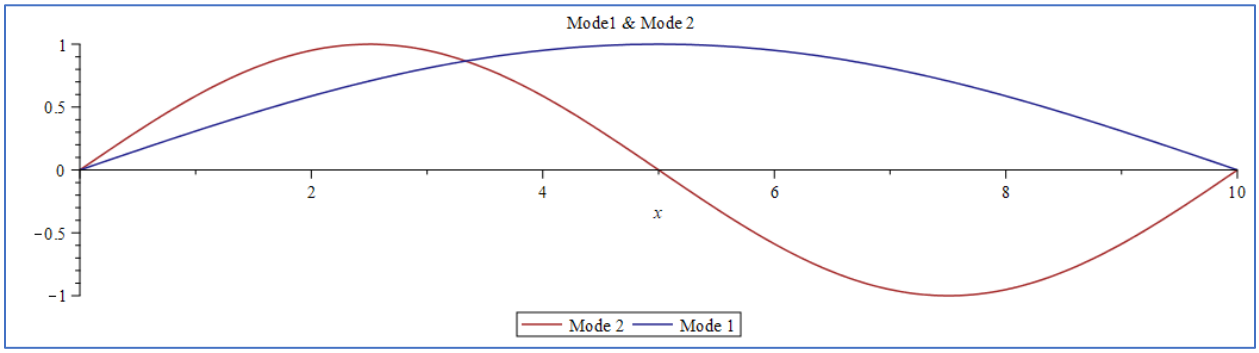

Figure A1.3: First and second buckling mode of the pin-pin column from Figure A1.1.

Bibliography

[1] A. Palmeri and A. Cicirello, “Physically-based Dirac’s delta functions in the static analysis of multi-cracked Euler-Bernoulli and Timoshenko beams,” *Int. J. Solids Struct.*, vol. 48, no. 14–15, pp. 2184–2195, 2011, doi: 10.1016/j.ijsolstr.2011.03.024.

[2] F. Giunta and A. Cicirello, “On the analysis of jointed Euler-Bernoulli beams with step changes in material and cross-section under static and dynamic loads,” *Eng. Struct.*, vol. 179, pp. 66–78, 2019, doi: 10.1016/j.engstruct.2018.10.036.

[3] A. Cicirello and A. Palmeri, “Static analysis of Euler-Bernoulli beams with multiple unilateral cracks under combined axial and transverse loads,” *Int. J. Solids Struct.*, vol. 51, no. 5, pp. 1020–1029, 2014, doi: 10.1016/j.ijsolstr.2013.11.030.

[4] M. I. Friswell and J. E. T. Penny, “Crack Modeling for Structural Health Monitoring,” *Struct. Heal. Monit. An Int. J.*, vol. 1, no. 2, pp. 139–148, 2002, doi: 10.1177/1475921702001002002.

[5] Q. S. Li, “Classes of exact solutions for buckling of multi-step non-uniform columns with an arbitrary number of cracks subjected to concentrated and distributed axial loads,” *Int. J. Eng. Sci.*, vol. 41, no. 6, pp. 569–586, 2003, doi: 10.1016/S0020-7225(02)00181-7.

[6] M. Salama, T. ABDEL-LATEEF, M. Dabaon, and O. ABDEL-MOEZ, “Buckling of Columns With Sudden Change in Cross Section,” 2000.

[7] N. Zdravković, M. Prof, and M. Savković, “Energy method in efficient estimation of elastic buckling critical load of axially loaded three-segment stepped column,” *FME Trans.*, vol. 41, pp. 222–229, 2013.

[8] M. Salama, “Buckling loads of columns with suddenly changing cross-section subjected to combined end and intermediat axial forces,” 2009.

[9] Q. S. Li, “Exact solutions for buckling of non-uniform columns under axial concentrated and distributed loading,” *Eur. J. Mech. - A/Solids*, vol. 20, no. 3, pp. 485–500, 2001, doi: https://doi.org/10.1016/S0997-7538(01)01143-3.

[10] Q. S. Li, “Analytical solutions for buckling of multi-step non-uniform columns with arbitrary distribution of flexural stiffness or axial distributed loading,” *Int. J. Mech. Sci.*, vol. 43, no. 2, pp. 349–366, 2001, doi: 10.1016/S0020-7403(00)00017-5.

[11] Q. Li, “Buckling Analysis of Multi-Step Non-Uniform Columns,” *Adv. Struct. Eng.*, vol. 3, pp. 139–144, 2000.

[12] Q. S. Li, “Buckling of multi-step non-uniform beams with elastically restrained boundary conditions,” *J. Constr. Steel Res.*, vol. 57, no. 7, pp. 753–777, 2001, doi: https://doi.org/10.1016/S0143-974X(01)00010-4.

[13] F. Arbabi and F. Li, “Buckling of Variable Cross-Section Columns: Integral-Equation Approach,” vol. 117, no. 8, pp. 2426–2441, 1992.

[14] S. Caddemi, I. Caliò, and F. Cannizzaro, “Closed-form solutions for stepped Timoshenko beams with internal singularities and along-axis external supports,” *Arch. Appl. Mech.*, vol. 83, no. 4, pp. 559–577, 2013, doi: 10.1007/s00419-012-0704-7.

[15] M. H. SADD, “Deformation: Displacements and Strains,” in *Elasticity*, Fourth Edi., no. 4, M. H. SADD, Ed. 2020, pp. 31–55.

[16] M. L. Gambhir, *Stability Analysis and Design of Structures*, 1st ed. Patiala, India: Springer, 2004.

[17] C. H. Yoo and S. C. Lee, “Chapter 3 - Beam-Columns,” C. H. Yoo and S. C. B. T.-S. of S. Lee, Eds. Boston: Butterworth-Heinemann, 2011, pp. 155–198.

[18] R. T. Ratay, “Column.” McGraw-Hill Education, Jul. 19, 2021, doi: 10.1036/1097-8542.150200.

[19] J. Erochko, *An Introduction to Structural Analysis*, First. Ottawa: Jeffrey Erochko.

[20] S. P. Timoshenko, J. M. Gere, and W. Prager, “Theory of Elastic Stability, Second Edition,” *J. Appl. Mech.*, vol. 29, no. 1, pp. 220–221, 1962, doi: 10.1115/1.3636481.

[21] L. F. M. da Silva, A. Öchsner, and R. D. Adamas, *Handbook of Adhesion Technology*. Berlin, 2011.

[22] F. Arbabi, *Structural Analysis and Behavior*. McGraw-Hill, 1991.

[23] I. G. N. O. University, “Unit 11 - Energy methods and applications,” in *Indeterminate Structures-II*, IGNOU, 2017, pp. 35–77.

[24] P. F. Rizos, N. Aspragathos, and A. D. Dimarogonas, “Identification of crack location and magnitude in a cantilever beam from the vibration modes,” *J. Sound Vib.*, vol. 138, no. 3, pp. 381–388, 1990, doi: 10.1016/0022-460X(90)90593-O.

[25] F. Farassat, “An introduction to generalized functions with some applications in aerodynamics and aeroacoustics NASA TP 3428 Corrected Copy,” no. May, 1994.

[26] L. Salasnich, *Quantum Physics of Light and Matter*, 1st ed. Springer, Cham, 2014.

[27] A. Saichev and W. Woyczynski, “Appendix C: Distributions, Fourier Transform, Divergent Series,” in *Distributions in the physical and engineering sciences. Volume 2, Linear and nonlinear dynamics in continuous media*, no. May, New York: Birkhäuser, 2013.